Elsevier Editorial System(tm) for Coordination Chemistry Reviews
Manuscript Draft

Manuscript Number: CCR-D-12-00110R1

Title: Twists and turns: studies of the complexes and properties of bimetallic complexes featuring phenylene ethynylene and related bridging ligands.

Article Type: Special Issue: Electron Transfer

Keywords: molecular electronics; mixed valence; ruthenium; molybdenum; spectroelectrochemistry; DFT.

Corresponding Author: Dr Paul J. Low,

Corresponding Author's Institution:

First Author: Paul J. Low

Order of Authors: Paul J. Low

Abstract: The concept of a molecular-based electronic technology has been evolving for over 50 years, and the development of molecular designs for such components over this period has drawn heavily on studies of intramolecular charge transfer in mixed-valence complexes and related systems. Recent advances in methods for the assembly and measurement of device characteristics of metal|molecule|metal junctions have brought the realisation of the considerable promise of the area within a tantalisingly close reach. This review presents a selective review of the chemistry, spectroscopic properties and electronic structures of bimetallic complexes [{LxM}(μ-bridge){MLx}]n+ based primarily, but not exclusively, on the Ru(PP)Cp' and Mo(dppe)(η-C7H7) fragments and alkynyl based bridging ligands. The molecular design strategies that lead to a wide spectrum of electronic characteristics in these systems are described. Examples range from weakly coupled mixed-valance complexes through more strongly coupled systems in which the electronic states of the bridging ligand are intimately involved in electron transfer processes to complexes. An argument is made that the latter are better described in terms of redox non-innocent bridging ligands supported by metal-based donor substituents rather than strongly coupled mixed valence complexes. The significance of these results on the further development of metal complexes for use as components within a hybrid molecular electronics technology are discussed.

Correspondence to: Prof. Paul J. Low
Department of Chemistry
Durham University
South Rd, Durham, DH1 3LE, UK
T: +44 (0)191 334 2114
F: +44 (0)191 384 4737
E: p.j.low@durham.ac.uk

Twists and turns: studies of the complexes and properties of bimetallic complexes featuring phenylene ethynylene and related bridging ligands.

Paul J. Low

Department of Chemistry, Durham University, South Rd, Durham, DH1 3LE, UK

Abstract

The concept of a molecular-based electronic technology has been evolving for over 50 years, and the development of molecular designs for such components over this period has drawn heavily on studies of intramolecular charge transfer in mixed-valence complexes and related systems. Recent advances in methods for the assembly and measurement of device characteristics of metal|molecule|metal junctions have brought the realisation of the considerable promise of the area within a tantalisingly close reach. This review presents a selective review of the chemistry, spectroscopic properties and electronic structures of bimetallic complexes $[\{L_xM\}(\mu\text{-bridge})\{ML_x\}]^{n+}$ based primarily, but not exclusively, on the Ru(PP)Cp' and Mo(dppe)(η-C_7H_7) fragments and alkynyl based bridging ligands. The molecular design strategies that lead to a wide spectrum of electronic characteristics in these systems are described. Examples range from weakly coupled mixed-valance complexes through more strongly coupled systems in which the electronic states of the bridging ligand are intimately involved in electron transfer processes to

complexes. An argument is made that the latter are better described in terms of redox non-innocent bridging ligands supported by metal-based donor substituents rather than strongly coupled mixed valence complexes. The significance of these results on the further development of metal complexes for use as components within a hybrid molecular electronics technology are discussed.

Graphical Abstract

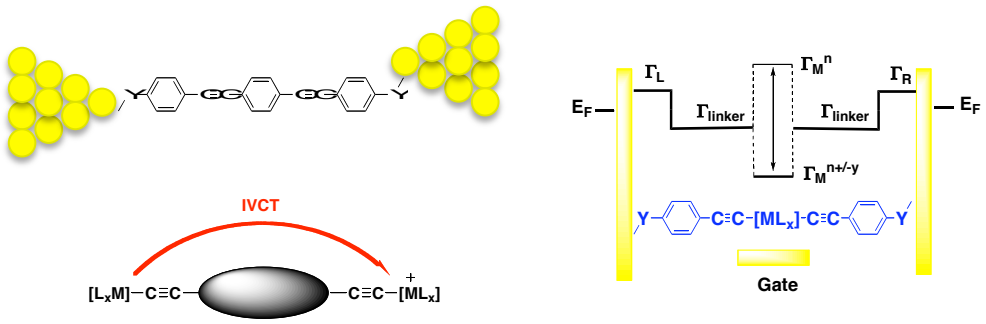

Highlights

- The use of spectroelectrochemical based studies and DFT computations to probe electronic structure in a range of open-shell ligand-bridged bimetallic complexes is presented.
- A summary of the relationships between bridging ligands in mixed-valence chemistry and the design criteria for molecular components for electronics.

- Design strategies for metal complex based components for molecular electronics are discussed.

Keywords: molecular electronics; mixed valence; ruthenium; molybdenum; spectroelectrochemistry; DFT.

Abbreviations

ap = 2-anilinopyridinate

pz = pyrazine

DBU = 1,8-diazabicycloundec-7-ene

1. Introduction

Electron transfer reactions are arguably the simplest subset of all chemical reactions, yet they underpin essentially every aspect of chemistry and biology [1-4]. In relatively recent times the understanding of these elementary processes has been exploited in the design of advanced optoelectronic materials [5] and devices for solar energy harvesting and conversion [6-8], as well as served to stimulate further exploration of electron exchange in a wider variety of molecular and nanoscale frameworks [9-12]. Although earlier enthusiasm for single molecule electronics from the mid 1970's and 1980's waned with the realisation of the magnitude of the challenges associated with developing this technology, the success of plastic electronics (e.g. OLED devices) and development of ever more reliable and accessible methods for measurements of single molecule conductance properties in metal | molecule | metal junctions [13, 14] and methods for the assembly of molecules within device-type platforms has led to another dramatic surge in interest in the topic [15]. The near-future potential for molecular electronics is now widely recognised, and the International Technology Roadmap for Semiconductors (ITRS) has begun to include molecular targets within its future materials agenda [16]. The integration of functional molecular components within electronic devices is a paradigm shift from conventional CMOS technology. [17] Consequently, exploration of the science which underpins this emerging high technology sector provides opportunities for the design and synthesis of novel molecular products en route to future industrial processes. In recognition of the importance of this area, major manufacturers have now established research programmes encompassing molecular electronic concepts [see, for example, 18-22].

Whilst the vast majority of studies with molecular junctions conducted to date have concentrated on studies of surface binding and trans-molecule conductance of short chain organic oligo(arylene ethynylene) systems [23-25], metal complexes are beginning to migrate from the prototypical systems with which to study intramolecular electron transfer in solution towards functional molecular materials in hybrid solid-state / molecule assemblies [see, for example, 26-37]. As has been noted elsewhere [38, 39], metal complexes offer numerous advantages in the design of molecules for use in single molecule electronics. These include the synthetic flexibility in terms of molecular length, conformational rigidity, steric bulk through appropriate choice of ancillary ligands, and control over the orbital energy and spin state at the metal center(s) through redox processes (Figure 1) [40]. The modular construction of metal complexes on surfaces has been elegantly demonstrated [41], which provided an interesting counter-point to the assembly of organic molecules in a junction *in situ* [42], and demonstrated an alternative method for the assembly of metal complexes within device structures to assembly strategies based on pre-preparation of the entire molecular component.

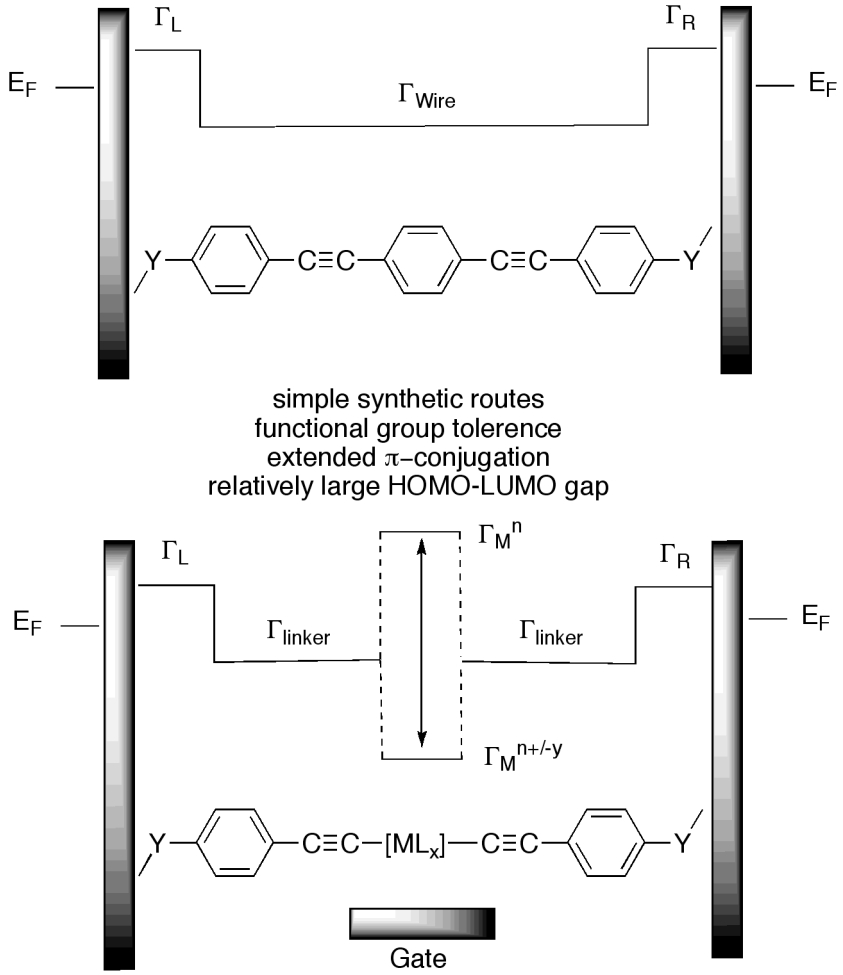

Figure 1 A schematic showing a prototypical organic (top) and organometallic (bottom) component within two- (top) and three-(bottm) terminal junctions. The junction conductance can be described in terms of the Landauer formalism

$G = \frac{2e^2}{h} \times \tau_L \times \tau_B \times \tau_R$ where e is the electron charge, h is Planck's constant and τ_L, τ_B and τ_R are the transmission coefficient of the left contact, the molecular bridge and the right contact, respectively. The introduction of a redox active molecule and a gate electrode offers a mechanism through which to tune Γ_B.

Perhaps the most fascinating prospect for metal complexes in molecular electronics lies in the capacity to bring frontier orbitals in and out of resonance with the contacting electrodes either through bias or change of molecular redox state at moderate potentials, or through the introduction of spin or Coulomb blockades [34, 43]. Nevertheless, many challenges still remain for molecular electronics in general, and organometallic moltronics in particular. High amongst the list of these challenges lies the development of chemical structure / device electronic property maps and the engineering challenges associated with fabrication of three-terminal device platforms that permit the full range of electrochemically accessible molecular redox states to be utilised to enhance junction characteristics [44, 45].

The challenges inherent in the fabrication and study of molecules contacted by even only two macroscopic contacts has led to a substantial interest in bimetallic model systems for molecular components in which charge transfer properties can be studied in solution using spectroscopic methods. Since the earliest studies of the Creutz-Taube ion, $[\{Ru(NH_3)_5\}_2(\mu\text{-pz})]^{5+}$, mixed valence derivatives in particular have played a vital role in both fundamental and applied studies involving electron transfer reactions in metal complexes [2, 46]. Consequently, transition metal complexes in which two (or more) metal atoms are linked through a common bridging ligand have been a target for synthetic chemists.

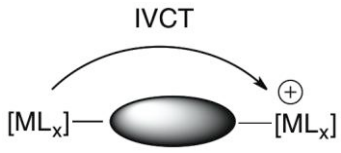

Figure 2. A schematic of a mixed valence complex; the intervalence charge transfer (IVCT) transition contains information concerning the electronic structure (localised

vs delocalised) and electronic coupling between the metal centers, and also provides information concerning the mixing of the bridge with the metallic states.

However, the use of bimetallic complexes, [{L_xM^n}(μ-bridge){M^nL_x}], as precursors to mixed valence derivatives, [{L_xM}(μ-bridge){$M^{(n\pm y)}L_x$}], and hence models of molecular wires in device structures, lies alongside the growing body of work that has re-ignited awareness of the redox activity of supporting and bridging ligands (i.e. ligand redox non-innocence) [47]. Further complications arise in the middle ground of electronic structures where bridge and metal states mix, leading to significant deviations from the well-known Hush two-state model of electronic coupling in mixed valence systems, whilst retaining some spectroscopic characteristics associated with mixed valency [48-51]. Identifying the electronic characteristics of the redox products derived from [{L_xM^n}(μ-bridge){M^nL_x}] systems therefore requires application of a range of physical and spectroscopic methods which provide information across a range of timescales, and is often supported by computational investigations and which precede discussions of the electron transfer characteristics of these species. The difficulties of using DFT based computations to model the electronic structure and charge transfer transitions in localised mixed valence systems is well documented [52], but there is considerable optimism regarding the potential for local hybrid and gradient functionals to satisfactorily model long-range charge transfer processes [53-55]. Nevertheless, the combination of DFT calculations with appropriately chosen functionals and spectroscopic data provides a powerful method for the assessment of electronic structure, distinguishing metal and ligand contributions to the stabilisation of unpaired charges, and contributing to the further

refinement of theories concerning intramolecular charge transport in both organic compounds and organometallic complexes.

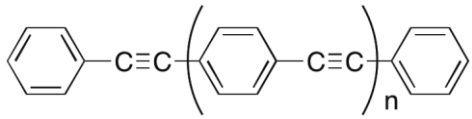

Figure 3 The oligo(phenylene ethynylene) motif.

The ability of molecular frameworks derived from the oligo(phenylene ethynylene) motif (Figure 3) to support intramolecular charge transfer over considerable distances [56] through super-exchange or hopping mechanisms [57-60] has long been recognised as an attribute of immense potential application for the design of molecular scale components for electronics [61-63]. For the same reasons, of the myriad of bridging ligands available to facilitate the construction of [{L_xM^A}(μ-bridge){M^BL_x}] complexes and associated open shell derivatives, diethynyl aromatic systems can be identified as particularly popular motifs for the study of intramolecular electron transfer processes and the construction of 'wire-like' metal complexes [30, 64]. This activity is further driven in no small part by the synthetic accessibility of the ligand precursors and the well-developed routes to metal alkynyl complexes.

The tools provided by Hush and others which allow extraction of electronic information from spectroscopically observable parameters in mixed valence complexes [{L_xM^n}(μ-bridge){$M^{n\pm y}L_x$}] [48, 65, 66] have been widely used to explore a vast range of molecular structures with a view to assessing intramolecular coupling between the metallic sites, and hence their 'wire-like' properties [67-69]. Of

course, this method of analysis pre-supposes the 'mixed-valence' nature of the object of study, and the prevalence of redox non-innocence in many π-conjugated ligand structures when associated with relatively electron rich, heavier members of the late transition series urges a degree of care before undertaking such analyses.

In this personal account, the cross-section of trans-molecule conductance in oligo(phenylene ethynylene) systems and intramolecular electron transfer processes in bimetallic complexes featuring phenylene ethynylene and related ynyl-based bridging ligands will be selectively explored and compared. A brief overview of the electronic structure and dynamic properties of the prototypical oligophenylene ethynylene, 1,4-bis(phenylethynyl)benzene (1), will be provided by way of introduction to phenylene ethynylene systems and the use of this and related fragments to support charge transfer in both molecular junctions and bimetallic complexes. Synthetic methods available for the preparation of phenylene ethylene oligomers and complexes derived from them are also described. In many cases, ynyl-ligated complexes exhibit well-behaved one-electron redox chemistry. The nature of the redox active orbitals can be varied from metal to ynyl-ligand by judicious choice of the metal and supporting ligands, and explored through application of spectroelectrochemical and computational methods. These ideas concerning metal vs ligand redox activity in organometallic complexes containing ynyl-derived ligands are also selectively summarised.

2. Twists and turns: Rotational conformers in the prototypical molecular wire oligo(phenylene ethynylene)

The seminal work of Allara, Tour and Weiss established the 1,4-bis(phenylethynyl)benzene (**1**, BPEB) motif as a molecular wire amenable to study in metal|molecule|metal junctions when augmented by suitable surface contacting groups [70]. Some 15 years after the original Allara, Tour and Weiss papers, the BPEB scaffold remains the basis of current molecular wire designs, augmented by functional groups designed to improve surface contacts, influence the distribution of π-electron density and modulate the *I-V* characteristics of the junction [71]. These investigations concerning conductance of molecular junctions run parallel to studies of intramolecular electron transfer processes in bimetallic complexes that feature this motif as a bridging ligand.

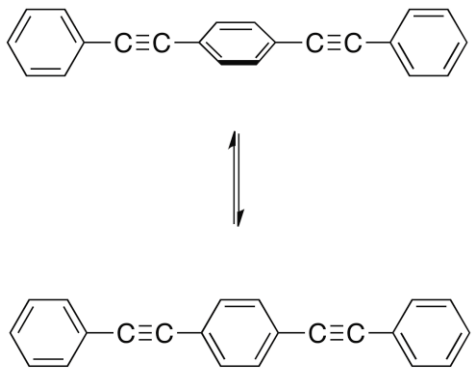

1

Figure 4. A representation of the planar form of 1,4-bis(phenylethynyl benzene) (**1**) and a representative 'twisted' conformer. The barrier to rotation is only 2.7 kcal mol^{-1} [75].

These complementary areas of investigation (conductance studies of metal|molecule|metal junctions and intramolecular charge transfer studies in $\{L_xM^n\}$(μ-bridge)$\{M^nL_x\}$ systems) are both driven by the extended π-conjugated

backbone of BPEB. The extent of delocalisation is highly sensitive to the molecular conformation, with planar conformations offering more extended delocalisation pathways along the long molecular axis [72-74]. An analysis of the torsional motions of the parent molecule, 1,4-bis(phenylethynyl)benzene and the central-ring deuterated derivative 1,4-bis(phenylenethynyl-2,3,5,6-tetradeuteriobenzene, using cavity ring-down spectroscopy revealed a low barrier to rotation of the phenyl(ene) rings in BPEB around the alkynyl linkers (2.7 kcal mol^{-1}) [75], a value consistent with earlier estimates [76-79]. Since this is comparable with kT at ambient temperatures, samples of BPEB and related systems are usually found as a mixture of all available conformers, with nearly free rotation of the phenyl(ene) rings around the long molecular axis [80], unless additional steric constraints [81, 82], templating backbones [83] intramolecular tethers [84, 85] or hydrogen bonding interactions [86, 87] are introduced. The distribution of conformers can also be biased towards the more highly delocalised planar conformer at lower temperatures in fluid or frozen solution [88], through interactions at the air-water interface in appropriately substituted derivatives [89], and by alignment in stretched polyethylene films containing the phenylene ethynylene system of interest [90]. Photoexcitation offers an alternate avenue for transient control of the molecular conformation, without significant disruption to the bonding pattern along the molecular backbone [91]. The S_1 state of BPEB has a deeper potential well than the ground state [75, 92], and photoexcitation followed by rapid relaxation to the lowest vibrational level leads to increased population of the planar $S_1(v=0)$ state, from which fluorescent emission takes place in line with Kasha's Rule [88].

Within condensed phases, BPEB derivatives tend to adopt planar conformations, whilst in Langmuir-Blodgett films of BPEB derivatives, H-aggregates are commonly observed [93-98]. In self assembled films based on gold-thiol interactions, BPEB derivatives tend to give dense, well packed monolayers (tilt angle to the surface ca. 30-40 °), in which the planar conformation is dominant [99]. Conformational switching was originally suggested as a mechanism to account for the stochastic switching observed in STM based imaging experiments [100], but later investigations revealed the fluxionality of the gold-sulfur contact to be the source of the observed variable conductance of thiol-contacted molecules within Au|S-molecule-S|Au junctions [101, 102].

Whilst gold-thiol remains the work-horse contacting chemistry for the assembly of molecules on conducting (gold) substrates, the fluctionality [102] and diversity of the Au-S contact leads to multiple conductance signatures [103], which can be exacerbated by differences in surface structure and hence the number of coordination sites on the surface leading to variation in conductance values of, for example, 1,4-benzenedithiol from 5 x 10^{-5} G_0 to 0.1 G_0 (Figure 5). Given that the contact morphology (site of binding, molecular tilt, etc) is sensitive to the site of surface binding [104, 105], the choice of measurement method (e.g. break-junction vs $I(s)$) can lead to differences in conductance measurements in even simple α,ω-alkanedithiols [106].

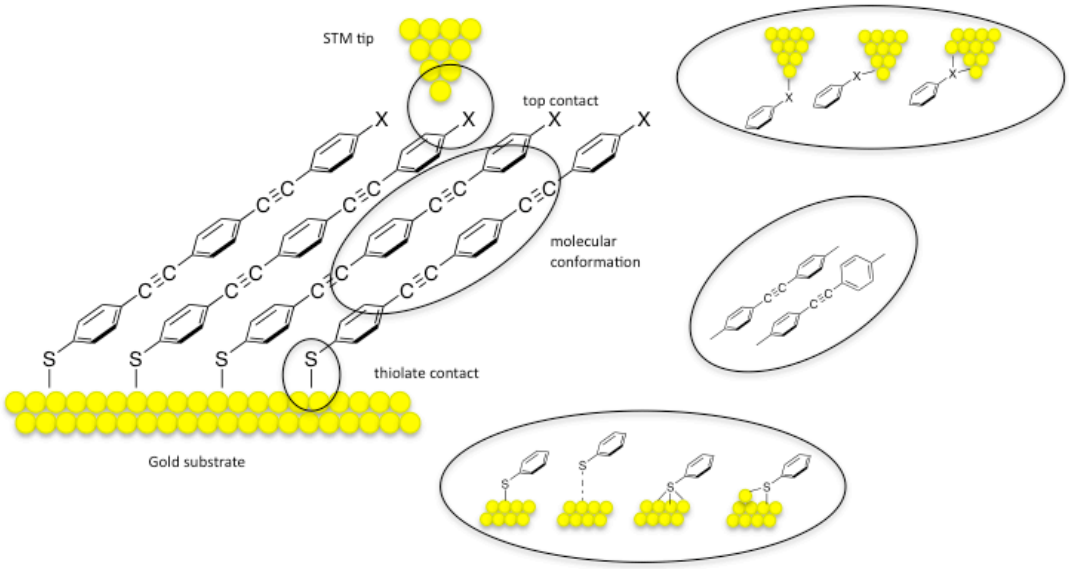

Figure 5. The diversity of top and bottom contacts between a molecule and the macropscopic electrode interfaces (illustrated here for a gold substrate and STM tip) are highly variable, giving rise to a range of conductance values for the junction.

Alternative contacting groups to the thiol moiety have also been identified, with terminal- [107] and trimethylsilyl-protected [94] alkynyl moieties, amines [93, 108, 109], pyridines [110], isocyanides [111], dimethylphosphines [112], metal complexes [113, 114] and direct formation of a substrate-carbon bond [115, 116] emerging as useful alternate contacts, although the formation of multiple stable junctions with a range of conductance profiles still an issue. Given that in addition to the nature of the contact, the number of molecules in the junction [110], contacts between molecular π-systems and electrode surface [117], presence of adjacent surface adatoms and molecular π-systems [25] can all influence the conductance of the junction, the identification of new, physically robust contacts remains a priority for the development of molecular electronics [118], including organometallic based components [17, 41, 119, 120].

3. Phenylene ethynylenes: From prototypical alkyne ligand to prototypical molecular wire and back again.

The electronic considerations that have directed so much attention to phenylene ethynylene based systems as molecular components within metal|molecule|metal junctions have also led to considerable interest in charge transfer processes within molecular systems bearing ligands derived from phenylene ethynylenes. However, interest in the use of phenylethynyl based ligands far pre-dates thoughts of using such complexes as models or components for molecular electronic systems. It is probably fair to suggest that phenyl acetylene has been the work-horse alkyne ligand used in the development of σ-alkynyl ligand chemistry. The availability, ready purification, and convenient boiling point range of phenylacetylene, together with the moderate acidity of the alkynyl proton which assists the formation of nucleophilic acetylide anions, made it something of a ligand of choice for the early, pioneering synthetic efforts [121]. The phenyl moiety also provided a scaffold for the introduction of additional alkynyl moieties, and complexes and polymers containing diethynylbenzene ligands were also quickly prepared.

In more recent times, the introduction of electron withdrawing groups to the these themes has been extended to include a wide range of donor-acceptor complexes and dendritic structures for electro-optical applications [122, 123], and necessitated access to a much wider range of functionalised alkynes. The development of the chemistry of functionalised metal alkynyl complexes is therefore something of a remarkable circular story. The development of Cu(I) mediated transmetallation to prepare Group 10 alkynyl complexes by Hagihara and Sonogashira [124-128] evolved to the Sonogashira cross-coupling reaction [130, 131]. The Sonogashira cross-coupling

protocol now provides access to a vast array of organic alkynes bearing almost every imaginable functional group. In turn, these alkynes are used in a variety of contexts to develop functionalised metal alkynyl complexes.

The compatibility of the Sonogashira cross-coupling protocol with trimethyl silyl and propan-2-ol based ethynyl protecting groups, the chemoselectivity of aryl iodides over aryl bromides, and the simple functional group transformations that can be used to introduce halide substituents permits the simple iterative assembly of phenylene ethynylene systems of considerable length and diverse peripheral functionality [132]. Extended phenylene ethynylene compounds are also readily prepared on large scale from quinones (benzoquinone, naphthaquinone, anthraquinone) via the sequential addition of alkynyl nucleophiles followed by reduction (Scheme 1). At –78°C only monosubstitution of the quinone takes place, with the second addition requiring temperatures above –40°C. This provides a convenient method through which to transform a cheap, symmetric quinone to differentially substituted diols, which can be subsequently reduced ($SnCl_2$) to the corresponding aromatic derivatives [133, 134]. These synthetic protocols, together with alkyne metathesis reactions, provide the new aromatic alkynyl compounds used in the further development of metal alkynyl chemistry.

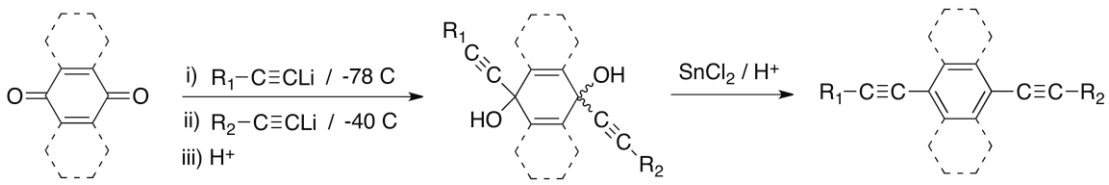

Scheme 1. The ‘palladium-free’ synthesis of arylene ethynylenes from quinones [133].

The rearrangement of terminal alkynes in the presence of more electron-rich metal centers to vinylidene complexes, followed by deprotonation has been widely exploited as a convenient route to metal alkynyl complexes, and probably represents the most commonly employed route in current use (Scheme 3) [135]. As part of a study of extended π-conjugated alkynyl-based ligands, metal diynyls represent a key conceptual advance from simpler alkynyl complexes [136]. Although access to terminal diyne reagents, HC≡CC≡CR, is becoming simpler [137-139], these fascinating species are still not widely employed in transition metal chemistry, and care must be taken when manipulating these sterically unencumbered, highly conjugated compounds. Terminal diynes also have a tendency to undergo a formal 1,4-H shift, although likely proceeding through a series of deprotonation / protonation steps [140], giving rise to highly reactive butatrienylidene complexes (Scheme 2) [141].

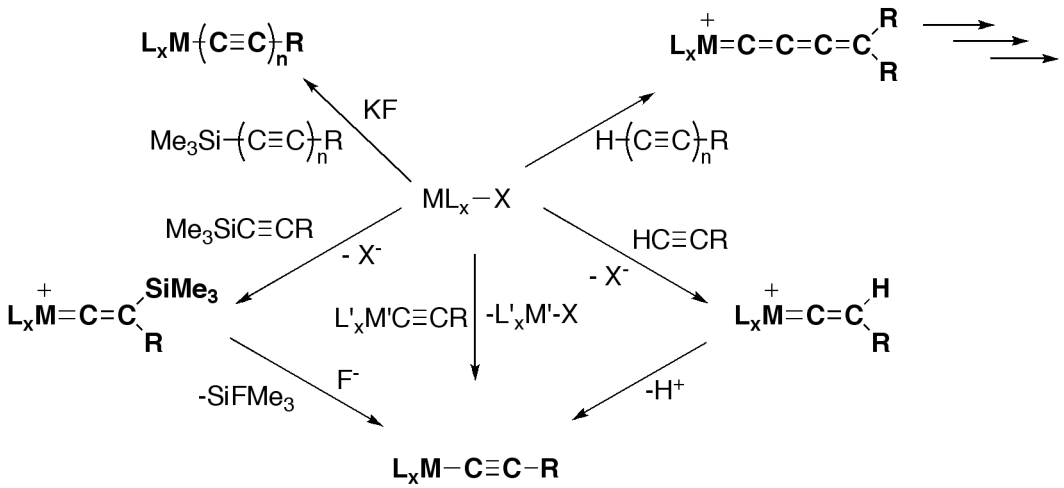

Scheme 2. A selection of common methods for the formation of metal ynyl complexes, intermediates and associated products.

Given the prevalence of trimethylsilyl protecting groups in synthetic alkyne chemistry, the use of $Me_3SiC{\equiv}CR$ precursors directly in the preparation of transition metal alkynyl complexes has been explored as a work-around to the preparation and manipulation of terminal ynyl and polyynyl compounds. Typically 'desilylation-metallation' reactions are conducted in the presence of a source of fluoride ions (KF or NBu_4F being commonly employed) and proceed at moderate temperatures to give the alkynyl complexes in good yield [142-144]. These reactions likely proceed by a sequence of initial formation a π-alkyne complex, followed by 1,2-silyl shift and desilylation [145-149], although mechanistic detail has not been established in all cases (Scheme 2). A competing *in situ* desilylation reaction to give the terminal alkyne in situ before entry to the conventional protio-vinylene chemistry cannot be excluded from every scenario. Nevertheless, silyl-protected alkynes are now established as convenient reagents for the preparation of metal alkynyl complexes.

Transmetallation reactions also provide convenient entry to $\{L_nM\}C{\equiv}CR$ complexes, with reactions of alkynyl Grignard reagents, alkali metal salts [150, 151], Group 11 or trialkyl tin alkynyl reagents with metal complexes bearing some suitable labile ligand or leaving group, $\{L_nM\}X$, having been explored (Scheme 2). Grignard reagents and alkali metal salts of alkynyl anions, although largely superseded due to the experimental simplicity of alternative procedures and the lack of compatibility between the nucleophilic alkynyl anions, or the bases used to generate them, and supporting ligands on the metal (e.g. CO), are still capable of providing entry to valuable product classes, such as the $[Ru_2(ap)_4(C{\equiv}CR)]$ systems developed by Ren [152]. The $Cu^{(I)}$-based transmetallation reactions have met with great success for less electron-rich metal fragments [153]. Although $[Cu(C{\equiv}CR)]_n$ species are prone to

explosive decomposition and the use of $[Cu(C{\equiv}CR)(PPh_3)]_4$ reagents tends to give products in which the copper fragment is π-coordinated by the transferred alkynyl ligand, the use of catalytic quantities of Cu(I) and Cu(C≡CR) species generated in situ significantly reduces both the hazards and formation of π-complex by-products [154, 155]. Silver(I) alkynyl reagents, which are also rather sensitive, have also been used as alkynyl transfer reagents [156]. Transmetallation reactions with stannyl-substituted alkynes have also been shown to be a viable synthetic strategy, although the use of toxic and / or deliquescent tin reagents does limit the wider appeal of these methods [157- 162]. Interestingly, $[RhCl(PMe_3)_4]$ undergoes an oxidative addition reaction with both $Me_3SnC{\equiv}CR$ and HC≡CR to give mer-trans-$[Rh(C{\equiv}CR)_2(SnMe_3)(PMe_3)_3]$ [163] or cis,cis-$[Rh(H)(C{\equiv}CR)(PMe_3)_4]^+$ species [164], respectively. Related neutral hydrides have been obtained by elimination of methane in reactions of $[Rh(Me)(PMe_3)_4]$ with terminal alkynes [164]. The use of $Me_3SnC{\equiv}CPh$ and $Me_3SnC{\equiv}CC_6H_4C{\equiv}CSnMe_3$ has permitted access to mono and bimetallic ruthenium complexes from the otherwise rather unreactive *trans*-$RuCl_2(dppe)_2$ [165].

Recently gold alkynyl complexes and intermediates have begun to attract attention as intermediates in catalytic cycles in which the alkyne is transferred from the gold centre to another (catalytically active) metal [166]. The propensity of gold alkynyl complexes to enter into transmetallation reactions, together with the simple preparation of these compounds from terminal or silyl protected alkynes and diynes, also makes them convenient reagents in their own right in the preparation of metal alkynyl complexes [167]. The relatively low π-acidity of $[Au(PPh_3)]^+$ and high covalency of the Au-X bonds is also convenient, serving to prevent the π-coordination of the gold fragment to the alkynyl product.

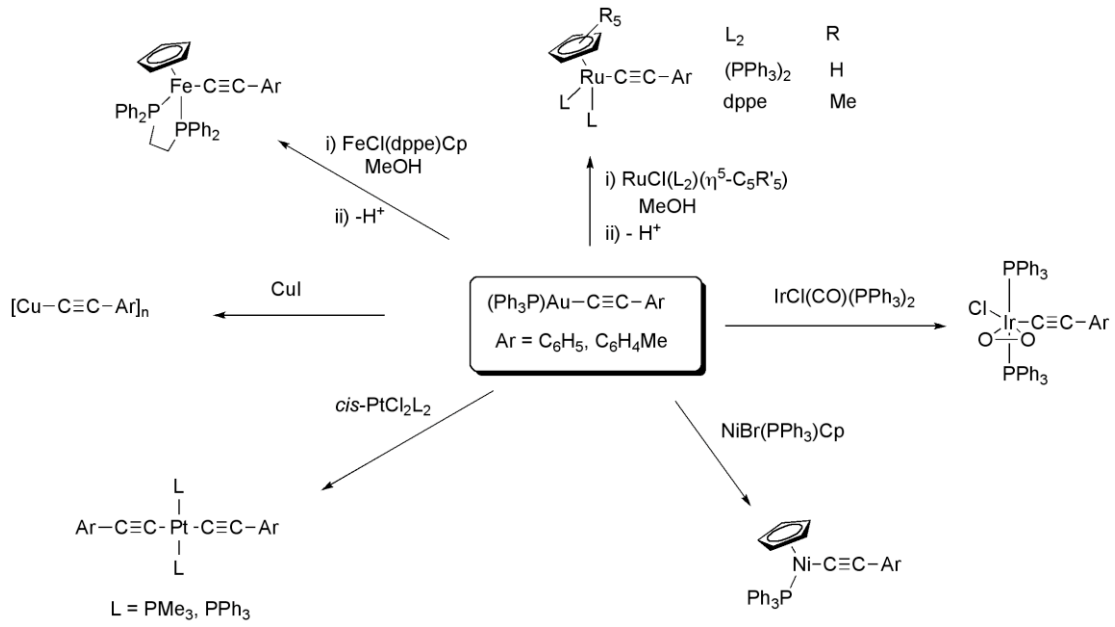

Scheme 3. The use of [Au(C≡CAr)(PPh_3)] in the preparation of metal alkynyl complexes by transmetallation reactions [167].

Another strategy that is finding increased application in recent times involves chemical modification of a ligand within the metal coordination environment [168]. In this context of metal alkynyl and polyynyl complexes, early examples of such processes would include the deprotonation of terminal ynyl ligands (or masked equivalents such as –C≡C$SiMe_3$ [169, 170] and terminal vinylidenes [171, 172]) and subsequent reactions with electrophiles [173-175]. The high nucleophilicity of the alkynyl C_β carbon in complexes such as [Ru(C≡CH)(dppe)Cp*] also raises interesting options for 'chemistry on the complex' synthetic strategies based on direct reactions of this species with electrophiles [176, 177]. However, with a view to the preparation of the phenyl ethynyl based systems the Sonogashira cross-coupling reaction using

either terminal ynyl complexes $\{L_nM\}\{(C\equiv C)_xH\}$ or $\{L_nM\}(C\equiv CArC\equiv CH)$ [154, 173, 178, 179] or arylhalide substituted metal σ-ethynyl complexes [180] as coupling partners with aryl halides or 1-alkynes, respectively, has been shown to be a powerful, if not yet widely exploited, synthetic strategy.

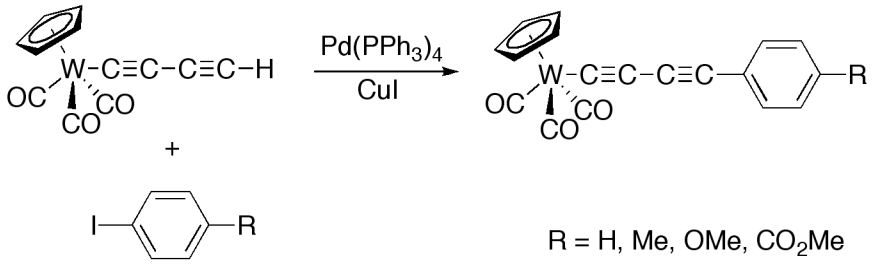

Scheme 4. An early example of 'chemistry on the complex' used to prepare aryl buta-1,3-diyl ligands [154, 173]

Other 'chemistry on the complex' strategies of direct relevance to the preparation of phenylene ethynyl ligand derivatives take advantage of the parallel reactivity of the pendent C≡CH moiety in $[Ru(C\equiv C–1,4\text{-}C_6H_4\text{-}C\equiv CH)(PPh_3)_2Cp]$ (1) with simple organic terminal alkynes [181]. The complex $[Ru(C\equiv C–1,4\text{-}C_6H_4\text{-}C\equiv CSiMe_3)(PPh_3)_2Cp]$ (2) is conveniently prepared from the 1:1 stoichiometric reaction of $RuCl(PPh_3)_2Cp$ with $Me_3SiC\equiv C–1,4\text{-}C_6H_4\text{-}C\equiv CSiMe_3$ in the presence KF in methanol. The mono-metallated complex 2 precipitates under these conditions before activation / desilylation of the second ethynyltrimethylsilyl moiety [143]. Subsequent reaction with $[NBu_4]F$ in a thf/methanol solvent mixture in which the precursor is more soluble affords the useful building block 1, which can be used in the preparation of a wide range of phenylene ethynlene derivatives by Sonogashira or Hay cross or homo-coupling reactions, or used in the preparation of bi- and

polymetallic derivatives through the usual methods of metallation associated with terminal alkynes (Scheme 5) [181].

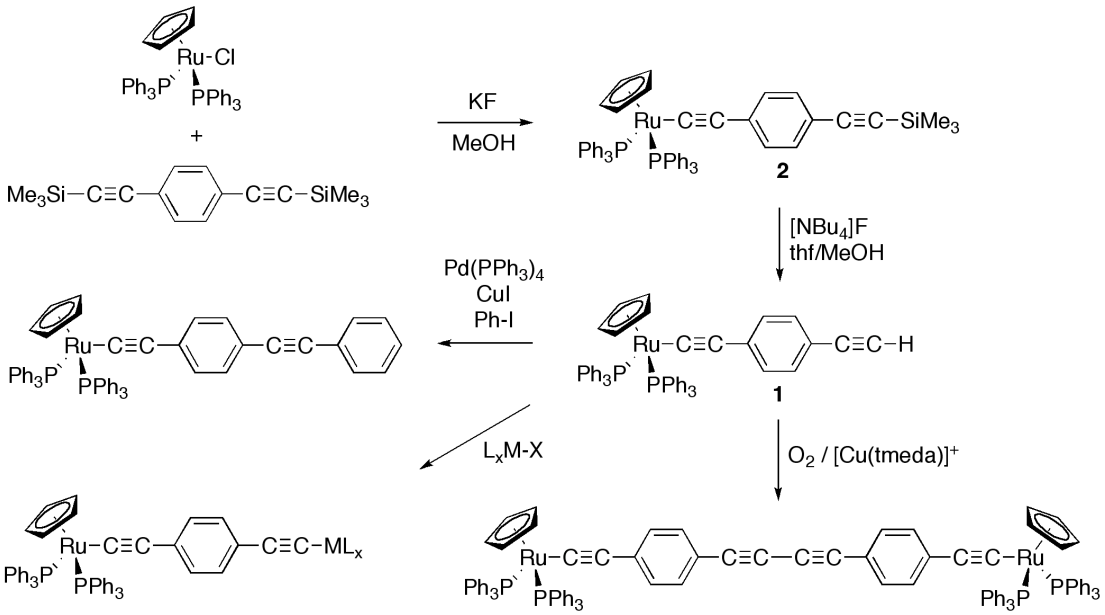

Scheme 5. The preparation of phenylene ethynylene complexes from [Ru(C≡C–1,4-C_6H_4-C≡CH)$(PPh_3)_2$Cp] using 'chemistry on the complex' concepts.

4. Building bridges: the mononuclear complexes [Ru(C≡CR)(PP)Cp´] and [Mo(C≡CR)(dppe)(η-C_7H_7)]

Before considering the electronic structure of bimetallic complexes, it is useful to first understand the electronic structure of the (conceptual) mono-metallic building blocks and metal-ligand interactions therein. The electronic structure of the half-sandwich d^6 Ru(II) complexes [Ru(C≡CR)(PP)Cp´] have been explored in increasing levels of detail over the past 20 years [182-184], and important contributions from studies of related ynyl species should not be forgotten [185-189]; however a comprehensive review of metal alkynyl bonding is beyond the scope of this review. The elementary

features of the bonding descriptions are summarised in terms of a fragment orbital approach in Figure 6 [182, 191]. The {Ru(PP)Cp´} fragment (P = phosphine based ligand, Cp´ = η-C_5H_5, C_5Me_5 etc) can be considered as a square pyramidal ML_5 fragment, with three of the ligand sites occupied by the facially capping Cp ligand. Using the coordinate system defined in Figure 6, the principle interactions between the metal center and the alkynyl ligand can be identified in ADF calculations as arising from overlaps of the metal d_{z^2} orbital and the alkynyl lone pair, which gives rise to a strong σ-bond, and weaker π-interactions between d_{xz} and d_{yz} with the C≡C π-obitals. In a d^6 metal system the σ-bonding and both bonding and anti-bonding π-combinations are populated, the later giving rise to the HOMOs. The relative energies, and hence contribution to the HOMOs, of the metal and alkynyl fragment orbitals are sensitive to the supporting ligands on the metal and substituents, and length of the ynyl chain [182, 191]. Consequently, chemical control around the molecular scaffold can be used to tune the electronic characteristics of the complex (Figure 6). Similar conclusions are also drawn from DFT analyses [192, 193], and the composition of the HOMO in [Ru(C≡CAr)$(PH_3)_2$Cp] (B3LYP/3-21G*) is found to vary from Ru:C_2Ar = 30:67 (Ar = C_6H_5) to 11:86 (Ar = $C_{14}H_8$). There is not a significant amount of structural distortion or orbital re-ordering on reducing the electron count by 1e to simulate oxidation, and the β-LUSO in [Ru(C≡CAr)$(PH_3)_2$Cp]$^+$ offers similar composition to the HOMO of the neutral precursor.

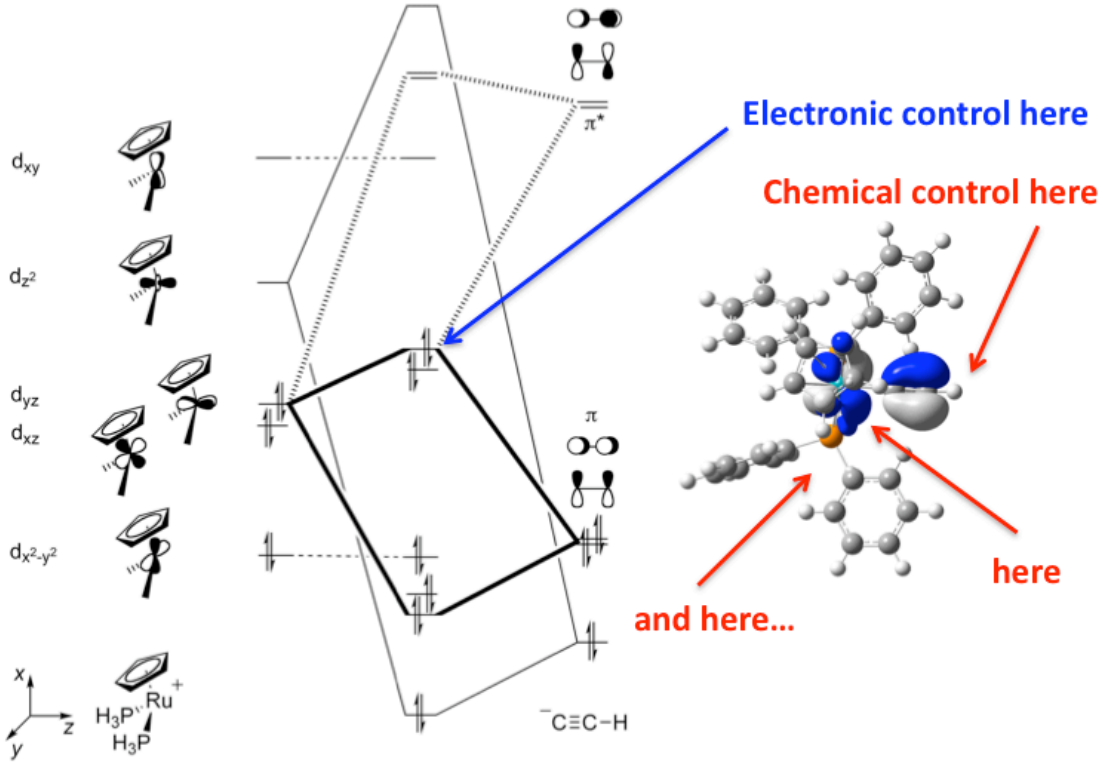

Figure 6. A qualitative MO scheme for the Ru(C≡CH)(PH_3)$_2$Cp fragment, adapted from [182, 191]. The energy and composition of the frontier orbitals is sensitive to the nature of the alkynyl substituent, the metal (e.g. Ru vs Fe) and supporting ligands.

These calculations indicating the significant contribution from the alkynyl ligand to the frontier orbitals of [Ru(C≡CAr)(PP)Cp´] systems are strongly supported by the available experimental evidence. The redox potentials of complexes of this type are strongly influenced by the electronic nature of the Ar group which provides the first clues to the substantial role of the ligand in the redox events associated with these molecules [183, 193]. Infra-red spectroelectrochemistry has proven to be a very valuable tool through which to study these rather reactive products of oxidation [194, 195]. Oxidation causes a substantial decrease in the ν(C≡C) frequency in complexes [Ru(C≡CAr)(dppe)Cp*] (Ar = C_6H_4Me, $\Delta\nu$(C≡C) = –143 cm^{-1}; Ar = $C_{14}H_8$, $\Delta\nu$(C≡C)

= –116 cm^{-1}) [183, 193], and the observation of products derived from coupling of ligand-centered radicals in preparative scale experiments [184, 196].

As the alkynyl ligand is extended from arylacetylide derivatives to ethynyl tolan (diphenylacetylene) based ligands, a similar pattern of behaviour emerges [192]. However, while the HOMO in $[Ru(C{\equiv}CC_6H_4C{\equiv}CC_6H_4OMe)(PH_3)_2Cp]$ ($Ru:C{\equiv}CC_6H_4:C{\equiv}CC_6H_4OMe$ = 18:55:21) and β-LUSO in $[Ru(C{\equiv}CC_6H_4C{\equiv}CC_6H_4OMe)(PH_3)_2Cp]^+$ ($Ru:C{\equiv}CC_6H_4:C{\equiv}CC_6H_4OMe$ = 19:47:24) are calculated to be delocalised over the entire chain, the greatest contribution arises from the phenyl ethynyl moiety coordinated to the metal center (Figure 7). This is in complete agreement with results from IR spectroelectrochemical studies of $[Ru(C{\equiv}CC_6H_4C{\equiv}CC_6H_4OMe\text{-}4)(dppe)Cp^*]^{n+}$ (n = 0, 1), which show the initial two band ν($RuC{\equiv}C/C{\equiv}CC_6H_4OMe$) pattern 2060s/2207w cm^{-1} shifting to 1923s/2206m cm^{-1} on oxidation, and indicating the bonding in the remote ethynyl anisyl moiety to be little affected by the oxidation process save for a more substantial dipole moment along the C≡C axis.

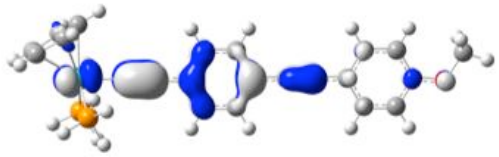

Figure 7. A plot of the HOMO in $[Ru(C{\equiv}CC_6H_4C{\equiv}CC_6H_4OMe)(PH_3)_2Cp]$, with contour values at ±0.04 $(e/bohr^3)^{1/2}$.

The UV-vis-NIR spectra of the one-electron oxidation products derived from mono-nuclear ruthenium acetylide complexes also contain features of considerable interest

to discussions concerning the electronic structure of these species. The electronic spectra of [Ru(C≡CAr)(PP)Cp′] species are usually dominated by transitions from the metal-ethynyl based HOMOs to the ligand π^* orbitals, and which tail into the visible region and are responsible for the yellow to orange colour of these complexes. These transitions may be likened in the most general terms as MLCT in character, although such descriptions lack an element of precision and do not describe the important contributions from the ethynyl ligand to the donor state. Additional ligand centred π-π* transitions can also be identified, the energy of which is, naturally, strongly dependent on the nature of the alkynyl ligand [192]. On one-electron oxidation to $[Ru(C{\equiv}CAr)(PP)Cp']^+$, these bands shift to lower energy in keeping with the largely ligand based character of the HOMO, and in addition new lower energy features can be observed in the visible spectrum, which TD DFT calculations suggest can be described in terms of transitions from occupied orbitals with substantial RuCp character to the metal-ligand based β-LUSO. At lower energy still, in the NIR region one or more very weak bands which can be likened to *d-d* transitions within an octahedral d^5 system are found, although again the substantial mixing of the metal d and alkynyl π-ligands would suggest a description in terms of a dπ/dπ transition may be more accurate (Figure 8). Similar descriptions have also been noted in closely related complexes based on the *trans*-$[Ru(C{\equiv}CR)Cl(dppe)_2]$ motif [197, 198].

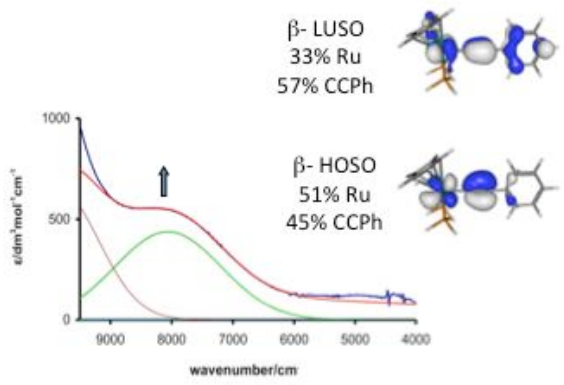

Figure 8. The NIR spectrum of $[Ru(C{\equiv}CC_6H_4Me\text{-}4)(PPh_3)_2Cp]^+$ generated in a spectroelectrochemical cell, with plots (± 0.04 $(e/bohr^3)^{1/2}$) and composition of the β-HOSO and β-LUSO.

The molybdenum alkynyl complexes $[Mo(C{\equiv}CR)(dppe)(\eta\text{-}C_7H_7)]$ popularised by Mark Whiteley offer distinctly different electronic characteristics to $[Ru(C{\equiv}CR)(PP)Cp']$ species, despite the apparent electronic and structural similarities. Whilst both are half-sandwich, d^6 systems derived from 4d metals, the molybdenum systems $[Mo(C{\equiv}CR)(dppe)(\eta\text{-}C_7H_7)]$ offer formal oxidation potentials some 600 - 400 mV less positive than the analogous complexes $[Ru(C{\equiv}CR)(dppe)Cp^*]$. Furthermore, the range of $E_{1/2}$ values offered by the Mo-based alkynyl complexes $[Mo(C{\equiv}CC_6H_4X)(dppe)(\eta\text{-}C_7H_7)]$ (X = H, NH_2, OMe, Me, CHO) (spanning a range of ca. 160 mV) is much less sensitive to the electronic character of the alkynyl substituent than in the analogous Ru-based series, $[Ru(C{\equiv}CC_6H_4X)(dppe)Cp^*]$, which vary by over 300 mV for the same substituents [183, 190, 199]. These striking differences in oxidation potential and range are mirrored in the shifts of ν(C≡C) frequency on oxidation, with the Mo based examples exhibiting much smaller shifts to lower frequency than the Ru analogues (e.g. $[Ru(C{\equiv}CC_6H_4Me)(dppe)Cp^*]^{0/+1}$ $\Delta\nu(C{\equiv}C)$ -145 cm^{-1}; $[Mo(C{\equiv}CC_6H_4Me)(dppe)(\eta\text{-}$

$C_7H_7)]^{0/+1}$ $\Delta\nu(C\equiv C)$ -33 cm^{-1}). The explanation for these differences can be traced back to the differences in electronic structures, and in particular the different metal-based frontier orbitals offered.

An examination of the frontier orbitals of the model system [Mo(C≡CC_6H_5)(dppe)(η-C_7H_7)] reveals an important stabilisation of the $d_{x^2-y^2}$ and d_{xy} orbitals by δ-interactions with the empty e_2 orbitals of the $\{C_7H_7\}^+$ ligand, whilst the d_{yz} and d_{xz} orbitals (filled in a d^6 Mo(I) electron counting system) are stabilised by π-backbonding interactions from the e_1 ligand orbitals (Figure 9). These metal-ligand interactions with the e-type orbitals of the $\{C_7H_7\}^+$ ring are more important than in the case of the isoelectronic $\{C_5H_5\}^-$ due to the lower energy of the ring orbitals as ring size increases, which especially favors the increased interactions of the metallic orbitals with the e_2 system in the case of the larger ring [200- 203]. The net consequence is that the d_{z^2} remains relatively high in energy, being somewhat destabilised by the ring a-type orbital, and contributes substantially to the molecular HOMO. The overlap of the d_{z^2} orbital, which is directed towards the C_7H_7 ring centroid under the coordinate systems that permits the strong metal-ring π- and δ-interactions, with the alkynyl ligand π-type orbitals is limited by symmetry constraints. As a result of these electronic and symmetry constraints, the redox processes associated with this system are largely confined to the change in population of d_{z^2}, a fact inferred by Phil Rieger many years ago from the consideration of the well-resolved isotropic EPR spectra of these complexes [204]. Similar electronic structure arguments apply to the analogous W complexes [W(C≡CR)(dppe)(η-C_7H_7)]$^{0/+1}$ [205], although reduction in the ring size to C_5H_5 and orbital reordering, as in [Mo(C≡CR)(CO)(dppe)Cp], leads to more alkynyl character in the frontier molecular orbitals [206].

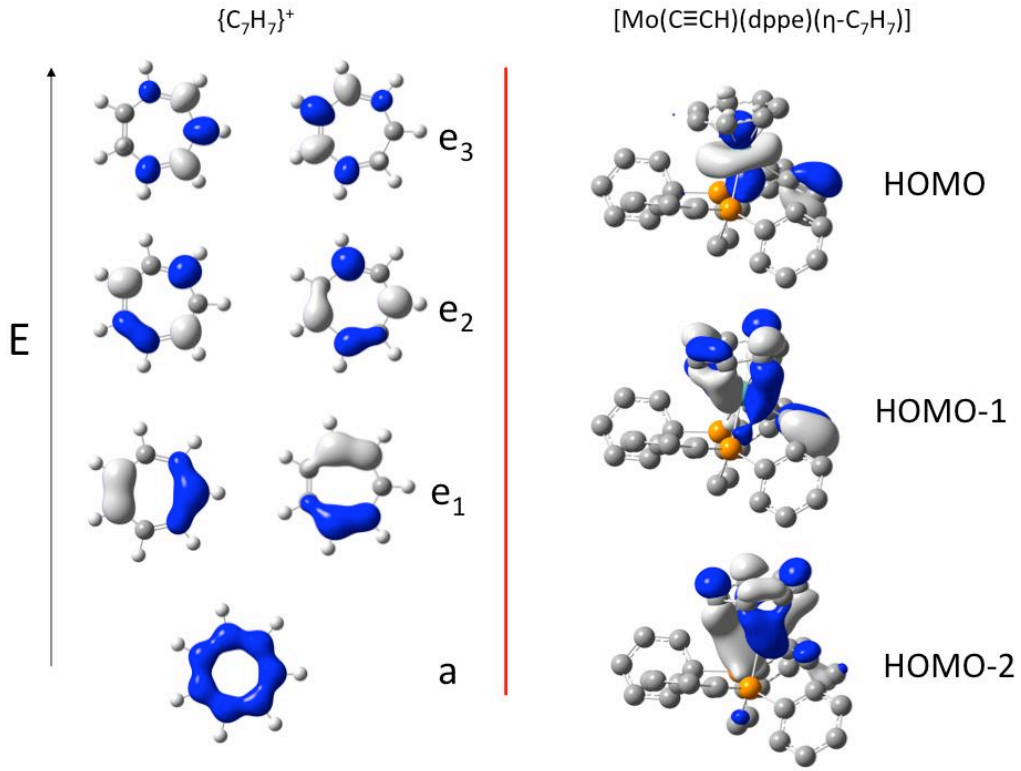

Figure 9. The key ligand orbitals from the $\{C_7H_7\}^+$ fragment (plotted with contours at ±0.06 $(e/bohr^3)^{1/2}$ for clarity), and the frontier orbitals of [Mo(C≡CH)(dppe)(η-C_7H_7)] ((±0.04 $(e/bohr^3)^{1/2}$) (adapted from a Figure by Mark Whiteley).

However, the alkynyl ligand is not entirely innocent even in the C_7H_7-alkynyl systems, as is evidenced by the observation of hyperfine coupling to substituents on the alkynyl ligand in EPR and ENDOR spectra [207] and slow formation of bis(vinylidene) dimers through C_β-C_β radical homo-coupling reactions which take place in solutions of the alkynyl [208] and diynyl [209] radicals (Scheme 6).

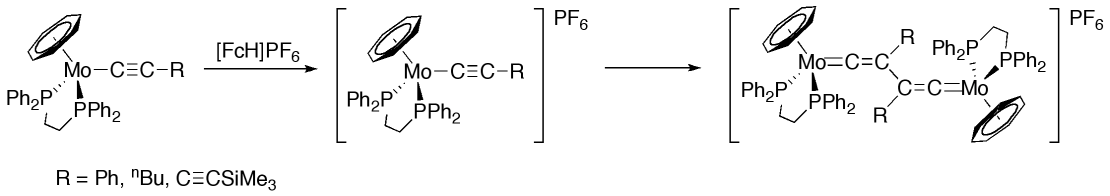

Scheme 6. The oxidative coupling of $[Mo(C{\equiv}CR)(dppe)(\eta\text{-}C_7H_7)]^+$ radicals [208, 209].

The contrasting electronic characteristics, but similar structural features of metal alkynyl complexes based on $[Ru(C{\equiv}CR)(PP)Cp']$ and $[Mo(C{\equiv}CR)(dppe)(\eta\text{-}C_7H_7)]$, have provided the opportunity to compare and contrast the electron structure of bimetallic complexes $\{(\eta\text{-}C_yR_y)(PP)M\}(\mu\text{-}C{\equiv}CXC{\equiv}C)\{M(PP)(\eta\text{-}C_yR_y\}]^{n+}$ (n = 0, 1, 2; M = Ru; PP = $(PPh_3)_2$, dppe; $\eta\text{-}C_yR_y$ = Cp, Cp*; M = Mo; PP = dppe; $\eta\text{-}C_yR_y$ = $\eta\text{-}C_7H_7$) as a function of both the metal auxiliary and the diethynyl ligand C≡CXC≡C. Depending on the nature of both, the monocation radicals with n = 1 can either be described in terms of metal-based mixed-valency, or as metal-stablised ligand radicals, as described below.

5. Deceptively simple: All-carbon bridges

The chemistry and electron transfer characteristics of all-carbon bridged systems $[\{L_nM\}\{\mu\text{-}(C{\equiv}C)_n\}ML_n]^{n+}$ have been reviewed on several previous occasions [187, 210-213] so only a brief summary is presented here. The C_2 moiety represents the most elementary carbon-based bridging ligand beyond carbide complexes [214, 215], and has a close structural and electronic relationship with the ubiquitous, but still fascinating, conjugated bridging ligand, cyanide [216, 217]. Despite the large number of complexes with μ-CN ligands and the substantial number of studies of the redox chemistry and CN mediated charge transfer processes within these systems, it is only

relatively recently that the redox chemistry, electronic structure and intramolecular charge transfer properties of μ-C_2 complexes have been explored [218]. Homo and hetero bimetallic Group 8 complexes featuring a μ-η^1,η^1-C_2 ligand have been prepared by double deprotonation of [M(C=CH_2)(dppe)Cp′]PF_6 (3) and subsequent reactions with [M′(thf)(dppe)Cp′] [172]. The C_2 compounds [{Cp′(dppe)M}(μ-C≡C){M′(dppe)Cp′}] (4) were readily protonated to give the analogous μ-C_2H complexes. However, treatment with one or two equivalents of [FcH]PF_6 decreased the electron density in the C_2 fragment to give more readily handled mono and di-cations $[4]^+$, $[4]^{2+}$ as their PF_6^- salts (Scheme 7).

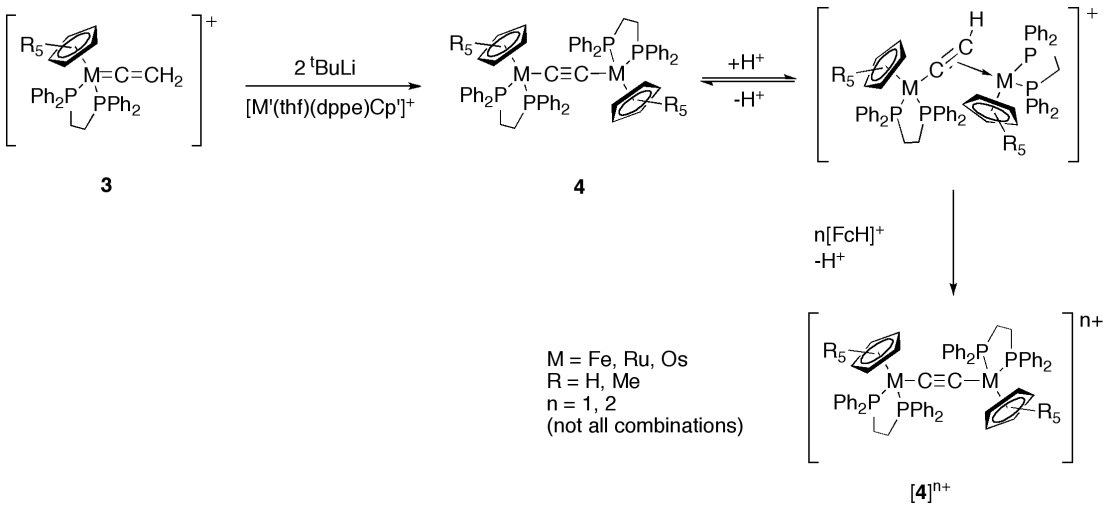

Scheme 7. The preparation of bimetallic complexes [{L_nM}(μ-C≡C)ML_n]$^{n+}$ [172].

Longer chain examples with C_4, C_6 and C_8 ligands [{Ru(PP)Cp′}$_2${μ-$(C≡C)_m$}] were readily prepared from KF mediated metalladesilylation reactions between $RuCl(PPh_3)_2Cp$ and $Me_3Si(C≡C)_mSiMe_3$ (m = 2, 3, 4) [143, 219]. Complexes containing C_4 chains with more electron-donating supporting ligands were obtained from oxidative dimerisation and deprotonation of Ru(C≡CH)(dppx)Cp* (dppx =

dppm, dppe) [220], Fe(C≡CH)(dppe)Cp* [221], Os(C≡CH)(dppe)Cp* [222] and [Mo(C≡CH)(dppe)(η-C_7H_7)] [51] which convincingly illustrates the radical character of the alkynyl ligand in the 17-e^- intermediates $[M(C{\equiv}CH)L_n]^+$ [223]. Oxidative dimersation of Ru(C≡CC≡CLi)(dppe)Cp* in the presence of [{$CuCl(PPh_3)$}$_4$] gives the electron-rich C_8 complex in excellent (85%) yield [175]. The μ-C_{14} complex [{Ru(dppe)Cp*}$_2${μ-C≡C)$_7$}] was assembled in a remarkably efficient variant of the Cadiot-Chodkiewicz coupling, from reaction of [Ru{$(C{\equiv}C)_2Au(PPh_3)$}(dppe)Cp*] with $I(C{\equiv}C)_3I$ in the presence of a mixed Pd(0)/Cu(I) catalyst [224].

This library of complexes has allowed an examination of the effects of both chain extension and metal substitution in all-carbon ligand bridged bimetallic complexes. In the case of the homo-bimetallic ruthenium series [{Ru(PP)Cp′}$_2${μ-$(C{\equiv}C)_m$}] the HOMOs are derived from the out-of-phase combination of metal (approximately d_{xz} and d_{yz}) with the C_n π-system (Figure 10) [189, 225-227]. These orbitals are delocalised over the M-C_n-M chain and well separated from the other frontier orbitals, and are π anti-bonding in character with respect to the M-C_α and C_β-C_γ, C_δ-C_ε etc bonds, and bonding between C_α-C_β, C_γ-C_δ, etc. The carbon content of these frontier orbitals increases with increasing chain length in the case of the ruthenium series, and other examples featuring the heavier, late transition metal elements [228].

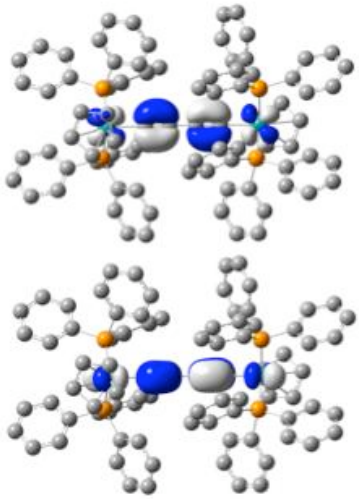

Figure 10. The HOMO and HOMO–1 calculated for [{Ru(PPh_3)$_2$Cp}$_2$(μ-C≡CC≡C)] (5) illustrating the nodal pattern, with contours at ±0.04 (e/bohr^3)$^{1/2}$.

Oxidation of these complexes can be well described in terms of the sequential depopulation of these frontier orbitals, which results in a gradual evolution of cumulenic and subsequently carbynic character in the carbon-based bridging ligand (Scheme 8), a point firmly established from both computational studies, IR spectroscopic investigations carried out on the various members of the [{Ru(PP)Cp´}$_2${μ-(CC)$_m$}]$^{n+}$ redox series [226], and supported by crystallographic structure determination [220].

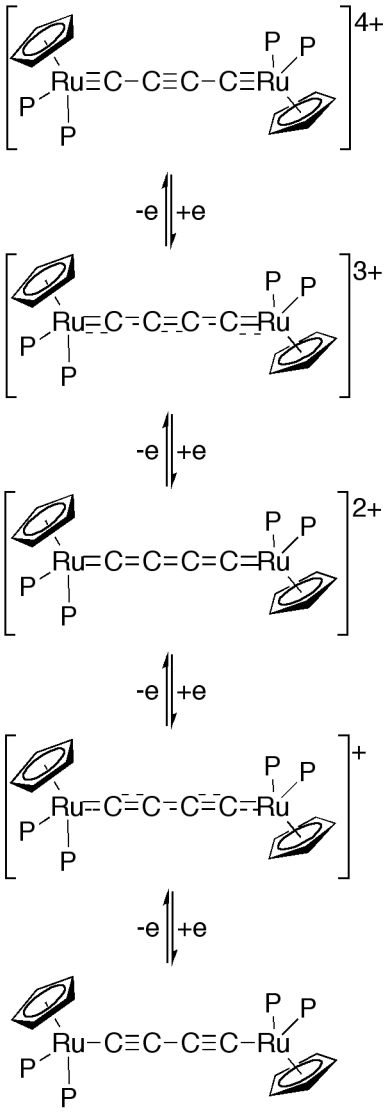

Scheme 8. The evolution of valence bond descriptions in the redox series $[\{Ru(PP)Cp'\}_2(\mu\text{-}C_4)]^{n+}$ (e.g. $[5]^{n+}$) (n = 0 - 4) [226].

In keeping with these simple valence bond representations, and the nature of the π-bond order revealed in the computational work, the neutral systems offer a relatively flat potential energy surface with regards to the relative orientation of the Ru(PP)Cp′ fragments. The *transoid* conformer is only slightly energetically favoured, and structural examples and polymorphs of $[\{Ru(PP)Cp'\}_2(\mu\text{-}C{\equiv}CC{\equiv}C)]$ based systems

illustrating Cp(0)-Ru…Ru'-Cp'(0) angles from –28.2° (*cisoid*) to 180° (*transoid*) have been crystallographically characterised (Cp(0) is the centroid of the Cp ring) [229]. Larger barriers to rotation are brought about by steric interactions between the supporting ligands in the C_2 series and by oxidation, which increases the Ru-C bond order [172]. In keeping with these electronic structure descriptions, the low energy NIR transitions observed in $[\{Ru(PP)Cp'\}_2\{\mu\text{-}(CC)_m\}]^+$ systems have considerable Ru(d)→[Ru(d)/C(π)]* (ca. MLCT) character. Similar descriptions apply for the low energy transitions in $[\{Os(dppe)Cp^*\}_2(\mu\text{-}C_4)]^+$ [221], but the higher energy of the iron d orbitals leads to more Fe(III)/Fe(II) mixed valence (Class III) character in the case of $[\{Fe(dppe)Cp^*\}_2(\mu\text{-}C_4)]^+$ [230]. Similarly, the greater metallic character also leads to a greater stabilisation of the triplet (HS) dicationic state in the dicationic systems $[\{M(PP)Cp'\}_2\{\mu\text{-}(C\equiv C)_m\}]^{2+}$ derived from iron, and in the shorter (m = 1) examples from the ruthenium series [172].

The difference in the electronic characteristics of Fe(C≡CR)(dppe)Cp* (more metallic character in the frontier orbitals) and Ru(C≡CR)(dppe)Cp* (more alkynyl character in the frontier orbitals) creates interest in the heterobimetallic complexes $[\{Cp^*(dppe)Fe\}(\mu\text{-}C\equiv CC\equiv C)\{Ru(PP)Cp'\}]^{n+}$ [n = 0, 1, 2; Ru(PP)Cp' = $Ru(PPh_3)_2Cp$ (**6**), Ru(dppe)Cp* (**7**)] [231]. The target complexes **6** and **7** were prepared in 70 – 80% yield from reaction of [FeCl(dppe)Cp*] with [Ru(C≡CC≡CH)(PP)Cp'] in the presence of a strong base (DBU) to facilitate deprotonation of the intermediate vinylidene (Scheme 9). Each half-sandwich Group 8 fragment offers frontier fragment orbitals of the same symmetry, and the nodal properties of the HOMO and HOMO–1 are similar to those of the homo-bimetallic analogues. These orbitals, whilst delocalised over the FeC≡CC≡CRu chain, are polarised towards the Fe centre with

calculated Hirschfeld charges on Fe and Ru in the model [{Cp(dHpe)Fe}(μ-C_4){Ru(dHpe)Cp}] –0.06 and +0.22, respectively and a calculated dipole moment of 1.05 D ($Fe^{\delta-}$←$Ru^{\delta+}$) (% composition Fe/C_α/C_β/$C_{\beta'}$/$C_{\alpha'}$/Ru: HOMO 18/17/11/11/18/12; HOMO–1 15/21/12/12/22/9). This polarisation is maintained on oxidation and whilst the total spin density is partitioned more or less equally over the metal centres and the C_4 chain in the mono-cation [{Cp(dHpe)Fe}(μ-C_4){Ru(dHpe)Cp}]$^+$ (M_2/C_4: 0.456/0.515) and the triplet dication [{Cp(dHpe)Fe}(μ-C_4){Ru(dHpe)Cp}]$^{2+}$ (M_2/C_4: 0.971/1.005). The contribution from the metals is greater on the Fe centre in both cases (Fe/Ru: monocation 0.290/0.166; triplet dication 0.602/0.369).

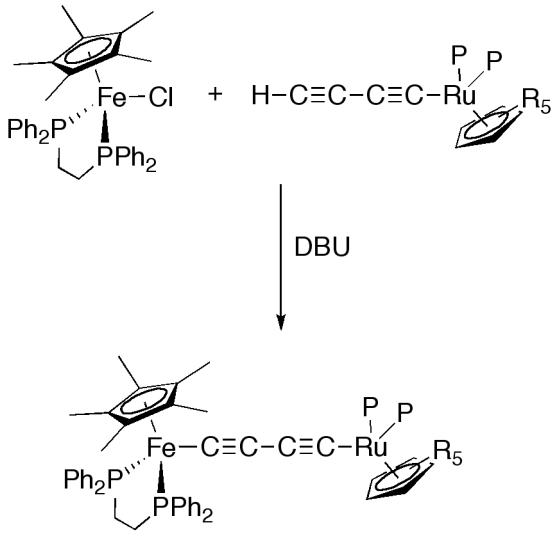

Ru(PP)Cp' = $Ru(PPh_3)_2Cp$ (**6**); Ru(dppe)Cp* (**7**)

Scheme 9. The preparation of [{Cp*(dppe)Fe}(μ-C≡CC≡C){Ru(PP)Cp′] 6 and 7 [231].

The IR, ^{57}Fe Mössbauer and ESR spectra of [{Cp*(dppe)Fe}(μ-C≡CC≡C){Ru(PP)Cp′}]$^{n+}$ (n = 1, 2) are consistent with this description in terms of

polarised electronic structure without complete evolution to an iron-localised oxidation giving rise to an Fe(III) centre. The IR spectra of the neutral complex feature a single (broad) ν(C≡C) band near 1965 cm^{-1}, which evolves to a two band ν(CC) pattern at progressively lower frequency in the mono and dications formed on oxidation. This is consistent with the increased polarisation along the Fe-C_4-Ru axis predicted from the computational results, whilst the evolution of the ν(CC) bands to lower frequencies indicates the involvement of the C_4 chain the redox event. In addition, the QS parameter of $[7]^{2+}$ is smaller at 273 K (1.069 mm s^{-1}) than at 80 K (1.113 mm s^{-1}) consistent with the thermal population of the higher energy triplet state at room temperature. There is no further change in the QS from 80 - 4 K, suggesting that the limiting triplet is reached at ca. 80 K in the solid state. Paramagnetic NMR studies suggest that the singlet / triplet energy gaps for $[\{Cp^*(dppe)Fe\}(\mu\text{-}C{\equiv}CC{\equiv}C)\{Ru(PP)Cp'\}]^{2+}$ ($Ru(PPh_3)_2Cp$ 350 cm^{-1}; Ru(dppe)Cp* 500 cm^{-1}) lie between the values obtained for the homo-bimetallic Fe (18 cm^{-1}) and Ru complexes (830 cm^{-1}). Whilst the singlet is lower in energy in all cases, the lowering of the gap with increasing spin density on metal centres, which is consequent of the substitution of Ru for Fe, increases the proportion of the thermally populated triplet state at ambient temperature.

Against this backdrop of a polarised electronic structure, the lowest energy, unique electronic transitions in $[\{Cp^*(dppe)Fe\}(\mu\text{-}C{\equiv}CC{\equiv}C)\{Ru(PP)Cp'\}]^{+}$ are assigned to $Ru \rightarrow Fe^{+}$ charge transfer processes, which are masked to some extent by a much more intense pseudo-LMCT transition (Figure 11). Assuming symmetrical band shape, an electron transfer distance approximated by the physical metal-metal separation and the weak coupling limit, the two state model gives a metal-metal coupling term of 230

($Ru(PPh_3)_2Cp$) to 310 (Ru(dppe)Cp*) cm^{-1}. Whilst these values are larger than for related Fe/Re mixed metal systems [232], the approximations inherent in the analysis, and their physical accuracy given the delocalised, albeit polarised, nature of the donor and acceptor orbitals must be borne in mind.

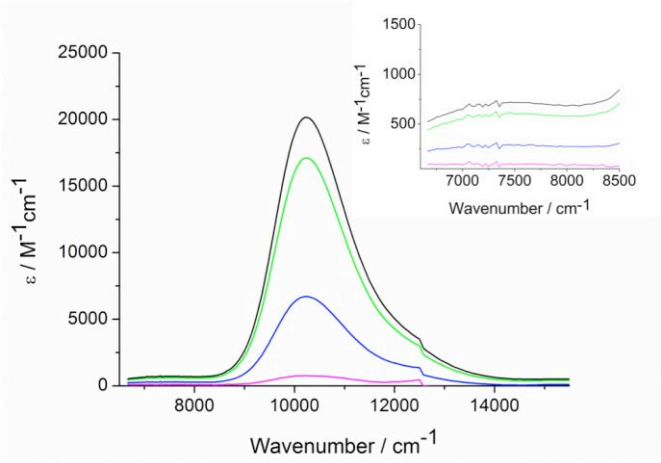

Figure 11. The unique low energy LMCT (10300 cm^{-1}) and IVCT (7300 cm^{-1}) transitions observed following spectroelectrochemical generation of $[6]^+$. The inset shows an expansion of the IVCT band.

Guided by these concepts, and given the more heavily metal localised frontier orbitals of the {Mo(C≡CR)dppe)(η-C_7H_7)} moiety, [{Mo(dppe)(η-C_7H_7)}$_2$(μ-C≡CC≡C)] (8) was an attractive target with a view to the preparation of a 'genuine' mixed-valence organometallic complex based on an all-carbon bridging ligand [51]. The complex 8 was obtained and isolated following oxidative coupling of two [Mo(C≡CH)(dppe)(η-C_7H_7)] complexes ([FcH]PF_6) to give the bis(vinylidene), and deprotonation ($KOBu^t$). However, prompt aerial oxidation took place, which provided a rather convenient entry point to [{Mo(dppe)(η-C_7H_7)}$_2$(μ-C≡CC≡C)]PF_6, $[8]PF_6$. Further oxidation with [FcH]PF_6 gave $[8][PF_6]_2$, which was crystallographically characterised (Scheme 10).

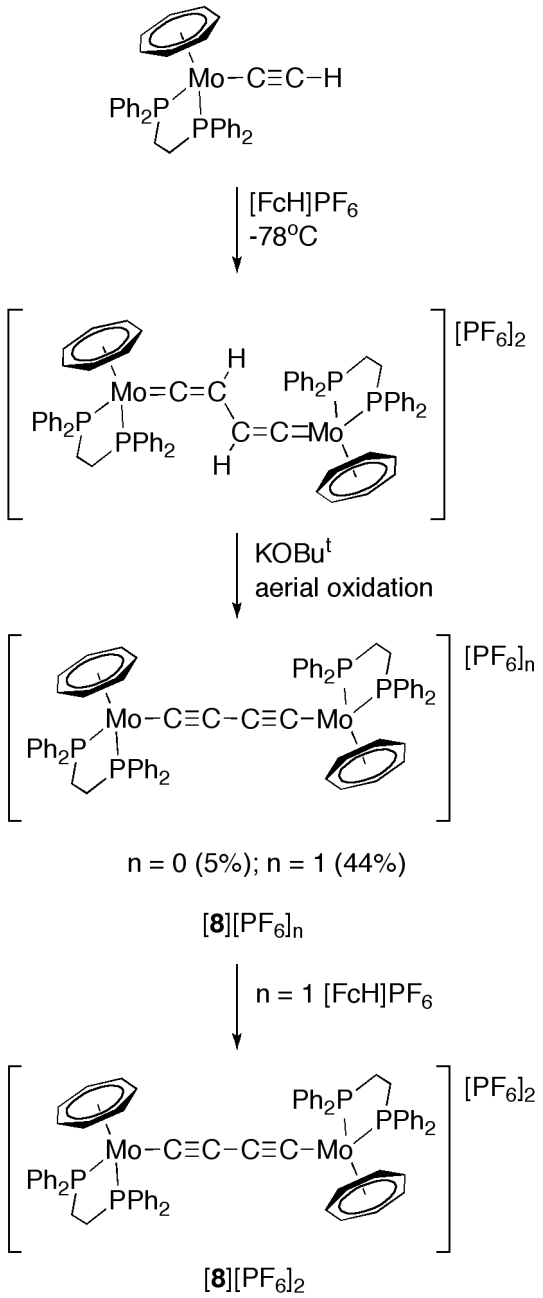

Scheme 10. The preparation of $[\{Mo(dppe)(\eta\text{-}C_7H_7)\}_2(\mu\text{-}C{\equiv}CC{\equiv}C)][PF_6]_n$ (n = 0, 1, 2)

The C_4 ligand in $[\{Mo(dppe)(\eta\text{-}C_7H_7)\}_2(\mu\text{-}C{\equiv}CC{\equiv}C)][PF_6]_2$, $[8][PF_6]_2$, exhibits significant alternating C≡C / C-C character, which contrasts the more cumulenic

character noted in both $[\{Ru(dppe)Cp^*\}_2(\mu\text{-}C_4)]^{2+}$ [220] and $[\{Re(PPh_3)(NO)Cp^*\}_2(\mu\text{-}C_4)]^{2+}$ [232b] and provides the first indications of the greater metallic character in the redox processes associated with the parent. The neutral system was IR silent in the ν(C≡C) region, but a Raman band was observed at 1939 cm^{-1}, both results indicating a largely symmetrical structure. The monocation exhibited a two band pattern with ν(CC) bands at 1930, 1868 cm^{-1}, the relative intensity of which did not change with solvent polarity or in the solid state. Thus, whilst different conformers of $[\{ML_n\}_2(\mu\text{-}C_4)]^{n+}$ are known to exhibit different ν(CC) bands (vide supra), in this case these IR features are also consistent with a valence localised (on the IR time scale) mixed-valence description of [8]PF_6, a point also consistent with NIR and ESR spectra. The Raman spectrum of the IR silent dication contains two bands, but given that these are enhanced to different extent using different excitation wavelengths, it would appear that the isolated sample contains two chemically distinct forms or species.

Turning attention to the electronic spectrum of the mono-cation $[8]^+$, two band envelopes were observed near 8650 cm^{-1} (apparent ε 8300 M^{-1} cm^{-1}) and 4020 cm^{-1} (apparent ε 2900 M^{-1} cm^{-1}), the latter tailing into the IR region. These band envelopes were deconvoluted into four Gaussian sub-bands, three of which were weak in intensity and exhibited a strong solvatochromic dependence (Figure 12). These sub-bands were therefore assigned to the three possible IVCT transitions in a mixed valence d^5/d^6 system based on pseudo-octahedral metal fragments. The less solvatochromic, much narrower and more intense component was assigned to an LMCT transition. Although the IVCT components were narrower than predicted from the Hush model, the involvement of the bridging ligand in the charge transfer process

is known to lead to narrowing of the IVCT band shape [48, 49]. The observation of both LMCT and IVCT components is a characteristic of the three-state model for weakly interacting mixed valence complexes, and points to a key role of the C_4 ligand in mediating the charge transfer process in this case.

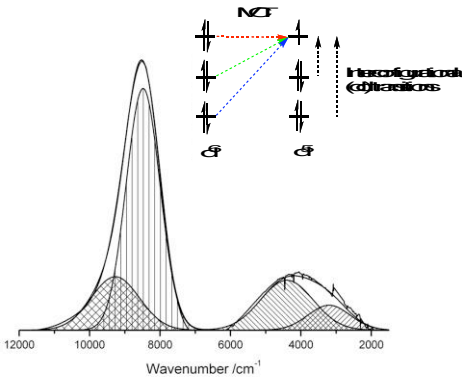

Figure 12. The NIR-IR spectrum of [{Mo(dppe)(η-C_7H_7)}$_2$(μ-C≡CC≡C)]PF_6 ([8]PF_6) in CH_2Cl_2, with deconvolution into IVCT and LMCT components [51]. The inset illustrates the metal-based transitions associated with a d^6/d^5 mixed valence complex derived from pseudo octahedral fragments [256].

Considerable insight can be gained into the dynamics of the electron transfer process by considering data from spectroscopic techniques that operate across a range of timescales [233]. Whilst the IR and NIR spectra are consistent with a localised mixed valence structure for $[8]^+$, no hyperfine data could be resolved from X-, S- or Q-band EPR spectra, despite the normally well-resolved EPR signatures of [MoX(dppe)(η-C_7H_7)]$^+$ radical arising from the largely isotropic distribution of spin in the d_{z^2} orbital. Rather, the EPR data are consistent with electron-exchange processes on the same time-scale as the measurement (10^8-10^{10} s^{-1}). Similar phenomena have been observed

for the slow electron exchange processes in $[\{WI(dppe)_2\}_2(\mu\text{-}C_4)]^+$ [234]. The dication $[\{Mo(dppe)(\eta\text{-}C_7H_7)\}_2(\mu\text{-}C{\equiv}CC{\equiv}C)]^{2+}$, $[\mathbf{8}]^{2+}$, was further examined by both EPR and magnetic susceptibility measurements, which revealed a strongly antiferromagnetically coupled ground state, with a thermally accessible triplet lying some 406 cm^{-1} higher in energy.

Electronic structure calculations on the model system $[\{Mo(dHpe)(\eta\text{-}C_7H_7)\}_2(\mu\text{-}C{\equiv}CC{\equiv}C)]$ (**8-H**) further illustrate the differences with the metal fragment orbitals offered by the Mo(PP)(η-C_7H_7) and M(PP)Cp based systems. The HOMO and HOMO–1 of **8-H** are comprised of both Mo (41%) and C_4 (40-41%) character, but in contrast to the Group 8 Cp derivatives, the Mo contribution arises not from a $d\pi$-orbital, but from d_{z^2} (Figure 13). Although attempts to construct computational models of the open shell (d^6/d^5) systems were not successful, the less efficient overlap between the metal d_{z^2} and carbon based π-orbitals evidenced in the closed shell (d^6/d^6) is likely the origin of the unique localised mixed valence character of the Mo system, which is in contrast to the more extensively delocalised (M = Fe) or heavily ligand based redox character (M = Ru) in $[\{M(PP)Cp'\}_2(\mu\text{-}C_4)]^+$ systems.

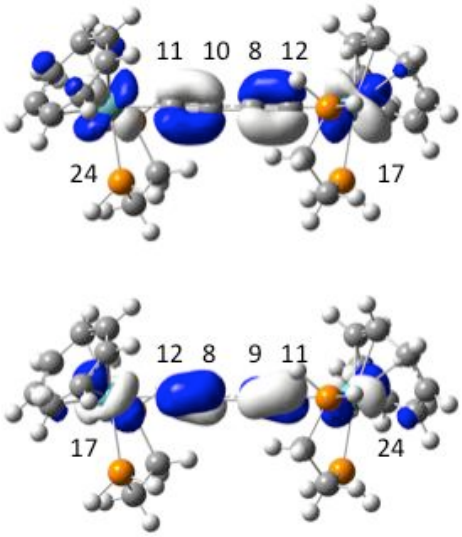

Figure 13. The HOMO (top) and HOMO–1 (bottom) from 8-H with contours at ±0.04 (e/bohr^3)$^{1/2}$, showing the % composition with respect to the Mo/C_α/C_β/$_\beta$′/C_α′/Mo′ chain.

6. Exploring the antipodes: Transmission of electronic effects through diethynylcarborane based bridging ligands.

Turning attention to further examples of systems in which mixed-valence descriptions are most appropriate, complexes featuring diethynyl para-carborane ligands provide a convenient point for discussion. The ethynyl moieties offer linear geometry, cylindrical symmetry and π-frontier orbitals of good symmetry match at least in the case of the Ru examples described above. The para-carboranyl moieties offer high symmetry along the C…C axis, excellent thermal and chemical stability and unusual 'three dimensional' aromatic character [235-237], the latter aspect of which has piqued curiosity in these cluster systems as a potential conduit for electronic effects across the cage [238-245]. The development of convenient synthetic routes to the bis(ethynyl)-*para*-carboranes 1,12-($Me_3SiC{\equiv}C)_2$-1,12-$C_2B_{10}H_{10}$ and 1,10-

$(Me_3SiC{\equiv}C)_2$-1,10-$C_2B_8H_8$ [246] has made these compounds available for use in the preparation of diethynylcarborane bridged bi- [247, 248] and polymetallic [244, 245] complexes (Scheme 11).

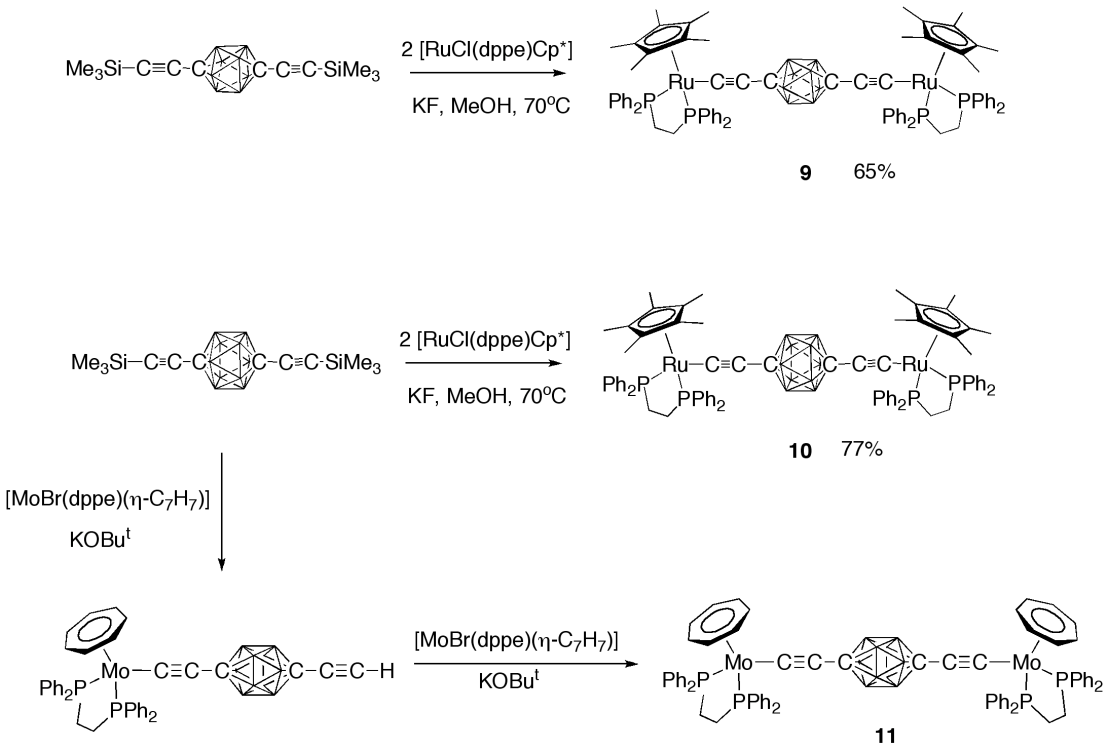

Scheme 11. The preparation of diethynyl carboranediyl bridged complexes 9, 10 [247] and 11 [249].

The compounds [{Ru(dppe)Cp*}$_2$(μ-1,10-C≡C-1,10-C_2B_8)] (9), [{Ru(dppe)Cp*}$_2$(μ-1,12-C≡C-1,12-C_2B_{10})] (10) [247] and [{Mo(dppe)(η-C_7H_7)}$_2$(μ-1,12-C≡C-1,12-C_2B_{10})] (11) [249] each undergo two sequential one-electron oxidation processes (9: 0.27, 0.39 V; 10: 0.32, 0.41 V; 11: -0.71, -0.63 V). The small difference in these oxidation potentials allows the comproportionation constant, K_C, to be calculated and gives a measure of the thermodynamic stability of the one-electron oxidation product with respect to disproportionation, but does not give direct information concerning

electronic structure. As discussed elsewhere [249-251], the stability of the intermediate charge state is dependent on a number of factors including inner and outer sphere reorganisation energies, differences in spin orbit coupling and ligand field effects associated with the different metal oxidation states in the case of metal-based redox processes, ion-pairing, Coulomb effects and so on, in addition to any contribution arising from 'delocalisation' of the charge within the molecular framework. The contribution of the terms other than the delocalisation energy can be significant, a point convincingly illustrated in a series of useful papers by the Geiger group, who have shown that even in the absence of strong intermolecular coupling, the separation of redox potentials in a molecule containing multiple redox sites can be tuned over a substantial range simply by the influence of ion-pairing effects [252-254]. In the present cases, the separation between the redox processes was only slightly dependent on the nature of the electrolyte anion, suggesting a more detailed examination of the electronic situation was warranted.

IR spectroelectrochemistry is a powerful tool for the investigation of structural change as a function of redox state [194, 195] on a relatively fast time scale [255]. The compounds **9**, **10** and **11** offer ν(C≡C) and ν(BH) bands that are convenient reporting groups through which to probe the effects of oxidation on the complexes, which together with comparative studies of mononuclear model systems allows the site of redox activity to be determined. On one-electron oxidation to $[\mathbf{9}]^{+}$ and $[\mathbf{10}]^{+}$, the ν(B-H) bands in **9** and **10** shifted ≤+10 cm^{-1} whilst the ν(C≡C) band near 2080 cm^{-1} was replaced by two relatively strong bands at 2065, 1990 cm^{-1} (**9**) / 2074, 2002 (**10**) cm^{-1}, which were superimposed in the tail of an electronic transition (vide infra). Further oxidation to $[\mathbf{9}]^{2+}$ and $[\mathbf{10}]^{2+}$ resulted in a collapse of the electronic transition, a

further small (≤+10 cm^{-1}) shift of the ν(B-H) bands and the appearance of a single, weak ν(C≡C) band ($[9]^{2+}$ 2006; $[10]^{2+}$ 2012 cm^{-1}) which compare with the analogous ν(C≡C) bands in the mononuclear systems [Ru(C≡C-1,10-$C_2B_8H_9$)(dppe)Cp*]$^+$ ($[12]^+$, 2006) and [Ru(C≡C-1,10-$C_2B_{10}H_{11}$)(dppe)Cp*]$^+$ ($[13]^+$, 2012 cm^{-1}). The substantial shift in the ν(C≡C) bands on oxidation indicates the ethynyl moiety is significantly involved in the redox processes, and the bridging carborandiyl moiety is much less involved.

These simple IR experiments are consistent with a description in terms of a localised electronic structure in which ground-state electron transfer is slow on the IR time scale (ca. 10^{-13} s). The low energy electronic transitions in $[9]^+$ and $[10]^+$ can each be deconvoluted into a sum of two Gaussian shaped components, arising from the dπ/dπ transitions noted above as being associated with 17-e^- [Ru(C≡CR)(PP)Cp′]$^+$ species, and an additional, more intense RuC≡C→[C≡CRu]$^+$ charge transfer transition. Whilst the dπ/dπ component is persistent upon oxidation to $[9]^{2+}$ and $[10]^{2+}$, the more intense component collapses, in keeping with the charge transfer (IVCT-like) assignment (Figure 14).

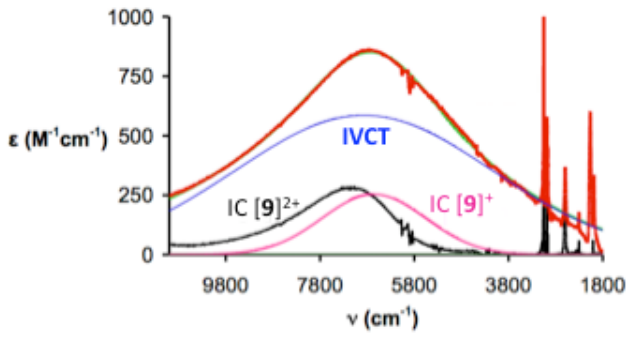

Figure 14. The NIR spectrum of $[9]^{+}$ showing deconvolution into a sum of IVCT and interconfigurational (IC) (or *d-d*) components, together with the spectrum of $[9]^{2+}$ illustrating the collapse of the IVCT component.

Although it is difficult to estimate the electron transfer distance in these systems given the involvement of the C≡C moieties in the redox active orbitals, it is helpful for comparison purposes to calculate the electronic coupling parameter H_{AB} using the relationships derived by Hush for two-state mixed valence systems. The half-height band width, $\Delta\nu_{1/2}$, of the 'IVCT' band obtained by deconvolution is somewhat broader than that predicted by the Hush model, but broadening of absorption bands in solution is not unexpected. Using the Ru…Ru separation as an upper estimate of the electron transfer distance, lower estimates of the coupling constants of 260 cm^{-1} ($[9]^{+}$) and 140 cm^{-1} ($[10]^{+}$) are obtained.

The Molybdenum complex 11 offers further opportunities to explore the behaviour of an organometallic 'mixed valence' system in which strongly metal localised redox character can be anticipated (vide supra) [248]. Good evidence for the metal localised nature of the redox processes $[11] \rightarrow [11]^{+} \rightarrow [11]^{2+}$ is found in the IR data, with the frequencies of the ligand based reporter groups ν(B-H) and ν(C≡C) remaining essentially unchanged by the progressive oxidation of the complex. The progress of the redox cycle was best monitored by the growth and decay of the low energy tail electronic transition. Well resolved EPR spectra are a feature of 17-e^{-} complexes [MoX(dppe)(η-C_7H_7)] complexes, and EPR analysis of $[11]^{n+}$ (n = 1, 2) together with reference spectra from the analogous mononuclear system [Mo(C≡C-1,12-C-$_2B_{10}H_{11}$)(dppe)(η-C_7H_7)]$^{+}$ ($[14]^{+}$) further support the description of the redox

chemistry in terms of metal centered processes. Thus, the EPR spectrum of $[\mathbf{11}]^+$ (from the PF_6^- salt) was essentially identical with that of $[\mathbf{14}]^+$, consistent with a description of $[\mathbf{11}]^+$ in terms of a localised d^5/d^6 mixed valence complex with thermal electron exchange slow on the EPR timescale. Further oxidation to $[\mathbf{11}]^{2+}$ was apparent by a small change in the isotropic g value, but no significant change in the hyperfine couplings. The dication therefore fits to a model in terms of two largely independent spin centers tethered by, but not strongly interacting through, the diethynyl carborane ligand. This illustrates a useful contrast with the C_4 bridged analogue discussed above; whilst the three-state model is most effective in the case of the C_4 bridged example, here the absence of a LMCT transition and the excellent fit of the NIR band shape to the Hush relationships indicate that the two-state model is more appropriate. The well-resolved EPR spectra in the case of the carboranyl derivative are indicative of slower electron-transfer in the absence of the additional bridge contribution to the charge transfer mechanism.

Compound $[\mathbf{11}]^+$ provides an excellent opportunity to explore the electron transfer characteristics of an organometallic 'mixed-valence' complex, free of complications arising from spin orbit coupling, strong metal-metal coupling, fast electron transfer, and mixing of the bridge- and metal-based states. The spectra of $[\mathbf{11}]^+$ and $[\mathbf{11}]^{2+}$ both feature LMCT type bands at energies greater than 20,000 cm^{-1}, similar to those observed for related arylacetylide complexes, but in the case of $[\mathbf{11}]^{2+}$ the much lower energy *d-d* type transitions were not resolved on the instrument used at the time. The NIR spectrum of $[\mathbf{11}]^+$ features a unique band envelope which can be deconvoluted into a sum of three IVCT and two *d-d* components (Figure 15).

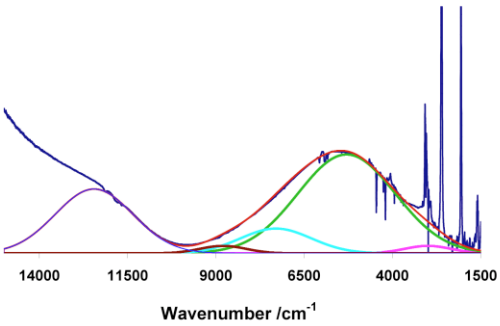

Figure 15 The NIR spectrum of $[11]^+$, showing deconvolution into two low intensity *d-d* bands and three IVCT components.

The observation of multiple IVCT and *d-d* bands in the spectra of mixed-valence complexes is not unknown, but more commonly observed in complexes of the heavier metal complexes in which spin orbit coupling effects are more significant [256, 257] and in systems in which the metal centers are found in a highly asymmetric ligand field [258, 259]. The relationships between these five transitions are summarized in terms of the simple *d*-orbital representation shown in the inset to Figure 12 and, if one neglects the reorganisation energy associated with the interconfigurational transitions, by the expressions (1) - (3), where λ is the reorganisation energy associated with the metal-to-metal charge transfer [257].

(1) $E_{IT(1)} = \lambda$

(2) $E_{IT(2)} \approx \lambda + E_{IC(1)}$

(3) $E_{IT(3)} \approx \lambda + E_{IC(2)}$

In the present case, analysis of the three IVCT transitions reveals different reorganisation energies, suggesting that the three intervalence transitions involve orbitals that are coupled to the ancillary ligands in substantively different fashion. Such suggestions are in agreement with the descriptions of the electronic structure of the mono-metallic alkynyl complexes [199]. The band-shape of the lowest energy IVCT transition fits extremely well to the Hush relationship $(\Delta\nu_{1/2})^2 = 16k_B T\lambda \ln 2$ [$(\Delta\nu_{1/2}(\text{calc}) = 3500\ \text{cm}^{-1}$; $\Delta\nu_{1/2}(\text{obs}) = 3200\ \text{cm}^{-1}$]. Assuming that the two-state model is appropriate for this transition, the intramolecular electron transfer rate k_{ET} can be calculated from the relationships :

$$\Delta G^*_{th} = (1 - 2H_{AB})^2/4\lambda$$

$$k_{ET} = \kappa\nu_n \exp(-\Delta G^*_{th}/RT)$$

assuming adiabatic electron transfer ($\kappa = 1$) and the nuclear frequency factor, ν_n, to be similar to the rate of bond vibrations (ca. $10^{12}\ s^{-1}$). The upper limit of k_{ET} is estimated to be $2.8 \times 10^9\ s^{-1}$. Since the rate of electron transfer is slow on the EPR timescale (ca. $10^9\ s^{-1}$) this upper estimate is reasonable. The other IT bands are considerably narrower than the Hush relationships would indicate, and likely a consequence of the greater mixing of the lower lying *d* orbitals with the ethynyl π-system of the bridging ligand.

Modelling charge transfer processes by DFT methods is beset by a large number of difficulties that arise from inaccuracies in the treatment of electron-hole correlation in the charge-separated state [260, 261], and computationally expeditious, but physically

unrealistic, neglect of environmental factors [262]. A work-around has been to employ functionals with a high amount of exact exchange [247, 248], although in more recent times considerable attention has been directed towards functionals with local gradient exchange terms [263, 264]. Nevertheless, TD DFT calculations using Hartree-Fock rich functionals have given models of $[9\text{-H}]^+$, $[10\text{-H}]^+$ and $[11\text{-H}]^+$ (in which the phosphine ligands present in the experimental systems have been replaced by simpler PH_3 and dHpe models) which qualitatively reproduce the observed spectroscopic features. The electronic structure calculations indicate that the carborane cage based orbitals reside much lower in energy than the metal / ethynyl d / π orbitals, and so contribute little to the frontier orbital character. The unoccupied cluster orbitals are also well removed from the frontier region, the consequence being that the cluster participates little to electronic transitions (MLCT / LMCT) in the visible - NIR region. In the case of $[9\text{-H}]^+$ and $[10\text{-H}]^+$ two transitions of moderate oscillator strength (intensity) are calculated with IVCT and IC character. Whilst in the case of $[11\text{-H}]^+$ accurate TD DFT results were not obtained, the electronic structure contains MOs of the appropriate character that could give rise to the five transitions (Figure 16).

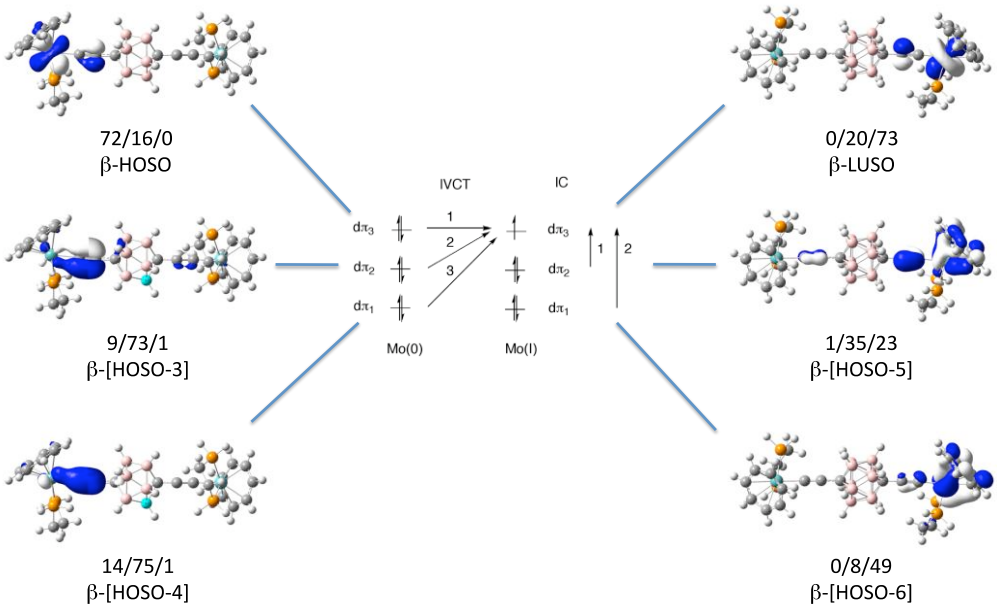

Figure 16. A selected group of MOs from $[11\text{-}H]^+$ which offer character in keeping with a simple d-orbital splitting diagram.

7. What goes around, comes around: Diethynyl phenylene and related bridges

The voltammetry of metal complexes of general form $[\{L_xM\}_2(\mu\text{-}C{\equiv}C\text{–}1,n\text{–}C_6H_4C{\equiv}C)]$ is generally characterised by the appearance of one 2e [265] or two 1e [see, for example 266-273] redox processes in solution and also grafted onto electrode surfaces [274]. Early studies exploring the electrochemical properties of $[\{L_xM\}_2(\mu\text{-}C{\equiv}C\text{–}1,n\text{–}C_6H_4C{\equiv}C)]$ systems were often based on assumptions of metal-centered redox character and consequently interpretations of spectroscopic data were based on the concepts of two-state mixed valency introduced by Hush and others [66, 256]. However, with the growing awareness of the redox-activity of many ligand systems [47, 187, 275-277], and the substantial deviations from the predictions of the two-state model that occur as the 'ligand' and 'mixed-valence' states mix [48, 278],

it is now quite clear that a careful exploration of the electronic structure is necessary before making such assignments [249]. The chemical reactivity of the alkynyl ligand in many metal σ-alkynyl radicals derived by electrochemical or chemical redox processes [223] clearly highlights the potential for redox non-innocent character in [{L_xM}$_2$(μ-C≡C–1,n–C_6H_4C≡C)] systems. Bimetallic alkynyl complexes based on the {Ru(PP)Cp′} (PP = $(PPh_3)_2$, dppe; Cp′ = η-C_5H_5, η-C_5Me_5) and {Mo(dppe)(η-C_7H_7)} fragments serve to illustrate these various issues.

The introduction of phenylene ethynylene based bridging ligands has significant consequences for the electronic structure, spectroscopic properties and charge transfer characteristics of complexes [{ML_n}$_2$(μ-C≡CArC≡C)]$^+$ when compared with the essentially mixed-valence characteristics of the carboranediyl spaced analogues. Early studies of group 8 complexes based on the [{ML_n}$_2$(μ-C≡CArC≡C)] revealed the compounds to undergo two sequential and well-separated one-electron anodic processes, with the combination of large K_C values, intense NIR transitions observed in the electronic spectra of the mono-cation radicals and calculations which indicated significant quinoidal character in the ligand being taken as evidence for highly delocalised electronic structures [273, 279, 280]. More recently, descriptions of the electronic character of such complexes in terms of ligand centered redox processes have been presented based on the basis of multiple spectroscopic investigations and consideration of a range of complexes with different length phenylene ethynylene bridges [271], and combinations of spectroelectrochemical and computational investigations [281].

The compounds [{*trans*-RuCl(dppe)$_2$}(μ-1,3-C≡CC_6H_4C≡C)] (15) and

[{Ru(dppe)Cp*}(μ-1,3-C≡CC_6H_4C≡C)] (16) serve to illustrate several of the key points in the analysis [282], and provide a convenient cross-over point between the largely metal (or metal-ethynyl) based properties of the carboranyl and arylene based systems. These compounds, and other examples of 1,3-diethynyl benzene bridged ruthenium complexes including [{*trans*-RuCl(dppm)$_2$}(μ-1,3-C≡CC_6H_4C≡C)] [279, 280] and the dendrimer building blocks [1,3-{L_nMC≡C}$_2$-5-HC≡CC_6H_3] [ML_n = *trans*-RuCl(dppm)$_2$ [283]; *trans*-RuCl(dppe)$_2$ [284, 285]; Ru(PPh_3)$_2$Cp [282]), are each observed to oxidise in two sequential one-electron steps, with a potential separation of the two half-wave potentials, ΔE, of 160 [{*trans*-RuCl(dppe)$_2$}(μ-1,3-C≡CC_6H_4C≡C)] - 190 [{Ru(dppe)Cp*}(μ-1,3-C≡CC_6H_4C≡C)] mV. In keeping with the redox non-innocence of the phenyelethynylene ligand, the oxidation potentials of complexes [Ru(C≡CC_6H_4R)(dppe)Cp*] are sensitive to the electronic character of the substituent, being tuned over some 350 mV through the introduction of strongly electron donating (R = NH_2) or withdrawing (R = NO_2) groups [183]. For example, the modest electron-withdrawing character of the carborane cage is reflected in the small anodic shift of the first oxidation potential of [{Ru(dppe)Cp*}$_2$(μ-1,10-C≡C-1,10-$C_2B_8H_8$)] and [{Ru(dppe)Cp*}$_2$(μ-1,12-C≡C-1,12-$C_2B_{10}H_{10}$)] relative to the prototypical phenylacetylide complex [Ru(C≡CPh)(dppe)Cp*]; in contrast, the introduction of a *meta*-{C≡CRu(dppe)Cp*} results in a small cathodic shift. The relatively small ΔE (ca. 100 - 150 mV) values in this series are largely a consequence of electrostatic / Coulombic effects, shielded by the combined effects of solvation and ion pairing [249], with some residual small electronic coupling which can be estimated from Hush-style analyses of the NIR spectra (vide infra).

The moderate potential separations observed for [{*trans*-RuCl(dppe)$_2$}(μ-1,3-

C≡CC_6H_4C≡C)] (15) and [{Ru(dppe)Cp*}(μ-1,3-C≡CC_6H_4C≡C)] (16) give rise to K_C values in the range 500 - 1600, indicating the equally moderate stability of the intermediate (mono-cationic) charge state towards disproportionation. The IR ν(C≡C) spectra of $[15]^{n+}$ and $[16]^{n+}$ (n = 0, 1, 2) and the mononuclear model systems [*trans*-RuCl(C≡CPh)$(dppe)_2]^{n+}$ (n = 0, 1) are summarised in Table 1. The IR data are clearly consistent with a localised description of the oxidation processes, with the removal of one electron affecting one RuC≡C moiety much more significantly than the other. The spectra of the mono-oxidised (n = 1) bimetallic complexes approximate a superposition of the spectra of the neutral (n = 0) and doubly oxidised (n = 2) systems, indicating little ground-state interaction between the two metal-ethynyl arms [282, 286, 287].

Table 1. Summary of ν(C≡C) frequencies for selected complexes.

compound	n = 0	n = 1	n = 2
[*trans*-RuCl(C≡CPh)$(dppe)_2]^{n+}$	2075	1910	
[Ru(C≡CPh)(dppe)Cp*]$^{n+}$	2072	1929	
[{*trans*-RuCl$(dppe)_2$}(μ-1,3-C≡CC_6H_4C≡C)]$^{n+}$	2063	2049, 1905	1909
[{Ru(dppe)Cp*}(μ-1,3-C≡CC_6H_4C≡C)]$^{n+}$	2063	2060, 1934	1938

This localised description is adequately reproduced by gas-phase DFT models using simplified ligand structures and the HF-rich functional MPW1K and the 3-21G* basis set for all atoms. An important aspect of these calculations is the large contribution from the bridging ligand (>70%) to the HOMO of the neutral model systems ([{*trans*-RuCl$(dHpe)_2\}_2$(μ-1,3-C≡CC_6H_4C≡C)] ([**15-H**]) and ([{Ru$(PH_3)_2$Cp}$_2$(μ-1,3-C≡CC_6H_4C≡C)] ([**16-H**]), and the confinement of the β-LUSO along one RuC≡CC_6H_4 moiety in [**15-H**]$^+$ and [**16-H**]$^+$ (% composition Ru / C≡C / C_6H_4 / C≡C / Ru: [**15-H**]$^+$ 21 / 32 / 34 / 7 / 2; [**16-H**]$^+$ 23 / 33 / 32 / 3 / 2). The β-HOSO is more

heavily concentrated on the alternate RuC≡C moiety (% composition Ru / C≡C / C_6H_4 / C≡C / Ru: 8 / 7 / 16 / 34 / 26 ([{*trans*-RuCl(dHpe)$_2$}$_2$(μ-1,3-C≡CC_6H_4C≡C)]$^+$; 5 / 4 / 15 / 31 / 29 ([{Ru(PH_3)$_2$Cp}$_2$(μ-1,3-C≡CC_6H_4C≡C)]$^+$) (Figure 17). Thus, whilst a description in terms of a localized (Class II) mixed valence complex is reasonable to a first approximation, the important contribution from the redox non-innocent bridging ligand to the stabilization of the unpaired electron must not be neglected.

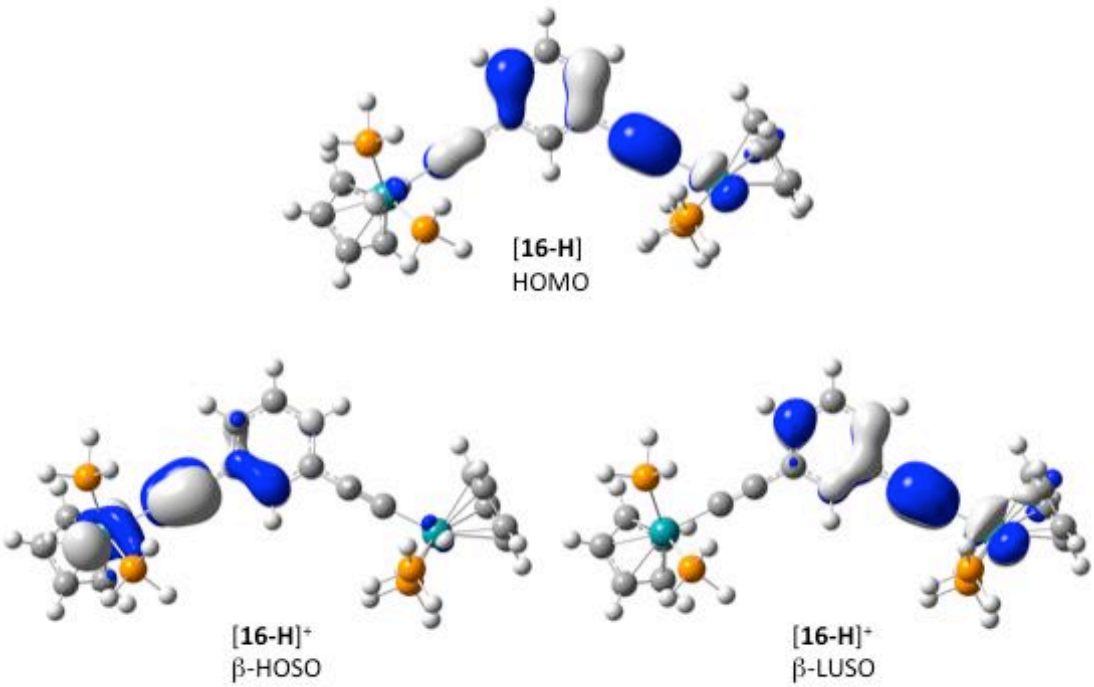

Figure 17. Plots of the HOMO of [**16-H**] and β-LUSO and β-HOSO of [**16-H**]$^+$ with contours at ±0.04 (e/bohr^3)$^{1/2}$.

The NIR spectra of [{*trans*-RuCl(dppe)$_2$}(μ-1,3-C≡CC_6H_4C≡C)]$^+$ and [{Ru(dppe)Cp*}(μ-1,3-C≡CC_6H_4C≡C)]$^+$ each contain two transitions of low intensity not present in the spectra of the closed shell precursors centered near 5800, 3750 cm^{-1}

([{*trans*-RuCl(dppe)$_2$}(μ-1,3-C≡CC_6H_4C≡C)]$^+$) and 7750, 4800 cm^{-1} ([{Ru(dppe)Cp*}(μ-1,3-C≡CC_6H_4C≡C)]$^+$) (Figure 18). On further oxidation to the dications, the lowest energy band collapses in line with its assignment as an intramolecular RuC≡C→[C_6H_4C≡CRu]$^+$ (pseudo-IVCT) charge transfer transition. The higher energy feature has more interconfigurational ($d\pi$-$d\pi$) character and grows in intensity in [{Ru(dppe)Cp*}(μ-1,3-C≡CC_6H_4C≡C)]$^{2+}$, but is masked by the low energy tail of the chloride-to-metal/ethynyl charge transfer band in [{*trans*-RuCl(dppe)$_2$}(μ-1,3-C≡CC_6H_4C≡C)]$^{2+}$. These assignments are supported by TDDFT calculations with the simple models. The half-height band width of the 'IVCT' component is in remarkably good agreement with the Hush two-state model (([{*trans*-RuCl(dppe)$_2$}(μ-1,3-C≡CC_6H_4C≡C)]$^+$) $\Delta\nu_{1/2(calc)}$ = 2900 cm^{-1}, $\Delta\nu_{1/2(obs)}$ = 3100 cm^{-1}; [{Ru(dppe)Cp*}(μ-1,3-C≡CC_6H_4C≡C)]$^+$ $\Delta\nu_{1/2(calc)}$ = 3300 cm^{-1}, $\Delta\nu_{1/2(obs)}$ = 3200 cm^{-1}). Assuming the crystallographically determined through space Ru…Ru distance (10.5 Å) from [1,3-{*trans*-RuCl(dppm)$_2$ C≡C}$_2$-5-HC≡CC_6H_3] [288] as an upper limit to the electron transfer distance (a estimate beset by difficulties in terms of allowing for the contribution of the carbon-rich ligand to the donor and acceptor sites) lower estimates for H_{ab} of 200 cm^{-1} ([{*trans*-RuCl(dppe)$_2$}(μ-1,3-C≡CC_6H_4C≡C)]$^+$) and 90 cm^{-1} ([{Ru(dppe)Cp*}(μ-1,3-C≡CC_6H_4C≡C)]$^+$) are obtained. Given the approximations involved, the values are entirely consistent with those from the carboranyl derivatives described above, although the involvement of the central portion of the bridging moiety in the electronic structures is quite distinct.

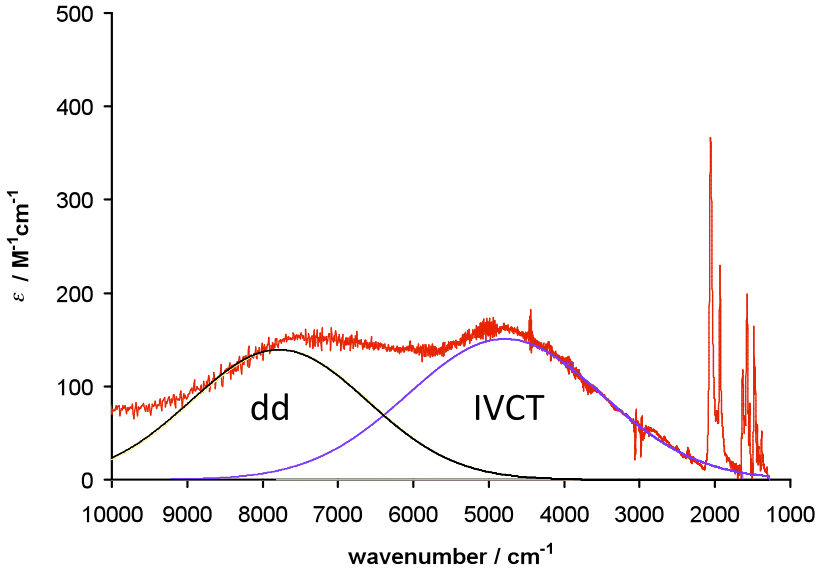

Figure 18. The NIR-IR region of spectroelectrochemically generated $[15]^{+}$, showing deconvolution into IVCT and interconfigurational / *d-d* components [282].

A few brief words concerning the electronic structures of the dications $[\{trans\text{-}RuCl(dppe)_2\}(\mu\text{-}1,3\text{-}C{\equiv}CC_6H_4C{\equiv}C)]^{2+}$ and $[\{Ru(dppe)Cp^*\}(\mu\text{-}1,3\text{-}C{\equiv}CC_6H_4C{\equiv}C)]^{2+}$ are also warranted, although detailed studies of the magnetic properties have not yet been undertaken. Computational analysis indicates the high-spin (HS) state to be energetically more stable than the low-spin (LS) form by ca. 36 kcal mol^{-1}, and the calculated frequencies from the HS state are also in better agreement with the experimental observations. Of some growing significance is the observation of a number of shallow energy minima on the potential energy surface, which differ in the degree of metal-bridging ligand mixing and energy by the orientation of the metal fragments RuP_4 and RuP_2Cp relative to the plane of the 1,3-substituted C_6H_4 ring. Similar conformational effects are now being more widely recognised in other

systems [278, 289-295], influencing the distribution of electron spin density [296] and being noted to affect intramolecular energy and electron transfer pathways [297, 298]. Some further aspects of conformational influence on electronic structure are discussed further below.

A simple consideration of resonance arguments would suggest that compounds derived from 1,4-diethynyl benzene should offer more delocalised structures than the 1,3-based isomers, and this is reflected in the design of wire-like molecules based on the phenylene ethynylene motif (vide supra). Unsurprisingly, many studies of $[\{ML_n\}_2(\mu\text{-}C{\equiv}C\text{-}1\text{-}4\text{-}C_6H_4C{\equiv}C)]$ complexes have drawn a conclusion of a delocalised electronc structure, with the corresponding $[\{ML_n\}_2(\mu\text{-}C{\equiv}C\text{-}1\text{-}4\text{-}C_6H_4C{\equiv}C)]^+$ cation radicals described in terms of strongly coupled 'mixed valence' electronic structures. However, in the case of relatively electron rich ruthenium d^6 derivatives, even early computations highlighted appreciable structural reorganisation within the diethynyl bridging ligand resulting from oxidation of the closed shell precursors [279, 280], and more recent descriptions have emphasised the ligand redox non-innocence of the bridging ligand in these cases [271, 281]. However, some features in the $\nu(C{\equiv}C)$ region of the IR spectra have been observed across a number of metal complexes with 1,4-diethynylbenzene derived bridging ligands which do not sit comfortably within a 'bridge localised' model, and which have provoked further exploration.

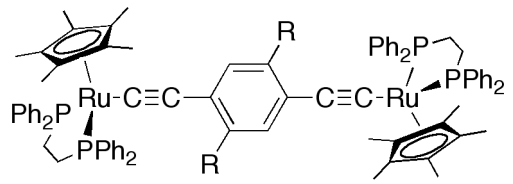

R = H (**17**), OMe (**18**)

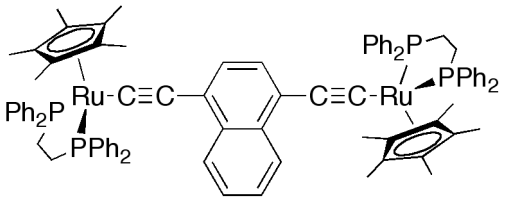

19

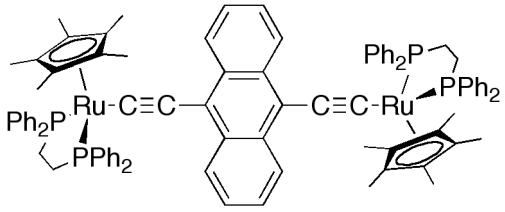

20

Figure 19. The complexes 17 - 20.

The family of complexes [{Ru(dppe)Cp*}$_2$(μ-C≡CArC≡C)] (HC≡CArC≡CH = 1,4-diethynylbenzene, 1,4-diethynyl-2,5-dimethoxybenzene, 1,4-diethynylnaphthalene, 9,10-diethynylanthracene) were prepared from the KF mediated reaction of trimethylsilyl protected ligand precursors and [RuCl(dppe)Cp*] in methanol (Figure 19) [299]. Each complex undergoes the familiar generic pattern of two well separated one-electron oxidation processes, at potentials rather more anodic than simpler mononuclear analogues (Table 2). Despite the variation in the structure of the aromatic bridging moiety, ΔE is ca 300 mV in each of 17 – 20. The UV-vis spectra of $[17]^+$ - $[20]^+$ contain structured bands consistent with an aromatic radical, whilst in the NIR region an intense band envelope is observed, which can be deconvoluted into three sub-bands, the lowest energy and most intense of which can be assigned to the

two MLCT transitions expected for a bridge-centered hole in a bimetallic complex $\{L_xM\}(\mu\text{-bridge})^+\{ML_x\}$ (Figure 20) [277, 281].

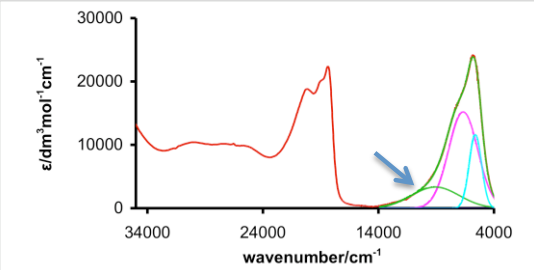

Figure 21. The UV-vis-NIR spectrum of $[17]^+$. The aryl radical band is found near 20,000 cm^{-1}. The NIR region is deconvoluted into a sum of three Gaussian shaped components. The IVCT-like component is highlighted by the arrow.

Examination of the IR spectra of $[17]^+$ revealed two ν(C≡C) bands, assigned to the symmetric and asymmetric stretch of the oxidised ligand, at frequencies between those of the neutral and doubly oxidised forms (Figure 21). These data are therefore strongly supportive of an interpretation based on the now familiar concept of redox non-innocent character associated with the ethynyl aromatic ligands of electron-rich Ru(II) d^6 complexes. However, the additional observation of a lower intensity NIR transition, the half-height bandwidth of which is in excellent agreement with the Hush two-state model and additional weak ν(C≡C) bands, also consistent with a localised mixed valence model, prompt consideration of a distribution of electronic states.

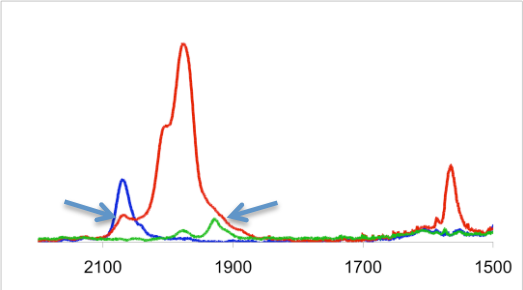

Figure 21. The IR spectrum of $[17]^+$. The weak bands associated with the mixed-valence form are highlighted by the arrows.

The distribution and mobility of electrons and holes in phenylene ethynylene based systems is known to be critically dependent on conformation and sensitive to conformational changes [300] and it is likely that conformational changes in the central aromatic ring system are responsible for the change in distribution of the hole in $[17]^+$-$[20]^+$ from bridge to metal, as the plane of the aromatic ligand rotates in and out of conjugation with the strongly electron-donating metal fragments (Scheme 12) [299].

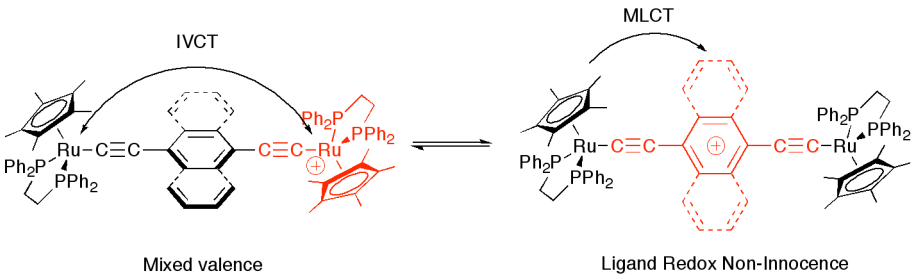

Scheme 12. A highly stylised and simplistic representation of the changes in relative conformation of metal and bridging ligand fragments and electronic structure in $[17]^+$ - $[21]^+$.

The electronic coupling parameter, H_{AB}, extracted from Hush-style analysis of the IVCT based contribution to the NIR band envelope in the series $[17]^+$ - $[20]^+$ is largely independent of the nature of the aromatic moiety in the bridging ligand (the deconvolution of $[20]^+$ being compromised somewhat by the overlap of the NIR band envelope with the tail of an anthracene based transition), falling in the narrow range 560 – 700 cm^{-1} (approximating the upper limit of the electron transfer distance as the average Ru…Ru separation in crystallographically determined systems). Such observations are consistent with de-coupling of the aromatic moiety from the superexchange pathway, but more investigations are required to explore the cross-over point from superexchange to hopping mechanism in these systems; a task which will be further complicated by the rotational dynamics of the ligand. It is rather pertinent at this point to note that interpolation of metal centers within the phenylene ethynylene (or other carbon-rich) backbone seem to enhance the efficient transfer of the charge along the molecular backbone [271, 276, 295, 301], a point which augers well for the construction of organometallic molecular components for use in molecular electronics.

Table 2. Summary of electrochemical data from selected alkynyl complexes, in CH_2Cl_2 / 0.1 M NBu_4BF_4, reported against SCE (FcH / FcH^+ = 0.46 V, Fc*H / $Fc*H^+$ = –0.07 V).

compound	E_1 / V	E_2 / V	DE / mV	K_C	reference
[Ru(C≡CPh)(dppe)Cp*]	0.25				183
[Ru(C≡C$C_6H_4NH_2$-4)(dppe)Cp*][a]	0.05				183
[Ru(C≡C$C_6H_4NO_2$-4)(dppe)Cp*][a]	0.40				183
[{Ru(dppe)Cp*}$_2$(μ-1,10-C≡C-1,10-$C_2B_8H_8$)]	0.27	0.39	0.12	116	247
[{Ru(dppe)Cp*}$_2$(μ-1,12-C≡C-1,12-$C_2B_{10}H_{10}$)]	0.32	0.41	0.09	35	247
[{Ru(dppe)Cp*}(μ-1,3-C≡CC_6H_4C≡C)]	0.18	0.34	0.16	500	282
[{Ru(dppe)Cp*}(μ-1,4-C≡CC_6H_4C≡C)]	0.01	0.30	290	0.8×10^5	299
[{Ru(dppe)Cp*}(μ-1,4-C≡C$C_6H_2(OMe)_2$C≡C)]	–0.14	0.17	310	1.7×10^5	299
[{Ru(dppe)Cp*}(μ-1,4-C≡C$C_{10}H_6$C≡C)]	–0.06	0.24	290	0.8×10^5	299
[{Ru(dppe)Cp*}(μ-9,10-C≡C$C_{14}H_8$C≡C)]	–0.17	0.13	300	1.2×10^5	299

[a] in 0.1 M NBu_4PF_6 / CH_2Cl_2 [183].

Although studies of [{Mo(dppe)(η-C_7H_7)}$_2$(μ-C≡CC_6H_4C≡C)]$^{n+}$ are still in progress, the members of a closely related redox series [{(η-C_7H_7)(dppe)Mo}(μ-C≡CC_6H_4C≡C){Fe(dppe)Cp*}]$^{n+}$ have been examined in some detail [302]. The [Fe(C≡CR)(dppe)Cp*] fragment presents a bonding arrangement similar to that of the ruthenium analogues, but offers more metallic character in the occupied frontier orbitals due to the 3d vs 4d character of the metals, and much more cathodic redox character. The complex [{(η-C_7H_7)(dppe)Mo}(μ-C≡CC_6H_4C≡C){Fe(dppe)Cp*}]$^+$ ([21]$^+$) therefore presented a useful opportunity to explore mixed-valance concepts in a carbon-rich bridged system in which the thermodynamic stability of the metal-based

oxidation processes are similar, but the extent of metal-bridging ligand mixing is differentiated on symmetry grounds.

Compound **21** was prepared via the intermediate mono-vinylidene, which exists as an equilibrium mixture, with the dominant contribution arising from proton migration to give the Mo-vinylidene form (Scheme 13). After deprotonation, the bis(alkynyl) species was obtained in high (>80%) yield. The cyclic voltammogram of **21** exhibits two reversible one-electron waves at –0.83 V and –0.56 V (vs. FcH/FcH^+ = 0 V; ΔE = 0.27 V), which were assigned to the Mo and Fe centers respectively on the basis of comparison with related mono-nuclear species; in this manner **21** is differentiated from other heterobimetallic complexes [{L_nM}(μ-C≡CC_6H_4C≡C){Fe(dppe)Cp*}] in presenting an intial oxidation event that is not iron-centred [303-305]. The comproportionation equilibrium lies far enough to the side of the monocation that samples of $[\mathbf{21}]^+$ could be isolated (as the PF_6^- salt) from reaction of **21** with $[\mathbf{21}]^{2+}$, the latter being prepared in turn by stoichiometric oxidation of **21** with two equivalents of [FcH]PF_6.

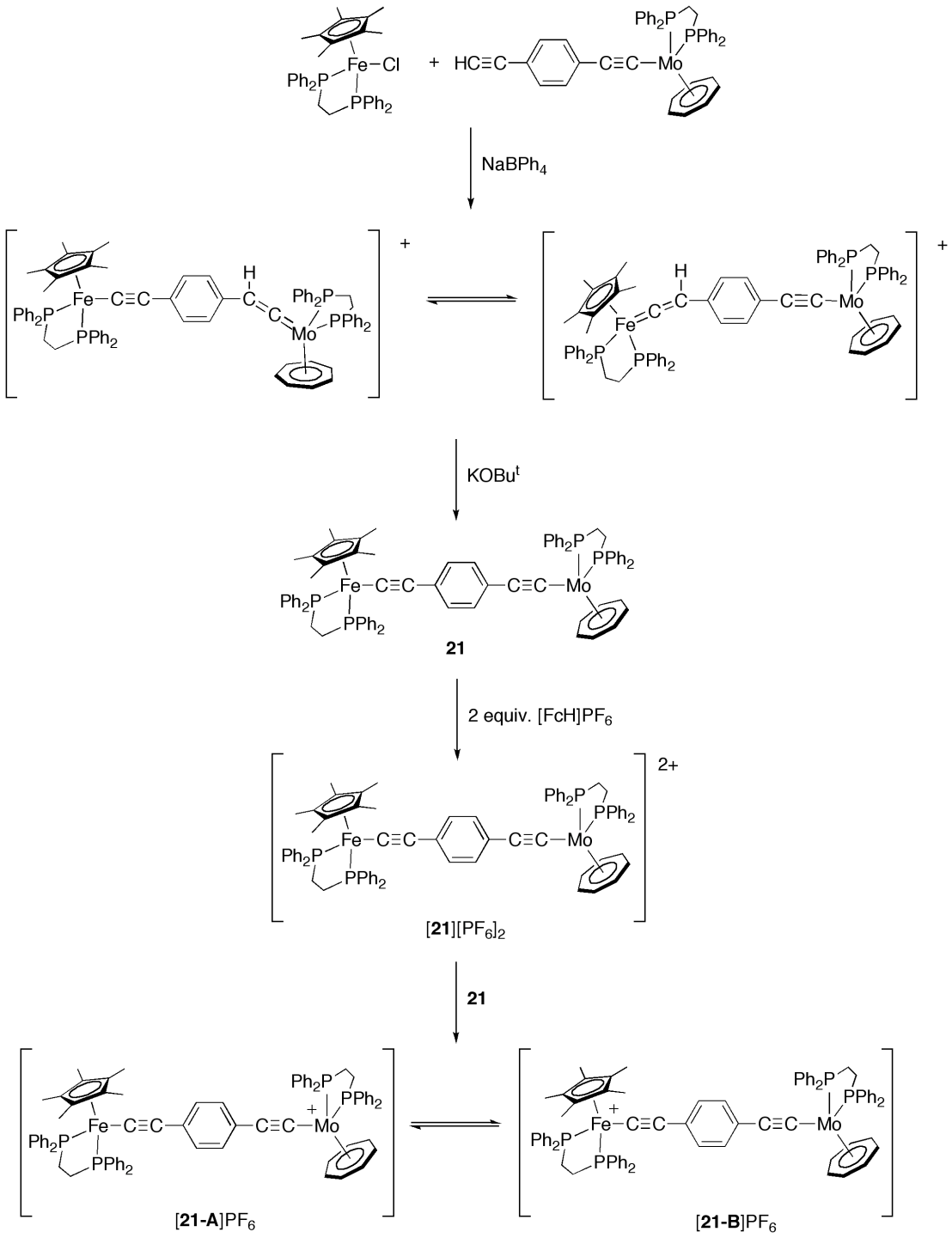

Scheme 13. The preparation of $[21]^{n+}$ (n = 0, 1, 2) [302].

Computational studies of 21 and the homometallic model systems $[\{Fe(dppe)Cp^*\}_2(\mu\text{-}C{\equiv}CC_6H_4C{\equiv}C)]^{n+}$ ($[22]^{n+}$) and $[\{Mo(dppe)(\eta\text{-}C_7H_7)\}_2(\mu\text{-}C{\equiv}CC_6H_4C{\equiv}C)]^{n+}$ ($[23]^{n+}$) reveal the progressive destabilisation of the HOMO and

reduction of the HOMO-LUMO gap upon substitution of {Fe(dppe)Cp*} for {Mo(dppe)(η-C_7H_7)}. Whilst Koopmans' theorem does not allow for structural and electronic relaxation upon changes in oxidation state, the HOMO energies do track with the trends in first oxidation potential. The nature of the HOMO is also metal dependent, being heavily comprised of the Mo d_{z^2} orbitals in the case of **21** (51% metal character, 48% from Mo) and the homobimetallic Mo (49%, equally distributed) system than the iron homobimetallic example (28% Fe character) (Figure 22).

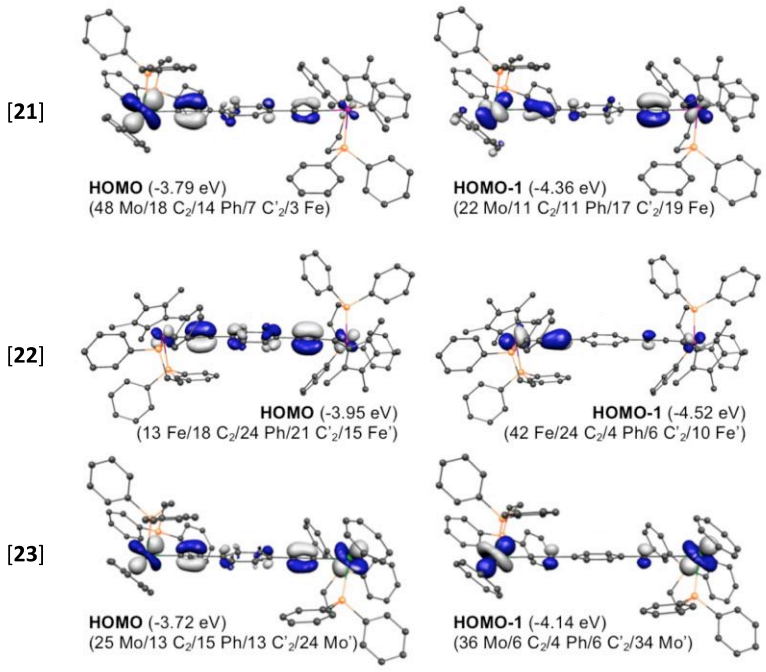

Figure 22. The HOMO and HOMO–1 from the computational models of **21**, **22** and **23** (adapted from [302]).

In the mono-cations, an important relationship exists between the orientation of the phenylene ring with respect to the metal fragments and the distribution of electron spin density across the molecular framework. In the lowest energy conformation the

ring is positioned to maximise overlap with the metal-based frontier orbitals in the β-LUSO. The aryl ring therefore lies approximately perpendicular to the plane of the C_7H_7 ring and parallel to the plane of the Cp* ring in $[\mathbf{21}]^+$, leading to a torsion angle between the planes defined by the centroid of each ring, the metal and the alkynyl C of –88°. In this conformation, spin density is rather more concentrated on the Fe center, likely due to the better stabilisation of charge arising from the additional mixing to the alkynyl fragment at the Fe fragment. However, single point calculations with different rotamers of $[\mathbf{21}]^+$ reveal that the spin density distribution can be shifted from one metal to the other in response to the relative orientation of the arene π-system and the metal fragments. The calculations are therefore consistent with the concept of an initial Mo-based oxidation, followed by geometric relaxation to the Fe(III)/Mo(II) isomer. The PES is fairly flat, and in the real systems the distribution of charge is likely to be rather sensitive to environmental factors which will influence the adopted conformation(s); this concept has been investigated in more details spectroscopically as described below.

The conformational dependence of the electronic structure represents a different example of conformation switching to that inferred from the studies of the homo-bimetallic Ru complex ($[\mathbf{17}]^+$), but serves to further underline the immense potential for fast time-resolved studies of the dynamics associated with the electron transfer mechanisms in these systems [297, 306, 307]. Experimental support for the idea of redox isomerism between the iron and molybdenum localised states comes from spectroscopic investigations. The closed shell system **21** is characterised by a single ν(C≡C) band at 2050 cm^{-1}, consistent with the ν(C≡C) bands in mononuclear alkynyl complexes featuring these metal auxillaries, and indicating little differentiation of the

metallic termini. Oxidation to $[21]^+$ in a spectroelectrochemical cell gives rise to a distinctive two band pattern, but with each principal band exhibiting a pronounced shoulder. The shoulder transitions are less pronounced in the solid state spectra of $[21]PF_6$, but the band asymmetry is still clearly evident. The splitting of ν(C≡C) bands can arise from Fermi coupling, or the presence of distinct geometric configurations [143, 308]. In the case of $[21]^+$ the additional features can also be evidence of the presence of the redox isomers, which are trapped on the IR timescale.

Further support for the environmental dependence of the electronic structure and dynamic electron exchange comes from EPR and Moessbuer spectroscopies. In fluid solution, the X-band EPR spectrum only resolves the characteristic 17-e^- $\{Mo(dppe)(\eta\text{-}C_7H_7)\}^+$ pattern, the 17-e^- $\{Fe(dppe)Cp^*\}^+$ fragment normally being EPR silent at room temperature due to fast relaxation processes. However, at 120 K in frozen glass, or in the solid state between 120 – 5 K, the X-band spectrum resembles a superposition of the $\{Mo(dppe)(\eta\text{-}C_7H_7\}^+$ and $\{Fe(dppe)Cp^*\}^+$ fragments, consistent with the presence of redox isomers in the sample. Furthermore, the magnitude of the hyperfine coupling constants to Mo and large g anisotropy associated with the Fe signal indicate the centers to be only weakly interacting and argues against substantial delocalisation on the EPR time-scale (10^{-9} s) (consistent with the IR spectra). On the slower Moessbuer timescale (10^{-7} - 10^{-8} s), only parameters consistent with an Fe(II) centre are observed in solid samples at 80 K, which therefore provides a convenient limit to the electron exchange rate.

The NIR spectrum of $[21]^+$ exhibits a solvatochromic band envelope which can be deconvoluted into three bands of similar half-height band width, and assigned to three

IVCT transitions (Figure 23). Given the facile electron exchange between the Fe and Mo sites, the reorganisation energy associated with charge transfer must be minimal, and hence the observation of a single set of IVCT transitions is not unexpected. Using the difference in electrode potentials to provide an estimate of the difference in energy of the two isomers and the Fe---Mo separation as an approximation of the electron transfer distance, if the the Hush two-state model holds, a coupling constant H_{AB} = 470 cm^{-1} can be extracted from the lowest energy IVCT transition. This value is smaller than in the analogous homobimetallic Fe complex (570 cm^{-1}), but larger than in systems containing more energetically miss-matched metal fragments [303-305].

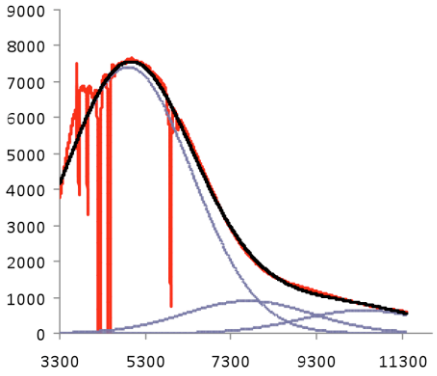

Figure 23. The NIR spectrum of [21]PF_6, illustrating the three band deconvolution (adapted from [302]).

Again, a few words are warranted on the electronic structure calculations concerning the dicationic state, $[21]^{2+}$. Whilst the homobimetallic iron system exhibits a small singlet-triplet energy gap, in the case of $[21]^{2+}$ the triplet lies much higher in energy (+10.6 kJ mol^{-1}) than the low spin, antiferromagnetically coupled ground state. The spin density is predominantly located on the metal centers, with the greater proportion on the Fe center, probably due to the greater stability conferred by the better mixing of the metal and ligand based orbitals.

8. A bridge too far: Oligo(phenylene)ethynylene bridging ligands

Although extended oligo(pheylene ethynylene) structures are known to be effective structures for the transmission of current in molecular junctions [vide supra], the insertion of additional phenylene ethynylene moieties between {Ru(PP)Cp´} [309] or *trans*-{RuCl(dppe)$_2$} centers [271, 310] significantly reduces the thermodynamic stability of the subsequent one-electron redox product, and in the case of [{Cp'(PP)Ru}$_2$(μ-C≡CC$_6$H$_4$C≡CC$_6$H$_2$(OMe)$_2$C≡CC$_6$H$_4$C≡C)] (Ru(PP)Cp' = Ru(PPh$_3$)$_2$Cp (**24a**), Ru(dppe)Cp* (**24b**) the electrochemical response is characterised by a two overlapping one-electron anodic processes which could not be resolved. The prompt disproportionation of [**24**]$^+$ prohibited spectroscopic investigation of this species, and prevented discussion of the intramolecular electron transfer characteristics in this species. However, the dications [**24**]$^{2+}$ could be accessed using spectroelectrochemical methods, and [{Ru(PH$_3$)$_2$Cp}$_2$(μ-C≡CC$_6$H$_4$C≡CC$_6$H$_2$(OMe)$_2$C≡CC$_6$H$_4$C≡C)]$^+$ ([**24-H**]$^{2+}$) modelled using DFT approaches.

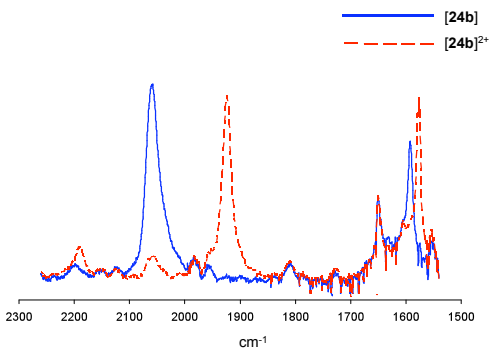

Figure 24. The ν(CC) bands in the IR spectra of [**24b**] and [**24b**]$^{2+}$

The observation of a relatively strong ν(C≡C) band in $[\mathbf{24}]^{2+}$ at 1926 (Ru(dppe)Cp*) and 1902 cm^{-1} in the *trans*-RuCl(dppe)$_2$ based analogue [271] confirms the redox non-innocent character of the phenylene ethynylene ligand. However, the presence of a weaker band at 2190 cm^{-1} is consistent with an organic alkyne and assigned to the 'inner' C≡C fragment argues against substantial cumulenic character (Figure 24), a conclusion which is consistent with DFT modelling which places the high-spin dication HS-$[\mathbf{24\text{-}H}]^{2+}$ some 0.17 eV lower in energy than the low-spin state. The β-LUSO and β-LUSO+1 in $[\mathbf{24\text{-}H}]^{2+}$ were largely localised on the Ru-C≡CC_6H_4- fragments, as was the majority of the calculated electron spin density (Figure 25).

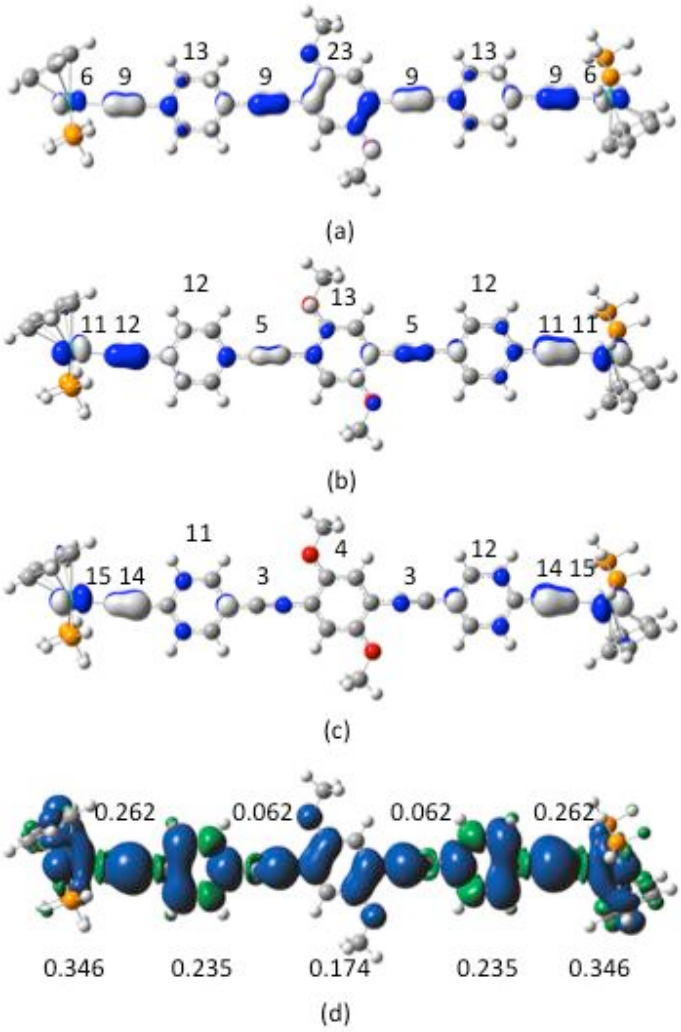

Figure 25. Plots and % composition of: (a) the HOMO of [24]; the (b) β -LUSO+1, (c) β-LUSO and (d) spin density of HS-$[24]^{2+}$.

Consequently, $[24]^{2+}$ and related systems are probably best described in terms of two independent, metal stabilised aryl ethynyl radicals [309]. These observations are consistent with the electronic structures of ethynyl tolan complexes such as $[Ru(C{\equiv}CC_6H_4C{\equiv}CC_6H_4OMe)(PP)Cp']^{n+}$ (n = 0, 1) described above [192].

9. Back around to the beginning: Conclusions

The studies described above, and many related studies by others, illustrate important ideas concerning molecular design strategies for engineering efficient coupling between metal centers in mixed valence bimetallic complexes featuring conjugated bridging ligands. Clearly, the match between the metal and ligand orbital energy and symmetry is essential to bring about strong coupling, a result embedded in the seminal work of Taube, Marcus and Hush. However, as the match between metal and ligand energies becomes closer, the involvement of the ligand in the charge transfer processes becomes increasingly important, leading to deviations from the Hush two-state model. The observation of LMCT transitions in the same region as IVCT bands is something of a signature of these processes, and helps to account for the faster electron transfer rate in $[\{Mo(dppe)(\eta\text{-}C_7H_7)\}_2(\mu\text{-}C{\equiv}CC{\equiv}C)]^+$ ($[8]^+$), when compared with $[\{Mo(dppe)(\eta\text{-}C_7H_7)\}_2(\mu\text{-}1,12\text{-}C{\equiv}C\text{-}1,12\text{-}C_2B_{10})]^+$ ($[11]^+$). The relatively poor symmetry match between the high-lying Mo d_{z^2} orbital offered by the {Mo(dppe)(η-C_7H_7)} fragment with the alkynyl π-orbitals limits the magnitude of metal-metal coupling through alkynyl-based bridging ligands, but simplifies descriptions and

models of electronic transitions in terms of metal-based states. The Group 8 {M(PP)Cp´} fragments offer frontier orbitals with better symmetry match to the alkynyl π-orbitals, and the different electronic characteristics of M = Fe (significant metal character) and Ru (significant alkynyl ligand character) based systems can be attributed to the relative energy of the 3*d* and 4*d* orbitals with respect to the organic π-system (Figure 6). The complexes $[\{L_xM\}(\mu\text{-}C{\equiv}CXC{\equiv}C)\{ML_x\}]^+$ ($\{ML_x\}$ = {Mo(dppe)(η-C_7H_7)}, {Fe(dppe)Cp*}, {Ru(PP)Cp'}) therefore exemplify the range of electronic structures from weakly coupled mixed-valence systems, through progressively more strongly coupled systems with concomitantly increasing bridging ligand character in the electronic states responsible for the low-energy (NIR) transitions, to systems where the redox activity is better considered in terms of a redox active organic fragment supported by metal *dπ*-donors.

So how does this relate back to the ideas of metal complexes as components within hybrid molecular electronic devices? There is a conceptual analogy between the Landauer-based descriptions of charge transport across a metal|molecule|metal molecular junction and charge transfer within a $[\{L_xM\}(\mu\text{-}C{\equiv}CXC{\equiv}C)\{ML_x\}]^+$ system. Whilst in the Landauer description the transport properties are considered in terms of the transmission across both left and right substrate-molecule contacts and the bridging molecule, in the mixed-valence analogue the metal-ligand interaction model the substrate-molecule contacts and the bridge present additional tunnel barriers, the height of which depend on the degree of delocalisation through the system and can be influenced by chemical composition (e.g. –C≡C-1,12-$C_2B_{10}H_{10}$-C≡C– vs –C≡CC≡C–) and molecular conformation (e.g. –C≡CArC≡C–). Although direct comparisons between transport across a molecular junction and the electronic

structure of a mixed valence complex have rarely been made, it is intriguing to note that in both platforms polyynyl based conduits provide more effective transport than oligo(phenylene ethynylene) based bridges / wires [311].

Several design rules for metal-based components for electronics stem from this analogy and observations drawn from studies of the electronic structure of 'wire-like' molecules: (a) the molecule-substrate contact (metal-bridge interaction) is an essential feature to ensure transport at low bias; (b) polyyne-based bridging moieties are particularly effective conduits; (c) interpolation of metal centers which offer d-orbital within good energy and symmetry match with C≡C π-orbitals within a polyyne chain is likely to both improve long-distance transport properties; (d) redox gating of charge transport should be achievable at low gate bias with metal complex-based molecular wires. The excellent understanding of the synthetic chemistry associated with the preparation of highly-conjugated, polymetallic metal complexes and the availability of spectroscopic and computational methods which permit detailed assessments of electronic structure provide a growing capacity to identify and rationalise the intricacies of conductance measurements in metal|molecule|metal junctions. Together with advances in nano-scale fabrication these advances bring great hope that a truly viable molecular electronics technology will be realised over the coming decade(s!).

Acknowledgements Thanks are due first and foremost to the pioneers of electron transfer theory and molecular electronics who have laid the foundations for the field. The dedicated and talented co-workers and colleagues whose names appear in the reference list are most sincerely thanked for their immense hard work, insight and good humour during the author's forays into the fascinating world of mixed valency

at the interface with molecular electronics. Many of the studies in the author's group have been supported by the EPSRC through project grants and a Leadership Fellowship, and this financial support is gratefully acknowledged.

References

[1] R.A. Marcus, N. Sutin, Biochem. Biophys. Acta, 811 (1985) 265.

[2] P.F. Barbara, T.J. Meyer, M.A. Ratner, *J. Phys. Chem.*, 1996, 100, 13148.

[3] J.F. Endicott, in J.A. McCleverty, T.J. Meyer (Eds.), *Comprehensive Coordination Chemistry II*, Elsevier Science Ltd, Oxford, 2004, pp 657 – 730.

[4] D.M. Stanbury, *Adv. Inorg. Chem.*, 2003, 54, 351.

[5] J.L. Bredas, D. Beljonne, V. Coropceanu, J. Cornil, Chem. Rev. 104 (2004) 4971.

[6] Y. Zhao, W.Z. Liang, Chem. Soc. Rev. 41 (2012) 1075.

[7] E.S. Andrreiadis, M. Chavarot-Kerlidou, M. Fontecave, V. Artero, Photochem. Photobiol. 87 (2011) 946.

[8] M.R. Wasielewski, Chem. Rev. 92 (1992) 435.

[9] J. Hankache, O.S. Wenger, Chem. Rev. 111 (2011) 5138.

[10] A. Heckmann, C. Lambert, Angew. Chem. Int. Ed. 51 (2012) 326.

[11] D. Wrobel, A. Graja, Coord. Chem. Rev. 255 (2011) 2555.

[12] C. Creutz, B.S. Brunschwig, N. Sutin, in J.A. McCleverty, T.J. Meyer (Eds.), *Comprehensive Coordination Chemistry II*, Elsevier Science Ltd, Oxford, 2004, pp 731 – 777.

[13] R.J. Nichols, W. Haiss, S.J. Higgins, E. Leary, S. Martin, D. Bethell, Phys Chem. Chem. Phys. 12 (2010) 2801.

[14] D.K. James, J.M. Tour, Chem. Mater. 16 (2004) 4423.

[15] R.F. Service, Science 294 (2001) 2442.

[16] http://www.itrs.net

[17] S.P. Cummings, J. Savchenko, T. Ren, Coord. Chem. Rev. 255 (2011) 1587.

[18] B. Gotsmann, H. Riel, E. Lörtscher, Phys. Rev. B 82 (2011) 1.

[19] E. Lörtscher, Chem. Phys. Chem. 12 (2011) 2887.

[20] E. Lörtscher, C. J. Cho, M. Mayor, M. Tschudy, C. Rettner, H. Riel, Chem. Phys. Chem. 12 (2011) 1677.

[21] E. Lörtscher, M. Elbing, M. Tschudy, C. von Hänisch, H. B. Weber, M. Mayor, H. Riel, Chem. Phys. Chem. 15 (2008) 2252.

[22] E. Lörtscher, J. W. Ciszek, J. Tour, H. Riel, Small, 2 (2006) 973.

[23] (a) J.M. Tour, Acc. Chem. Res. 33 (2000) 791. (b) A. Salomon, D. Cahen, S. Lindsay, J. Tomfohr, V.B. Engelkes, C.D. Frisbie, Adv. Mater. 15 (2003) 1881.

[24] W. Hong, D. Zsolt Manrique, P. Moreno-Garcia, M. Gulcur, A. Mishchenko, C.J. Lambert, M.R. Bryce, T. Wandlowski, J. Am. Chem. Soc. 134 (2012) 2292.

[25] S. Martin, I. Grace, M.R. Bryce, C. Wang, R. Jitchati, A.S. Batsanov, S.J. Higgins, C.J. Lambert, R.J. Nichols, J. Am. Chem. Soc. 132 (2010) 9157.

[26] J. Park, A.N. Pasupathy, J.I. Goldsmith, C. Chang, Y. Yalsh, J.R. Petta, M. Rinkoski, J.P. Sethna, H.D. Abruña, P.L. McEuen, D.C. Ralph, Nature 417 (2002) 722.

[27] W. Liang, M.P. Shores, M. Bockrath, J.R. Long, H. Park, Nature 417 (2002) 725.

[28] I.-W.P. Chen, M.-D. Fu, W.-H. Tseng, J.-Y. Yu, S.-H. Wu, C.-J. Ku, C.-h. Chen, S.-M. Peng, Angew. Chem. Int. Ed. 45 (2006) 5814.

[29] B.S. Kim, J.M. Beebe, C. Olivier, S. Rigaut, D. Touchard, J.G. Kushmerick, X.-Y. Zhu, C.D. Frisbie, J. Phys. Chem. C 111 (2007) 7521.

[30] C. Olivier, B.S. Kim, D. Touchard, S. Rigaut, Organometallics 27 (2008) 509.

[31] A.K. Mahapatro, J. Ying, T. Ren, D.B. Janes, Nano Lett. 8 (2008) 2131.

[32] M. Ruben, A. Landa, E. Lörtscher, H. Riel, M. Mayor, H. Görls, H. Weber, A. Arnold, F. Evers, Small 4 (2008) 2229.

[33] E. Leary, H. Van Zalinge, S.J. Higgins, R.J. Nichols, F.F. di Biani, P. Leoni, L. Marchetti, P. Zanello, Phys. Chem. Chem. Phys. 11 (2009) 5198.

[34] A.M. Ricci, E.J. Calvo, S. Martin, R.J. Nichols, J. Am. Chem. Soc. 132 (2010) 2494.

[35] A. Benameur, P. Brignou, E. Di Piazza, Y.-M. Hervault, L. Norel, S. Rigaut, New J. Chem. 35 (2011) 2105.

[36] L. Luo, A. Benameur, P. Brignou, S.H. Choi, S. Rigaut, C.D. Frisbie, J. Phys. Chem. C 115 (2011) 19955.

[37] P.J. Mohan, V.P. Georgiev, J.E. McGrady, Chemical Sci. 3 (2012) 1319.

[38] S.J. Higgins, R.J. Nichols, S. Martin, P. Cea, H.S.J. van der Zant, M.M. Richter, P.J. Low, Organometallics 30 (2011) 7.

[39] P.J. Low, Dalton Trans. (2005) 2821.

[40] F. Prins, M. Monrabal-Capilla, E.A. Osorio, E. Coronado, H.S.J. van der Zant, Adv. Mater. 23 (2011) 1545.

[41] M. Haga, K. Kobayashi, T. Terada, *Coord. Chem. Rev.*, 2007, 251, 2688.

[42] G.J. Ashwell, L.J. Phillips, B.J. Robinson, B. Urasinka-Wojcik, C.J. Lambert, I.M. Grace, M.R. Bryce, R. Jitchati, M. Tavasli, T.I. Cox, I.C. Sage, R.P. Tuffin, S. Ray, ACS Nano 4 (2010) 7401.

[43] (a) X. Chen, S. Yeganeh, L. Qin, S. Li, C. Xue, A.B. Braunschweig, G.C. Schatz, M.A. Ratner, C.A. Mirkin, Nano Lett. 9 (2009) 3974 (b) E.A. Osorio, K. Moth-Poulsen, H.S.J. van der Zant, J. Paaske, P. Hedegard, K. Flensberg, J. Bendix, T. Bjornholm, Nano Lett. 10 (2010) 105.

[44] C.A. Martin, J.M. van Ruitenbeek, H.S.J. van der Zant, Nanotechnology 21 (2010) 265201.

[45] H. Song, Y. Kim, Y.H. Jang, H. Jeong, M.A. Reed, T. Lee, Nature 462 (2009) 1039.

[46] D.E. Richardson, H. Taube, Coord. Chem. Rev. 60 (1984) 107.

[47] W. Kaim, Eur. J. Inorg. Chem. (2012) 343.

[48] B.S. Brunschwig, C. Creutz, N. Sutin, Chem. Soc. Rev. 31 (2002) 168.

[49] M. Lohan, F. Justaud, T. Roisnel, P. Ecorchard, H. Lang, C. Lapinte, Organometallics 29 (2010) 4804.

[50] M. Lohan, F. Justaud, H. Lang, C. Lapinte, Organometallics 31 (2012) DOI 10.1021/om300050t.

[51] E.C. Fitzgerald, N.J. Brown, R. Edge, M. Helliwell, H.N. Roberts, F. Tuna, A. Beeby, D. Collison, P.J. Low, M.W. Whiteley, Organometallics 31 (2012) 157.

[52] B. Kaduk, T. Kowalczyk, T. Van Voorhis, Chem. Rev. 112 (2012) 321.

[53] A.V. Arbuznikov, M. Kaupp, J. Chem. Phys. 136 (2012) 014111.

[54] J. Plotner, D.J. Tozer, A. Dreuw, J. Chem. Theory and Comp. 6 (2010) 2315.

[55] P. Wiggins, J.A.G. Williams, D.J. Tozer, J. Chem. Phys. 131 (2009) 091101.

[56] L.O. Palsson, C.S. Wang, A.S. Batsanov, S.M. King, A. Beeby, A.P. Monkman, M.R. Bryce, Chem. Eur. J. 16 (2010) 1470.

[57] Q. Lu, K. Liu, H. Zhang, Z. Du, X. Wang, F. Wang, ACS Nano 3 (2009) 3861.

[58] T. Hines, I. Diez-Perez, J. Hihath, H. Liu, Z.-S. Wang, J. Zhao, G. Zhou, K. Müllen, N. Tao, J. Am. Chem. Soc. 132 (2010) 11658.

[59] O.S. Wenger, Acc. Chem. Res. 44 (2011) 25.

[60] L. Luo, S.H. Choi, C.D. Frisbie, Chem. Mater. 23 (2011) 631.

[61] C. Joachim, J.K. Gimzewski, A. Aviram, Nature 408 (2000) 541.

[62] M. Kiguchi, S. Kaneko, ChemPhysChem 13 (2012) 1116.

[63] N.A. Zimbovskaya, M.R. Pederson, Phys. Reports 509 (2011) 1.

[64] S. Rigaut, J. Perruchon, L. Le Pichon, D. Touchard, P.H. Dixneuf, J. Organomet. Chem. 670 (2003) 37.

[65] C. Creutz, M.D. Newton, N. Sutin, *J. Photochem. Photobiol. A*, 1994, 82, 47.

[66] C. Creutz, *Prog. Inorg. Chem.*, 1983, 30, 1.

[67] F. Paul, C. Lapinte, Coord. Chem. Rev. 178 (1998) 431.

[68] A. Ceccon, S. Santi, L. Orian, A. Bisello, Coord. Chem. Rev. 248 (2004) 683.

[69] M.D. Ward, Chem Soc. Rev. 24 (1995) 121.

[70] L.A. Bumm, J.J. Arnold, M.T. Cygan, T.D. Dunbar, T.P. Burgin, L. Jones II, D.L. Allara, J.M. Tour, P.S. Weiss, Science 271 (1996) 1705.

[71] For a general review of the molecular backbone see: U.H.F Bunz, Chem. Rev.100 (2000) 1605.

[72] M. Levitus, K. Schmieder, H. Ricks, K.D. Schimizu, U.H.F. Bunz, M.A. Garcia-Garibay, J. Am. Chem. Soc. 123 (2001) 4259.

[73] M. Levitus, K. Schmieder, H. Ricks, K.D. Schimizu, U.H.F. Bunz, M.A. Garcia-Garibay, J. Am. Chem. Soc. 124 (2002) 8181.

[74] K. Schmieder, M. Levitus, H. Dang, M.A. Garcia-Garibay, J. Phys. Chem. A 106 (2002) 1551.

[75] S.J. Greaves, E.L. Flynn, E.L. Futcher, E. Wrede, D.P. Lydon, P.J. Low, S.R. Rutter, A. Beeby, J. Phys. Chem. A 110 (2006) 2114.

[76] J. Seminario, A. Zacarias, J. Tour, J. Am. Chem. Soc. 120 (1998) 3970.

[77] K. Okuyama, T. Hasegawa, M. Ito, N. Mikami, J. Phys. Chem. 88 (1984) 1711.

[78] A.V. Abramenkov, A. Almenningen, B.N. Cyvin, S.J. Cyvin, T. Jonvik, L.S. Khaikin, C. Romming, L.V. Vilkonv, Acta Chim. Scand. A42 (1988) 674.

[79] K. Inoue, H. Takeuchi, S.J. Konaka, Chem. Phys. A 105 (2001) 6711.

[80] S. Toyota, *Chem. Rev.*, 2010, 110, 5398.

[81] H.E. Zimmerman, J.R. Dodd, J. Am. Chem. Soc. 92 (1970) 6507.

[82] A. Beeby, K.S. Findlay, A.E. Goeta, L. Porrès, S.R. Rutter, A.L. Thompson, Photochem. Photobiol. Sci. 6 (2007) 982.

[83] H. Nakayama, S. Kimura, J. Phys. Chem. A 115 (2011) 8960.

[84] G.T. Crisp, T.P. Bubner, Tetrahedron 53 (1997)11881.

[85] R. Shukla, D.M. Brody, S.V. Lindeman, R. Rathore, J. Org. Chem. 71 (2006) 6124.

[86] W. Hu, Q. Yan, D. Zhou, Chem. Eur. J. 17 (2011) 7087.

[87] W. Hu, N. Zhu, W. Tang, D. Zhao, J. Org. Chem. 10 (2008) 2669.

[88] A. Beeby, K. Findlay, P.J. Low, T.B. Marder, J. Am. Chem. Soc. 124 (2002) 8280.

[89] J. Kim, T.M. Swager, Nature 411 (2001) 1030.

[90] D.D. Nguyen, N.C. Jones, S.V. Hoffmann, S.H. Anderson, P.W. Thulstrup, J. Spanget-Larsen, Chem. Phys. 392 (2012) 130.

[91] A. Beeby, K. Findlay, P.J. Low, T.B. Marder, P. Matousek, A.W. Parker, S.R. Rutter, M. Towrie, Chem. Commun. (2003) 2406.

[92] M.I. Sluch, G. Godt, U.H.F. Bunz, M.A. Berg, J. Am. Chem. Soc. 123 (2001) 6447.

[93] L.M. Ballesteros, S. Martin, G. Pera, P.A. Schauer, N.J. Kay, M.C. Lopez, P.J. Low, R.J. Nichols, P. Cea, Langmuir 27 (2011) 3600.

[94] G. Pera, S. Martin, L.M. Ballesteros, A.J. Hope, P.J. Low, R.J. Nichols, P. Cea, Chem. Eur. J. 16 (2010) 13398.

[95] A. Villares, G. Pera, S. Martin, R. Nichols, D.P. Lydon, L. Applegarth, A. Beeby, P.J. Low, P. Cea, Chem. Mater. 22 (2010) 2041.

[96] A. Villares, D.P. Lydon, B.J. Robinson, G.J. Ashwell, F.M. Royo, P.J. Low, P. Cea, Surf. Sci., 602 (2008) 3683.

[97] A. Villares, D.P. Lydon, P.J. Low, B.J. Robinson, G.J. Ashwell, F.M. Royo, P. Cea, Chem. Mater. 20 (2008) 258.

[98] A. Villares, D.P. Lydon, L. Porres, A. Beeby, P.J. Low, P. Cea, F.M. Royo, J. Phys. Chem. B 111 (2007) 7201.

[99] H. Hamoudi, P. Kao, A. Nefedov, D.L. Allara, M. Zharnikov, Beilstein J. Nanotechnol. 3 (2012) 12.

[100] Z.J. Donhauser, B.A. Mantooth, K.F. Kelly, L.A. Bumm, J.D. Monnell, J.J. Stapleton, D.W. Price Jr., A.M. Rawlett, D.L. Allara, J.M. Tour, P.S. Weiss, Science 292 (2001) 2303.

[101] A.M. Moore, A.A. Dameron, B.A. Mantooth, R.K. Smith, D.J. Fuchs, J.W. Ciszek, F. Maya, Y. Yao, J.M. Tour, P.S. Weiss, J. Am. Chem. Soc. 128 (2006) 1959.

[102] G.K. Ramachandran, T.J. Hopson, A.M. Rawlett, L.A. Nagahara, A. Primak, S.M. Lindsay, Science 300 (2003) 1413.

[103] M.T. González, J. Brunner, R. Huber, S. Wu, C. Schönenberger, M. Calame, New J. Phys. 10 (2008) 065018.

[104] X. Li, J. He, J. Hihath, B. Xu, S.M. Lindsay, N. Tao, J. Am. Chem. Soc. 128 (2006) 2135.

[105] M. Kamenetska, M. Koentopp, A.C. Whalley, Y.S. Park, M.L. Steigerwald, C. Nuckolls, M.S. Hybertsen, L. Venkataraman, Phys. Rev. Lett. 102 (2009) 126803.

[106] W. Haiss, S. Martin, E. Leary, H. van Zalinge, S.J. Higgins, L. Bouffier, R.J. Nichols, J. Phys. Chem. C 113 (2009) 5823.

[107] L.M. Ballesteros, S. Martín, M.C. Momblona, S. Marqués-González, M.C. Lopez, R.J. Nichols, P.J. Low, P. Cea, J. Phys. Chem. (2012) accepted, in press.

[108] L. Venkataraman, J.E. Klare, I.W. Tam, C. Nuckolls, M.S. Hybertsen, M.L. Steigerwald, Nano Lett. 6 (2006) 458.

[109] M.S. Hybertsen, L. Venkataraman, J.E. Klare, A.C. Whalley, M.L. Steigerwald, C. Nuckolls, J. Phys.: Condens. Matter. 20 (2008) 374115.

[110] B. Xu, N.J. Tao, Science 301 (2003) 1221.

[111] B.-S. Kim, J.M. Beebe, C. Olivier, S. Rigaut, D. Touchard, J.G. Kushmerick, X.-Y. Zhu, C.D. Frisbie, J. Phys. Chem. C 111 (2007) 7521.

[112] Y.S. Park, A.C. Whalley, M. Kamenetska, M.L. Steigerwald, M.S. Hybertsen, C. Nuckolls, L. Venkataraman, J. Am. Chem. Soc. 129 (2007) 15768.

[113] D. Millar, L. Venkataraman, L.H. Doerrer, J. Phys. Chem. C 111 (2007) 17635.

[114] S. Ballmann, W. Hieringer, D. Secker, Q. Zheng, J.A. Gladysz, A. Gorling, H.B. Weber, ChemPhysChem 11 (2010) 2256.

[115] Z.-L. Cheng, R. Skouta, H. Vazquez, J.R. Widawsky, S. Schneebeli, W. Chen, M.S. Hybertsen, R. Breslow, L. Venkataraman, Nature Nanotech. 6 (2011) 353.

[116] W. Chen, J.R. Widawsky, H. Vázquez, S.T. Schneebeli, M.S. Hybertsen, R. Breslow, L. Venkataraman, J. Am. Chem. Soc. 133 (2011) 17160.

[117] J.S. Meisner, M. Kamenetska, M. Krikorian, M.L. Steigerwald, L. Venkataraman, C. Nuckolls, Nano Lett. 11 (2011) 1575.

[118] S.M. Lindsay, M.A. Ratner, Adv. Mater. 19 (2007) 23.

[119] J.-M. Noël, B. Sjöberg, R. Marsac, D. Zigah, J.-F. Bergamini, A. Wang, S. Rigaut, P. Hapiot, C. Lagrost, Langmuir 25 (2009) 12742.

[120] C. Olivier, B.S. Kim, D. Touchard, S. Rigaut, Organometallics 27 (2008) 209.

[121] R. Nast, *Angew. Chem. Int. Ed.*, 1965, 4, 366.

[122] K.A. Green, M.P. Cifuentes, M. Samoc, M.G. Humphrey, Coord. Chem. Rev. 255 (2011) 2530.

[123] K.A. Green, M.P. Cifuentes, M.Samoc, M.G. Humphrey, Coord. Chem. Rev. 255 (2011) 2025.

[124] Y. Fujikura, K. Sonogashira, N. Hagihara, *Chem. Letters*, 1975, 1067

[125] K. Sonogashira, Y. Fujikura, T. Yatake, N. Toyoshima, S. Takahashi,N. Hagihara, J. Organomet. Chem. 145 (1978) 101.

[126] S. Takahashi, Y. Ohyama, E. Murata, K. Songashira, N. Hagihara, J. Polym. Sci., Polym. Chem. Ed. 18 (1980) 349.

[127] S. Takahashi, E. Murata, K. Songashira, N. Hagihara, J. Polym. Sci., Polym. Chem. Ed. 18 (1980) 661.

[128] K. Sonogashira, K. Ohga, S. Takahashi, N. Hagihara, J. Organomet. Chem. 188 (1980) 237.

[129] H. Yamaguchi, K. Shinohara, K. Sonogashira, K. Yamaguchi, J. Polym. Sci., Part A: Polym. Chem. 25 (1987) 2281.

[130] R. Chinchilla, C. Najera, Chem. Soc. Rev. 40 (2011) 5084.

[131] M. Schilz, H. Plenio, J. Org. Chem. 77 (2012) 2798.

[132] J.S. Schumm, D.L. Pearson, J.M. Tour, Angew. Chem. Int. Ed. 33 (1994) 1360.

[133] D.P. Lydon, D. Albesa-Jové, G.C. Shearman, J.M. Seddon, J.A.K. Howard, T.B. Marder, P.J. Low, Liq. Cryst. 35 (2008) 119.

[134] D.P. Lydon, L. Porrès, A. Beeby, T.B. Marder, P.J. Low, New J. Chem. 29 (2005) 972.

[135] M.I. Bruce, Chem. Rev. 91 (1991) 197.

[136] P.J. Low, M.I. Bruce, Adv. Organomet. Chem. 48 (2002) 71.

[137] K. West, C.S. Wang, A.S. Batsanov, M.R. Bryce, J. Org. Chem. 71 (2006) 8541.

[138] K. West, L.N. Hayward, A.S. Batsanov, M.R. Bryce, Eur. J. Org. Chem. (2008) 5093.

[139] K. West, C.S. Wang, A.S. Batsanov, M.R. Bryce, Org. Biomol. Chem. 6 (2008) 1934.

[140] F. Creati, C. Coletti, N. Re, Organometallics 28 (2009) 6603.

[141] M.I. Bruce, Coord. Chem. Rev. 248 (2004) 1603.

[142] M.I. Bruce, P.J. Low, A. Werth, B.W. Skelton, A.H. White, J. Chem. Soc., Dalton Trans. (1996) 1551.

[143] M.I. Bruce, B.C. Hall, B.D. Kelly, P.J. Low, B.W. Skelton, A.H. White, J. Chem. Soc., Dalton Trans. (1999) 3719.

[144] T. Weyland, C. Lapinte, G. Frapper, M.J. Calhorda, J.-F. Halet, L. Toupet, Organometallics 16 (1997) 2024.

[145] D. Schneider, H. Werner, Angew. Chem., Int. Ed. Engl. 30 (1991) 700 .

[146] C. Gauss, D. Veghini, H. Berke, Chem. Ber. Recueil 130 (1997) 183.

[147] R.W. Lass, H. Werner, Inorg. Chim. Acta 369 (2011) 288.

[148] H. Katayama, C. Wada, K. Taniguchi, F. Ozawa, Organometallics 21 (2002) 3285.

[149] H. Katayama, F. Ozawa, Organometallics 17 (1998) 5190.

[150] R. Nast, J. Moritz, J. Organomet. Chem. 117 (1976) 81.

[151] L. Ballester, M. Cano, A. Santos, J. Organomet. Chem. 229 (1982) 101.

[152] S.K. Hurst, T. Ren, J. Organomet. Chem. 660 (2002) 1.

[153] M.I. Bruce, M.G. Humphrey, J.G. Mattisons, S.K. Roy, A.G. Swincer, Aust. J. Chem. 37 (1984) 1955.

[154] M.I. Bruce, M.Z. Ke, P.J. Low, Chem. Commun. (1996) 2405.

[155] M.I. Bruce, P.J. Low, M.Z. Ke, B.D. Kelly, B.W. Skelton, M.E. Smith, A.H. White, N.B. Witton, Aust. J. Chem. 54 (2001) 453.

[156] N. St Fleur, J.C. Hili, A. Mayr, Inorg. Chim. Acta 362 (2009) 1571.

[157] L. Medei, O.V. Semeikin, M.G. Peterleitner, N.A. Ustynyuk, S. Santi, C. Durante, A. Ricci, C. Lo Sterzo, Eur. J. Inorg. Chem. (2006) 2582.

[158] A. La Groia, A. Ricci, M. Bassetti, D. Masi, C. Bianchini, C. Lo Sterzo, J. Organomet. Chem. 683 (2003) 406.

[159] K. Venkatesan, T. Fox, H.W. Schmalle, H. Berke, Eur. J. Inorg. Chem. (2005) 901.

[160] S. Kheradmandan, T. Fox, H.W. Schmalle, K. Venkatesan, H. Berke, Eur. J. Inorg. Chem. (2004) 3544.

[161] M.S. Khan, S.J. Davies, A.K. Kakkar, D. Schwartz, B. Lin, B.F.G. Johnson, J. Lewis, J. Organomet. Chem. 424 (1992) 87 .

[162] S.J. Davies, B.F.G. Johnson, M.S. Khan, J. Lewis, J. Chem. Soc., Chem. Commun. (1991) 187.

[163] S.J. Davies, B.F.G. Johnson, M.S. Khan, J. Lewis, J. Chem. Soc., Chem. Commun. (1991) 187.

[164] H.B. Fyfe, M. Miekuz, D. Zagarian, N.J. Taylor, T.B. Marder, J. Chem. Soc., Chem. Commun. (1991) 188.

[165] C.W. Faulkner, S.L. Ingram, M.S. Khan, J. Lewis, N.J. Long, P.R. Raithby, J. Organomet. Chem. 482 (1994) 139.

[166] M.H. Perez-Temprano, J.A. Casares, P. Espinet, *Chem. Eur. J.*, 2012, 18, 1864.

[167] W.M. Khairul, M.A. Fox, N.N. Zaitseva, M. Gaudio, D.S. Yufit, B.W. Skelton, A.H. White, J.A.K. Howard, M.I. Bruce, P.J. Low, Dalton Trans. (2009) 610.

[168] T. Ren, Chem. Rev. 108 (2008) 4185.

[169] M.E. Smith, R.L. Cordiner, D. Albesa-Jové, D.S. Yufit, F. Hartl, J.A.K. Howard, P.J. Low, Can. J. Chem. 84 (2006) 154.

[170] A. Wong, P.C.W. Kang, C.D. Tagge, D.R. Leon, Organometallics 9 (1990) 1992.

[171] R.L. Cordiner, M.E. Smith, A.S. Batsanov, D. Albesa-Jové, F. Hartl, J.A.K. Howard, P.J. Low, Inorg. Chim. Acta 359 (2006) 946.

[172] M.I. Bruce, K. Costuas, B.G. Ellis, J.F. Halet, P.J. Low, B. Moubaraki, K.S. Murray, N. Ouddaï, G.J. Perkins, B.W. Skelton, A.H. White, Organometallics 26 (2007) 3735.

[173] M.I. Bruce, M.Z. Ke, P.J. Low, B.W. Skelton, Organometallics 17 (1998) 3539.

[174] R.L. Cordiner, D. Corcoran, D.S. Yufit, A.E. Goeta, J.A.K. Howard, P.J. Low, Dalton Trans. (2003) 3541.

[175] M.I. Bruce, N. Scoleri, B.W. Skelton, J. Organomet. Chem. 696 (2011) 3473.

[176] M.I. Bruce, J.C. Morris, C.R. Parker, B.W. Skelton, J. Organomet. Chem. 696 (2011) 3292.

[177] M.I. Bruce, M.A. Fox, P.J. Low, B.K. Nicholson, C.R. Parker, W.C. Patalinghug, B.W. Skelton, A.H. White, Organometallics 31 (2012) 2639.

[178] M.I. Bruce, P.J. Low, M.Z. Ke, B.D. Kelly, B.W. Skelton, M.E. Smith, A.H. White, N.B. Witton, Aust. J. Chem. 54 (2001) 453.

[179] M.I. Bruce, J. Davy, B.C. Hall, Y.J. Van Galen, B.W. Skelton, A.H. White, Appl. Organomet. Chem. 16 (2002) 559.

[180] J. Courmarcel, G. Le Gland, L. Toupet, F. Paul, C. Lapinte, J. Organomet. Chem. 670 (2003) 108.

[181] M.I. Bruce, B.C. Hall, P.J. Low, B.W. Skelton, A.H. White, J. Organomet. Chem. 592 (1999) 74.

[182] J.E. McGrady, T. Lovell, R. Stranger, M.G. Humphrey, Organometallics 16 (1997) 4004.

[183] F. Paul, B.G. Ellis, M.I. Bruce, L. Toupet, T. Roisnel, K. Costuas, J.-F. Halet, C. Lapinte, Organometallics 25 (2006) 649.

[184] M.I. Bruce, A. Burgun, F. Gendron, G. Grelaud, J.-F. Halet, B.W. Skelton, Organometallics 30 (2011) 2861.

[185] D.L. Lichtenberger, S.K. Renshaw, A. Wong, C.D. Tagge, Organometallics 12 (1993) 3522.

[186] D.L. Lichtenberger, S.K. Renshaw, R.M. Bullock, J. Am. Chem. Soc. 115 (1993) 3276.

[187] K. Costuas, S. Rigaut, Dalton Trans. (2011) 5643.

[188] G. Frapper, M. Kertsz, Inorg. Chem. 32 (1993) 732.

[189] N. Ouddai, K. Costuas, M. Bencharif, J.-Y. Saillard, J.-F. Halet, C.R. Chem. 8 (2005) 1336.

[190] N. Gauthier, N. Tchouar, F. Justaud, G. Argouarch, M.P. Cifuentes, L. Toupet, D. Touchard, J.-F. Halet, S. Rigaut, M.G. Humphrey, K. Costuas, F. Paul, Organometallics 28 (2009) 2253.

[191] (a) J.D. Manna, K.D. John, M.D. Hopkins, Adv. Organomet. Chem. 38 (1995) 79. (b) O.F. Koentjoro, R. Rousseau, P.J. Low, Organometallics 20 (2001) 4502.

[192] W.M. Khairul, M.A. Fox, P.A. Schauer, D. Albesa-Jové, D.S. Yufit, J.A.K. Howard, P.J. Low, Inorg. Chim. Acta 374 (2011) 461.

[193] M.A. Fox, R.L. Roberts, W.M. Khairul, F. Hartl, P.J. Low, J. Organomet. Chem. 692 (2007) 3277.

[194] W. Kaim, J. Fielder, Chem. Soc. Rev. 38 (2009) 3373.

[195] S.P. Best, S.J. Borg, K.A. Vincent, in W. Kaim, A. Klein (Eds), *Spectroelectrochemistry*, RSC Publishing, 2008, pp 1-30]

[196] For early interpretations see M.I. Bruce, G.A. Koutsantonis, M.J. Liddell, E.R.T. Tiekink, J. Organomet. Chem. 420 (1991) 253.

[197] G.T. Dalton, M.P. Cifuentes, L.A. Watson, S. Petrie, R. Stranger, M. Samoc, M.G. Humphrey, Inorg. Chem. 48 (2009) 6534.

[198] B. Babgi, L. Rigamonti, M.P. Cifuentes, T.C. Corkery, M.D. Randles, T. Schwich, S. Petrie, R. Stanger, A. Teshome, I. Asselberghs, K. Clays, M. Samoc, M.G. Humphrey, J. Am. Chem. Soc. 131 (2009) 10293.

[199] N.J. Brown, D. Collison, R. Edge, E.C. Fitzgerald, M. Helliwell, J.A.K. Howard, H.N. Lacashire, P.J. Low, J.J.W. McDouall, J. Raftery, C.A. Smith, D.S. Yufit, M.W. Whiteley, Organometallics 29 (2010) 1261.

[200] M. Elian, M.M.L. Chen, D.M.P. Mingos, R. Hoffmann, Inorg. Chem. 15 (1976) 1148.

[201] M. Tamm, A. Kunst, T. Bannenberg, E. Herdtweck, R. Schmid, Organometallics 24 (2005) 3163.

[202] A. Glockner, T. Bannenberg, M. Tamm, A.M. Arif, R.D. Ernst, Organometallics 28 (2009) 5866.

[203] H. Wang, Y. Xie, R.B. King, H.F. Schaefer III, Eur. J. Inorg. Chem. (2008) 3698.

[204] P.H. Rieger, Coord. Chem. Rev. 135-136 (1994) 203.

[205] H.N. Lancashire, N.J. Brown, L. Carthy, D. Collison, E.C. Fitzgerald, R. Edge, M. Helliwell, M. Holden, P.J. Low, J.J.W. McDouall, M.W. Whiteley, Dalton Trans. 40 (2011) 1267.

[206] H.N. Roberts, N.J. Brown, R. Edge, R. Lewin, D. Collison, P.J. Low, M.W. Whiteley, Organometallics 30 (2011) 3763.

[207] E. Carter, D. Collison, R. Edge, E.C. Fitzgerald, H.N. Lancashire, D.M. Murphy, J.J.W. McDouall, J. Sharples, M.W. Whiteley, Dalton Trans. 39 (2010) 11424.

[208] R.L. Beddoes, C. Bitcon, A. Ricalton, M.W. Whiteley, J. Organomet. Chem. 367 (1989) C21.

[209] N.J. Brown, D. Collison, R. Edge, E.C. Fitzgerald, P.J. Low, M. Helliwell, Y.T. Ta, M.W. Whiteley, Chem. Commun. 46 (2010) 2253.

[210] M.I. Bruce, P.J. Low, Adv. Inorg. Chem. 50 (2004) 179.

[211] B. Xi, T. Ren, C.R. Chemie, 12 (2009) 321.

[212] P. Aguirre-Etcheverry, D. O'Hare, Chem. Rev. 110 (2010) 4839.

[213] M. Akita, T. Koike, Dalton Trans. (2008) 3523.

[214] G.A. Koutsantonis, J.P. Selegue, J. Am. Chem. Soc. 113 (1991) 2316.

[215] J.P. Selegue, Coord. Chem. Rev. 248 (2004) 1543.

[216] K.R. Dunbar, R.A. Heintz, Prog. Inorg. Chem. 45 (1997) 283.

[217] W. Kaim, Angew. Chem. Int. Ed. 50 (2011) 10498.

[218] S. Kherahmandan, K. Venkatean, O. Blacque, H.W. Schmalle, H. Berke, Chem. Eur. J. 10 (2004) 4872.

[219] M.I. Bruce, B.D. Kelly, B.W. Skelton, A.H. White, J. Organomet. Chem. 604 (2000) 150.

[220] M.I. Bruce, B.G. Ellis, P.J. Low, B.W. Skelton, A.H. White, Organometallics 22 (2003) 3184.

[221] (a) N. Le Narvor, C. Lapinte, J. Chem. Soc., Chem. Commun. (1993) 357. (b) F. Coat, C. Lapinte, Organometallics 15 (1996) 477. (c) F. Coat, M.-A. Guillevic, L. Toupet, F. Paul, C. Lapinte, Organometallics 16 (1997) 5988.

[222] M.I. Bruce, K. Costuas, T. Davin, J.F. Halet, K.A. Kramarczuk, P.J. Low, B.K. Nicholson, G.J. Perkins, R.L. Roberts, B.W. Skelton, M.E. Smith, A.H. White, Dalton Trans. (2007) 5387.

[223] P.A. Schauer, P.J. Low, Eur. J. Inorg. Chem. (2012) 390.

[224] A.B. Antonova, M.I. Bruce, B.G. Ellis, M. Guadio, P.A. Humphrey, M. Jevric, G. Melino, B.K. Nicholson, G.J. Perkins, B.W. Skelton, B. Stapleton, A.H. White, N.N. Zaitseva, Chem. Commun. (2004) 960.

[225] P. Belanzoni, N. Re, A. Sgamellotti, C. Floriani, J. Chem. Soc., Dalton Trans., 1997, 4773.

[226] M.I. Bruce, P.J. Low, K. Costuas, J.F. Halet, S.P. Best, G.A. Heath, J. Am. Chem. Soc. 122 (2000) 1949.

[227] M.I. Bruce, J.-F. Halet, B. Le Guennic, B.W. Skelton, M.E. Smith, A.H. White, Inorg. Chim. Acta, 350 (2003) 175.

[228] H. Jiao, K. Costuas, J.A. Gladysz, J.-F. Halet, M. Guillemot, L. Toupet, F. Paul, C. Lapinte, J. Am. Chem. Soc. 125 (2003) 9511.

[229] M.I. Bruce, B.G. Ellis, M. Gaudio, C. Lapinte, G. Melino, F. Paul, B.W. Skelton, M.E. Smith, L. Toupet, A.H. White, Dalton Trans. 2004, 1601.

[230] N. Le Narvor, L. Toupet, C. Lapinte, J. Am. Chem. Soc. 117 (1995) 7129.

[231] M.I. Bruce, K. Costuas, T. Davin, B.G. Ellis, J.F. Halet, C. Lapinte, P.J. Low, M.E. Smith, B.W. Skelton, L. Toupet, A.H. White, Organometallics 24 (2005) 3864.

[232] (a) F. Paul, W.E. Meyer, L. Toupet, H. Jiao, J.A. Gladysz, C. Lapinte, J. Am. Chem. Soc. 122 (2000) 9405. (b) M. Brady, W. Weng, Y. Zhou, J.W. Seyler, A.J. Amoroso, A.M. Arif, M. Böhme, G. Frenking, J.A. Gladysz, J. Am. Chem. Soc. 119 (1997) 775.

[233] J.J. Concepcion, D.M. Dattelbaum, T.J. Meyer, R.C. Rocha, Phil. Trans. R. Soc. A 366 (2008) 163.

[234] S.N. Semenov, O. Blacque, T. Fox, K. Venkatesan, H. Berke, J. Am. Chem. Soc. 132 (2010) 3115.

[235] J. Aihara, J. Am. Chem. Soc. 100 (1978) 3339.

[236] P.v.R. Schleyer, C. Maerker, A. Dransfield, H. Jiao, N.J.R.v.E. Hommes, J. Am. Chem. Soc. 118 (1996) 6317.

[237] R.B. King, Chem. Rev. 101 (2001) 1119.

[238] J. Vincente, M.-T. Chicote, M.M. Alavarez-Falcón, M.A. Fox, D. Bautista, Organometallics 22 (2003) 4792.

[239] H. Jude, H. Disteldorf, S. Fischer, T. Wedge, A.M. Hawkridge, A.M. Arif, M.F. Hawthorne, D.C. Muddiman, P.J. Stang, J. Am. Chem. Soc. 127 (2005) 12131.

[240] T.J. Wedge, A. Herzog, R. Huertas, M.W. Lee, C.B. Knobler, M.F. Hawthorne, Organometallics, 23 (2004) 482.

[241] D. Hablot, A. Sutter, P. Retailleau, R. Ziessel, Chem. Eur. J., 18 (2012) 1890.

[242] B.P. Dash, R. Satapathy, J.A. Maguire, N.S. Hosmane, New J. Chem. 35 (2011) 1955.

[243] R. Zeissel, G. Ulrich, J.H. Olivier, T. Bura, A. Sutter, Chem. Commun. 46 (2010) 7978.

[244] B. Le Guennic, K. Costuas, J.F. Halet, C. Nervi, M.A.J. Paterson, M.A. Fox, R.L. Roberts, D. Albesa-Jové, H. Puschmann, J.A.K. Howard, P.J. Low, C. R. Chemie 8 (2005) 1883.

[245] M.A. Fox, M.A.J. Paterson, C. Nervi, F. Galeotti, H. Puschmann, J.A.K. Howard, P.J. Low, Chem. Commun. (2001) 1610.

[246] M.A. Fox, T.E. Baines, D. Albesa-Jové, J.A.K. Howard, P.J. Low, J. Organomet. Chem. 691 (2006) 3889.

[247] M.A. Fox, R.L. Roberts, T.E. Baines, B. Le Guennic, J.F. Halet, F. Hartl, D.S. Yufit, D. Albesa-Jové, J.A.K. Howard, P.J. Low, J. Am. Chem. Soc. 130 (2008) 3566.

[248] N.J. Brown, H.N. Lancashire, M.A. Fox, D. Collison, R. Edge, D.S. Yufit, J.A.K. Howard, M.W. Whiteley, P.J. Low, Organometallics 30 (2011) 884.

[249] P.J. Low, N.J. Brown, J. Cluster Sci. 21 (2010) 235.

[250] D.M. D'Alessandro, F.R. Keene, Dalton Trans. (2004) 3950.

[251] D.M. D'Alessandro, F.R. Keene, Chem. Soc. Rev. 35 (2006) 424.

[252] F. Barrière, N. Camire, W.E. Geiger, U.T. Mueller-Westerhoff, R. Sanders, J. Am. Chem. Soc. 124 (2002) 7262.

[253] F. Barrière, W.E. Geiger, J. Am. Chem. Soc. 128 (2006) 3980.

[254] W.E. Geiger, F. Barrière, Acc. Chem. Res. 43 (2010) 1030.

[255] S.D. Glover, B.J. Lear, J.C. Salsman, C.H. Londergan, C.P. Kubiak, Phil. Trans. R. Soc. A 366 (2006) 177.

[256] K.D. Demadis, C.M. Hartshorn, T.J. Meyer, Chem. Rev. 101 (2001) 2655.

[257] R.C. Rocha, F.N. Rein, H. Jude, A.P. Shreve, J.J. Concepcion, T.J. Meyer, Angew. Chem. Int. Ed. 47 (2008) 503.

[258] S. Ibn Ghazala, F. Paul, L. Toupet, T. Roisnel, P. Hapiot, C. Lapinte, J. Am. Chem. Soc. 128 (2006) 2463.

[259] M.I. Chung, X. Gu, B.A. Etzenhouser, A.M. Spuches, P.T. Rye, S.K. Seetharaman, D.J. Rose, J. Zubieta, M.B. Sponsler, Organometallics 22 (2003) 3485.

[260] A. Dreuw, J.L. Weisman, M. Head-Gordon, J. Chem. Phys. 119 (2003) 2943.

[261] M.J.G. Peach, P. Benfield, T. Helgaker, D.J. Tozer, J. Chem. Phys. 128 (2008) 8425.

[262] M. Kaupp, M. Renz, M. Parthey, M. Stolte, F. Würthner, C. Lambert, Phys. Chem. Chem. Phys. 13 (2011) 16973.

[263] L. Weber, D. Eickhoff, T.B. Marder, M.A. Fox, P.J. Low, A.D. Dwyer, D.J. Tozer, S. Schwedler, A. Brockhinke, H.-G. Stammler, B. Neumann, Chem. Eur. J. 18 (2012) 1369.

[264] A.V. Arbuznikov, M. Kaupp, J. Chem. Phys. 136 (2012) 014111.

[265] See, for example, C. Egler-Lucas, O. Blacque, K. Venkatesan, A. Lopez-Hernandez, H. Berke, Eur. J. Inorg. Chem. (2012) 1536.

[266] L.D. Field, A.M. Magill, T.K. Shearer, S.B. Colbran, S.T. Lee, S.J. Dalgarno, M.M. Bhadbhade, Organometallics 29 (2010) 957.

[267] Y. Matsuura, Y. Tanaka, M. Akita, J. Organomet. Chem. 694 (2009) 1840.

[268] Q.Y. Hu, G. Jia, Can. J. Chem. 87 (2009) 134.

[269] L.-B. Gao, J. Kan, Y. Fan, L.-Y. Zhang, S.-H. Liu, Z.-N. Chen, Inorg. Chem. 46 (2007) 5651.

[270] L. Medei, O.V. Semeikin, M.G. Peterleitner, N.A. Ustynyuk, S. Santi, C. Durante, A. Ricci, C. Lo Sterzo, Eur. J. Inorg. Chem. (2006) 2582.

[271] A. Klein, O. Lavastre, J. Fiedler, Organometallics 25 (2006) 635.

[272] L.-B. Gao, L.-Y. Zhang, Z.-N. Chen, Organometallics 24 (2005) 1678.

[273] L.D. Field, A.V. George, F. Laschi, E.Y. Malouf, P. Zanello, J. Organomet. Chem. 435 (1992) 347.

[274] N. Gauthier, G. Argouarch, F. Paul, M.G. Humphrey, L. Toupet, S. Ababou-Girard, H. Sabbah, P. Hapiot, B. Fabre, Adv. Mater. 20 (2008) 1952.

[275] F.D. Pevny, E. Di Piazza, L. Norel, M. Drescher, R.F. Winter, S. Rigaut, Organometallics 29 (2010) 5912.

[276] (a) J. Maurer, M. Linseis, B. Sarkar, B. Schwederski, M. Niemeyer, W. Kaim, S. Zalis, C. Anson, M. Zabel, R.F. Winter, J. Am. Chem. Soc. 130 (2008) 259. (b) P. Mücke, M. Linseis, S. Zalis, R.F. Winter, Inorg. Chim. Acta 374 (2011) 36. (c) E. Wuttke, F. Pevny, Y.M. Hervault, L. Norel, M. Drescher, R.F. Winter, S. Rigaut, Inorg. Chem. 51 (2012) 1902.

[277] W.Y. Man, J.-L. Xia, N.J. Brown, J.D. Farmer, D.S. Yufit, J.A.K. Howard, S.H. Liu, P.J. Low, Organometallics 30 (2011) 1852.

[278] B.J. Lear, M.H. Chisholm, Inorg. Chem. 48 (2009) 10954.

[279] M.C.B. Colbet, J. Lewis, N.J. Long, P.R. Raithby, M. Younus, A.J.P. White, D.J. Williams, N.N. Payne, L. Yellowlees, D. Beljonne, N. Chawdhury, R.H. Friend, Organometallics 17 (1998) 3034.

[280] D. Beljonne, M.C.B. Colbert, P.R. Raithby, R.H. Friend, J.L. Brédas, Synth Met. 81 (1996) 179.

[281] D.J. Armitt, M.I. Bruce, M. Gaudio, N.N. Zaitseva, B.W. Skelton, A.H. White, B. Le Guennic, J.F. Halet, M.A. Fox, R.L. Roberts, F. Hartl, P.J. Low, Dalton Trans. (2008) 6763.

[282] M.A. Fox, J.D. Farmer, R.L. Roberts, M.G. Humphrey, P.J. Low, Organometallics 28 (2009) 5266.

[283] N.J. Long, A.J. Martin, F.F. di Biani, P. Zanello, J. Chem. Soc., Dalton Trans. (1998) 2017.

[284] S.K. Hurst, M.P. Cifuentes, M.G. Humphrey, Organometallics 21 (2002) 2353.

[285] C.E. Powell, S.K. Hurst, J.P. Morrall, M.P. Cifuentes, R.L. Roberts, M. Samoc, M.G. Humphrey, Organometallics 26 (2007) 4456.

[286] M.E. Stoll, S.R. Lovelace, W.E. Geiger, H. Schimanke, I. Hyla-Kryspin, R. Gleiter, J. Am. Chem. Soc. 121 (1999) 9343.

[287] C.G. Atwood, W.E. Geiger, J. Am. Chem. Soc. 122 (2000) 5477.

[288] I.R. Whittall, M.G. Humphrey, S. Houbrechts, J. Maes, A. Persoons, S. Schmid, D.C.R. Hockless, J. Organomet. Chem. 544 (1997) 277.

[289] (a) F. Paul, A. Bondon, G. da Costa, F. Malvolti, S. Sinbandhit, O. Cador, K. Costuas, L. Toupet, M.-L. Boillot, Inorg. Chem. 48 (2009) 10608. (b) K. Costuas, O. Cador, F. Justaud, S. Le Stang, F. Paul, A. Monari, S. Evangelisi, L. Toupet, C. Lapinte, J.-F. Halet, Inorg. Chem. 50 (2011) 12601.

[290] L. Bonniard, S. Kahlal, A.K. Diallo, C. Ornelas, T. Roisnel, G. Manca, J. Rodrigues, J. Ruiz, D. Astruc, J.-Y. Saillard, Inorg. Chem. 50 (2011) 114.

[291] A.C. Benniston, A. Harriman, P. Li, C.A. Sams, M.D. Ward, J. Am. Chem. Soc. 126 (2004) 13630.

[292] M.H. Chisholm, F. Feil, C.M. Hadad, N.J. Patmore, J. Am. Chem. Soc. 127 (2005) 18150.

[293] P.P. Romanczyk, K. Noga, A.J. Wlodarczyk, W. Nitek, E. Broclawik, Inorg. Chem. 49 (2010) 7676.

[294] F. Otón, I. Ratera, A. Espinosa, A. Tárranga, J. Veciana, P. Molina, Inorg. Chem. 49 (2010) 3183.

[295] C. Olivier, K. Costuas, S. Choua, V. Maurel, P. Turek, J.-Y. Saillard, D. Touchard, S. Rigaut, J. Am. Chem. Soc. 132 (2010) 5638.

[296] F. Paul, F. Malvolti, G. da Costa, S. Le Stang, F. Justaud, G. Argouarch, A. Bondon, S. Sinbandhit, K. Costuas, L. Toupet, C. Lapinte, Organometallics, 29 (2010) 2491

[297] J.M. Keller, K.D. Glusac, E.O.. Danilov, S. McIlroy, P. Sreerouthai, A.R. Cook, H. Jiang, J.R. Miller, K.S. Schanze, J. Am. Chem. Soc. 133 (2011) 11289.

[298] K. Glusac, M.E. Koese, H. Jiang, K.S. Schanze, J. Phys. Chem. B 111 (2007) 929.

[299] M.A. Fox, B. Le Guennic, R. L. Roberts, D.A. Brue, D.S. Yufit, J.A.K. Howard, G. Manca, J.-F. Halet, F. Hartl, P.J. Low, J. Am. Chem. Soc. 133 (2011) 18433.

[300] Y.A. Berlin, G.R. Hutchinson, P. Rempala, M.A. Ratner, J. Michl, J. Phys Chem. A 107 (2003) 3970.

[301] S.C. Jones, C. Coropceanu, S. Barlow, T. Kinnibrugh, T. Timofeeva, J.-L. Brédas, S.R. Marder, J. Am. Chem. Soc. 126 (2004) 11782.

[302] E.C. Fitzgerald, A. Ladjarafi, N.J. Brown, D. Collison, K. Costuas, R. Edge, J.-F. Halet, F. Justaud, P.J. Low, H. Meghezzi, T. Roisnel, M.W. Whiteley, C. Lapinte, Organometallics 30 (2011) 4180.

[303] N. Gauthier, C. Olivier, S. Rigaut, D. Touchard, T. Roisnel, M.G. Humphrey, F. Paul, Organometallics, 2008, 27, 1063

[304] N. Gauthier, G. Argouarch, F. Paul, L. Toupet, A. Ladjarafi, K. Costuas, J.-F. Halet, M. Samoc, M.P. Cifuentes, T.C. Corkery, M.G. Humphrey, Chem. Eur. J. 17 (2011) 5561.

[305] K.M.-C. Wong, S.C.-F. Lam, C.-C. Ko, N. Zhu, V.W.-W. Yam, S. Roué, C. Lapinte, S. Fathallah, K. Costuas, S. Kahlal, J.-F. Halet, Inorg. Chem. 42 (2003) 7086.

[306] L. Chen, J.E. Yarnell, K.D. Glusac, K.S. Schanze, J. Phys. Chem. B 114 (2010) 14763.

[307] J.M. Keller, K.S. Schanze, Organometallics 28 (2009) 4210.

[308] F. Coat, F. Paul, C. Lapinte, L. Toupet, K. Costuas, J.-F. Halet, J. Organomet. Chem. 683 (2003) 368.

[309] W.M. Khairul, M.A. Fox, P.A. Schauer, D.S. Yufit, D. Albesa-Jové, J.A.K. Howard, P.J. Low, Dalton Trans. 39 (2010) 11605.

[310] G.T. Dalton, M.P. Cifuentes, S. Petrie, R. Stranger, M.G. Humphrey, M. Samoc, J. Am. Chem. Soc. 129 (2007) 11882.

[311]. C. Wang, A.S. Batsanoc, M.R. Bryce, S. Martin, R.J. Nichols, S.J. Higgins, V.M. Garcia-Suárez, C.J. Lambert, *J. Am. Chem. Soc.*, 2009, 131, 15647.

Figure 1

Click here to download high resolution image

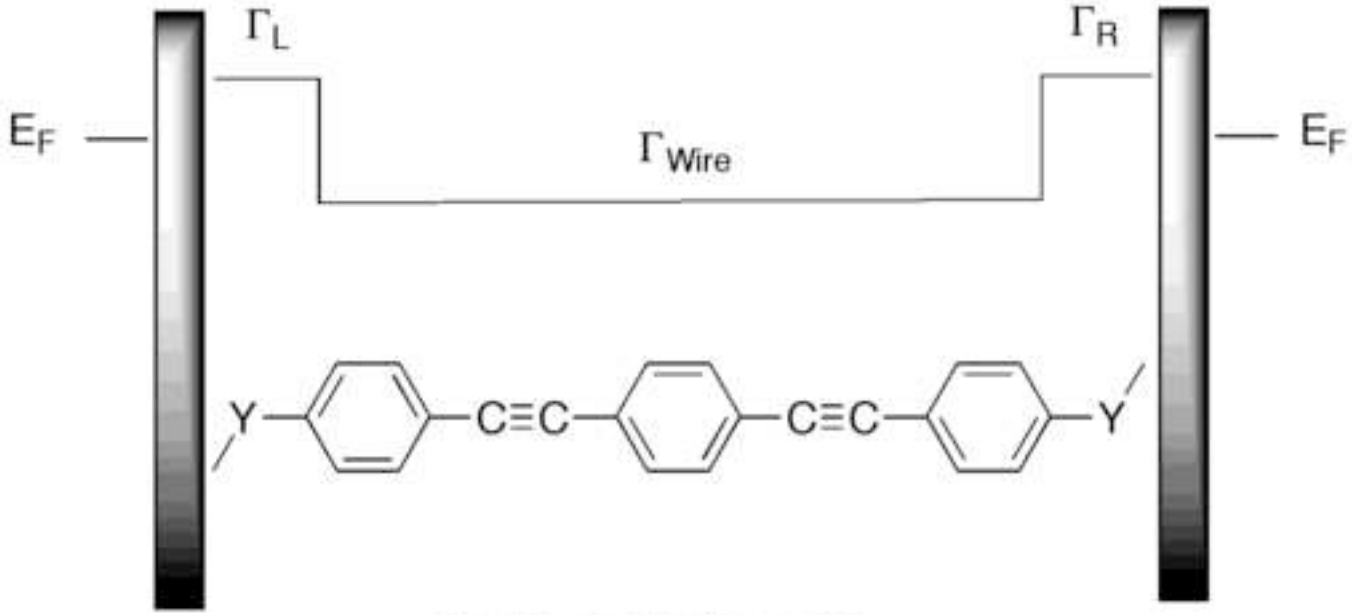

simple synthetic routes
functional group tolerence
extended π–conjugation
relatively large HOMO-LUMO gap

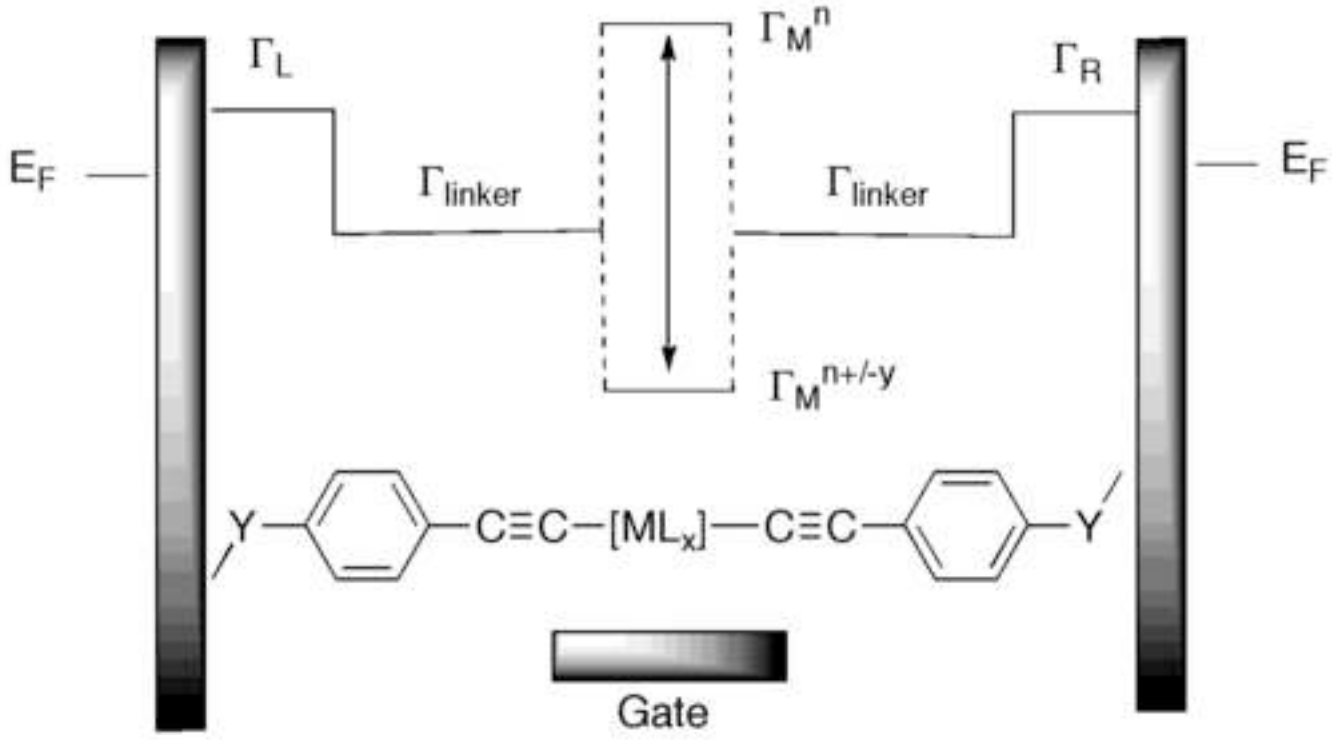

redox active over narrow potential range
tuneable electronic properties through M and L
chemically controlable high / low spin characteristics
modular synthesis
ML_x can serve as tunnel barrier or conduit

Figure 2

Click here to download high resolution image

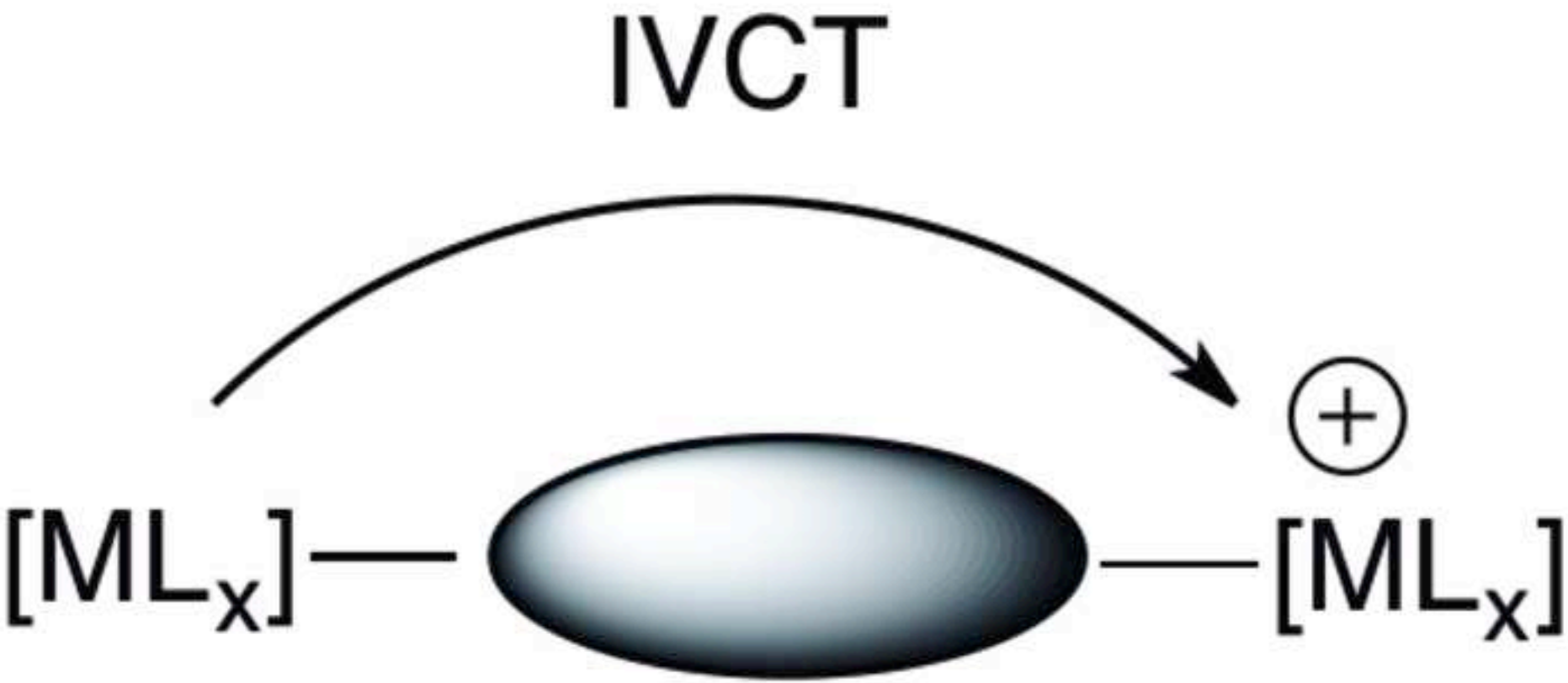

Figure 3

Click here to download high resolution image

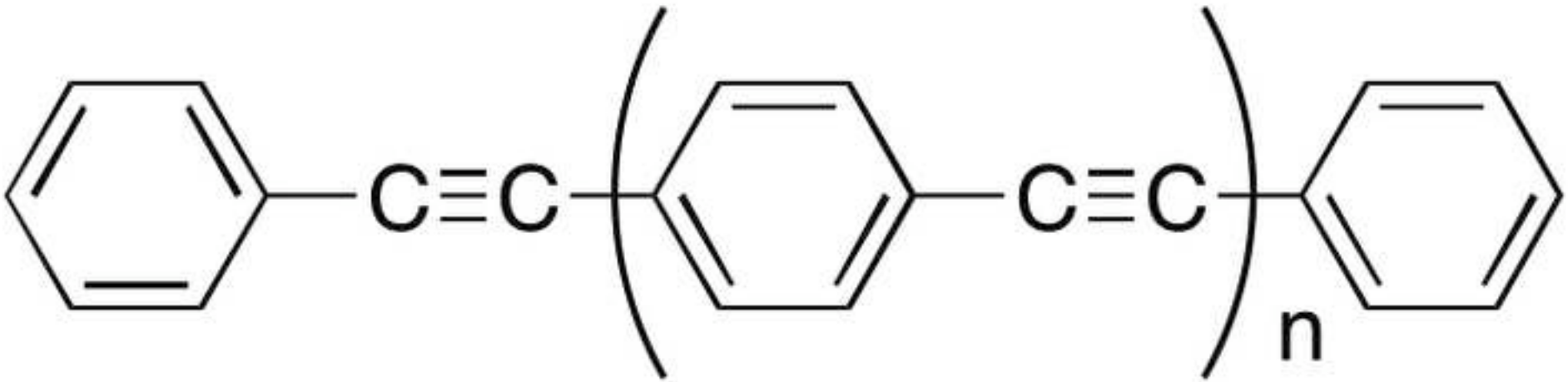

Figure 4

Click here to download high resolution image

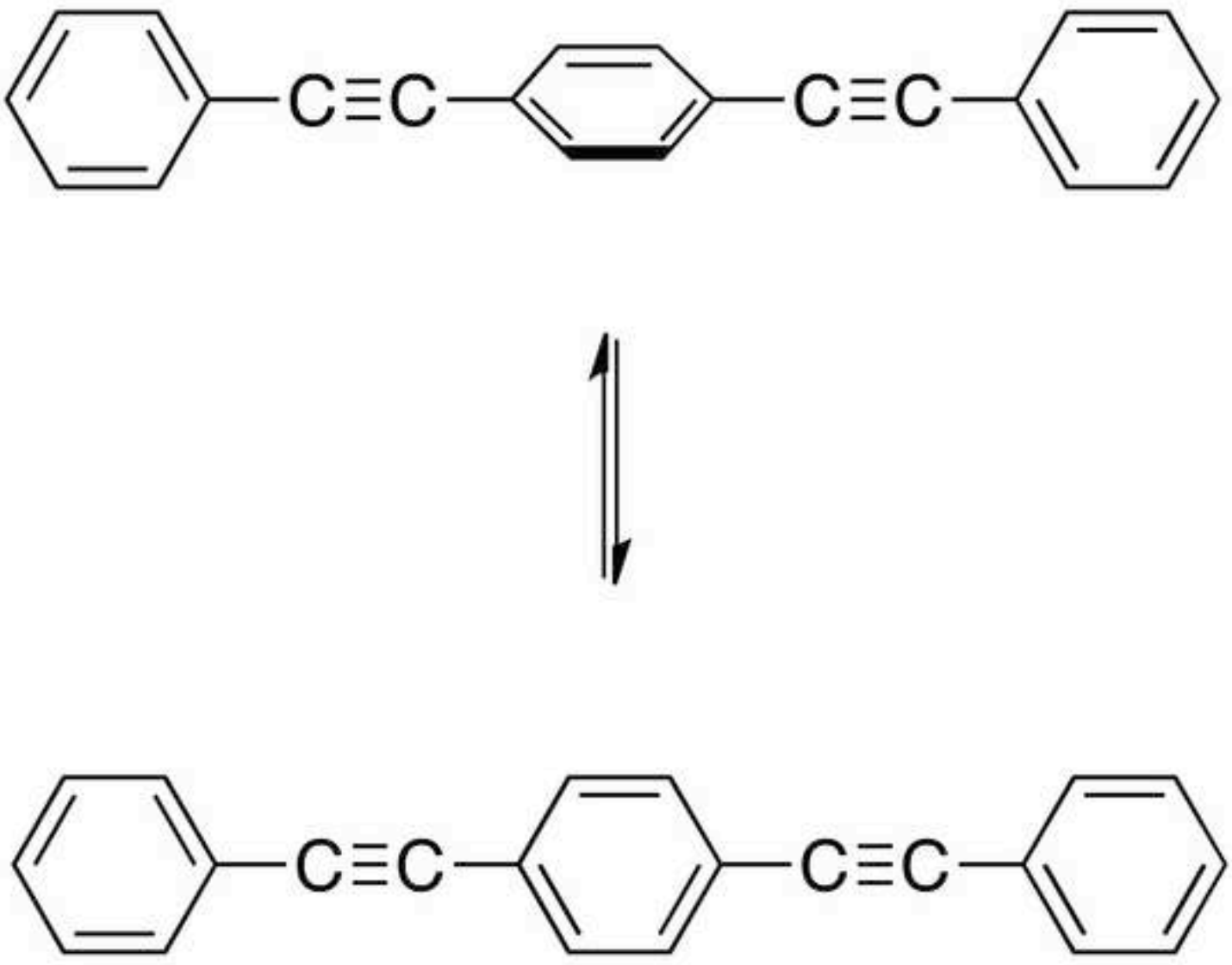

1

Figure 5

Click here to download high resolution image

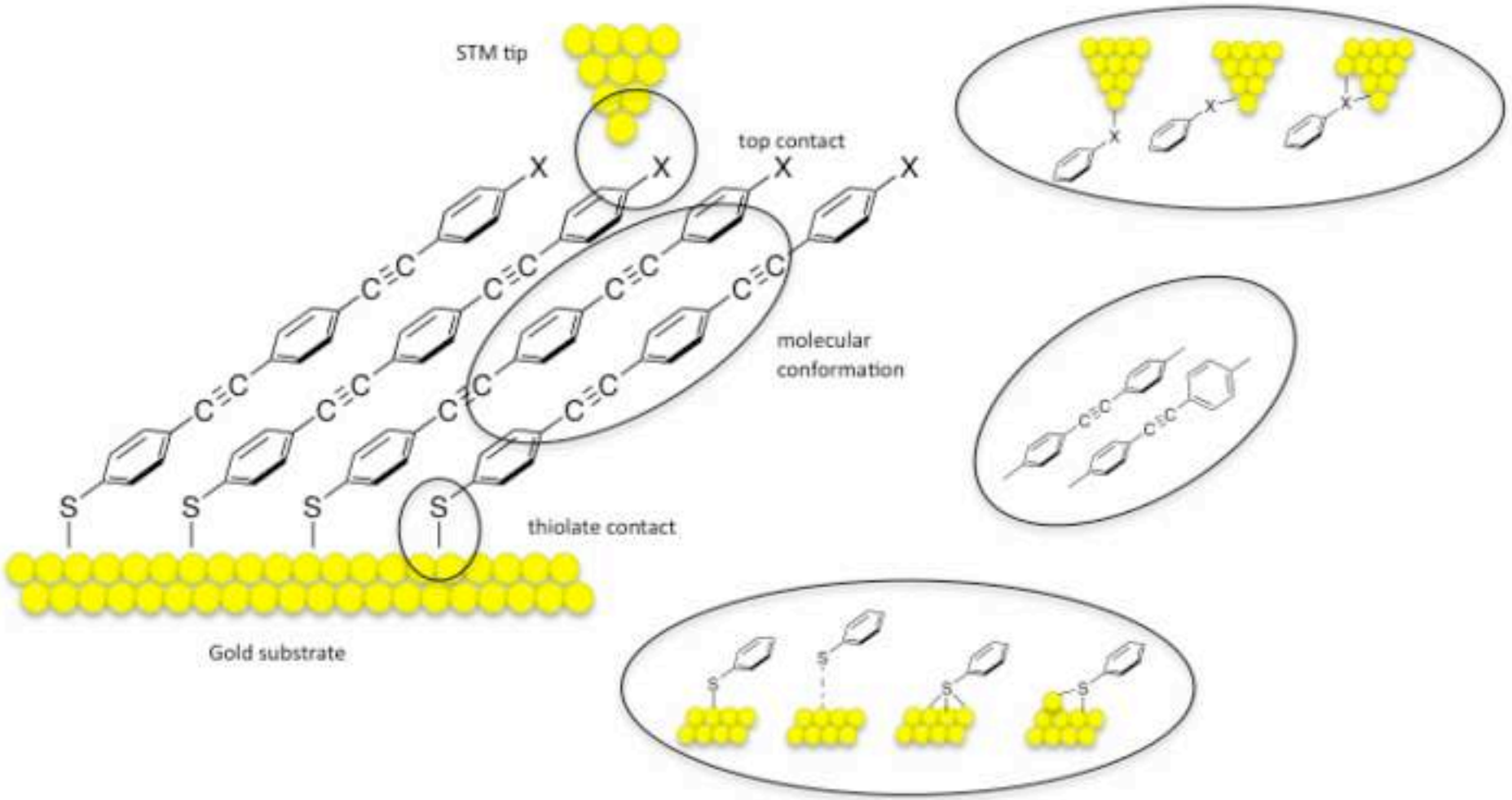

Figure 6

Click here to download high resolution image

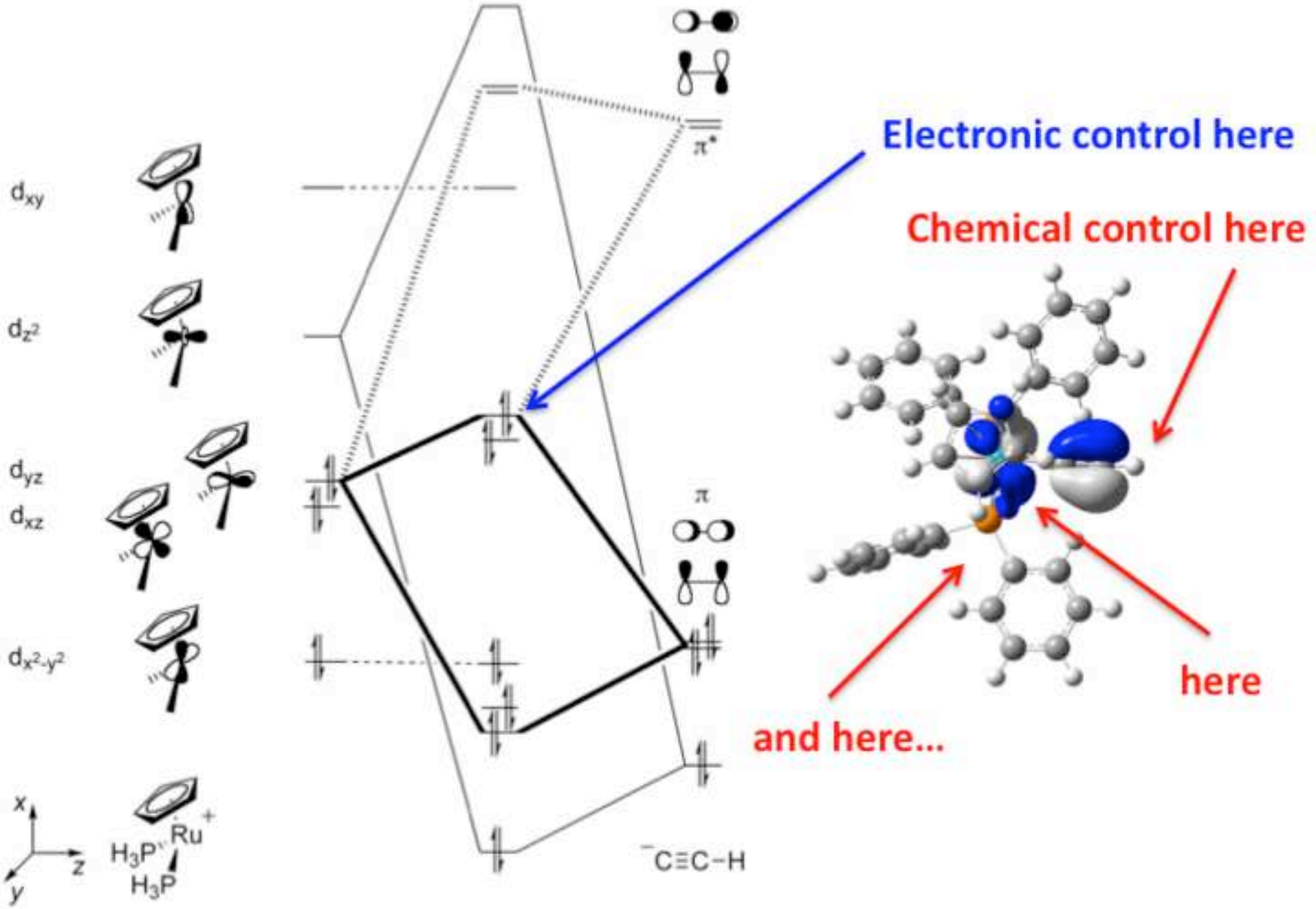

Figure 7

Click here to download high resolution image

Figure 8

Click here to download high resolution image

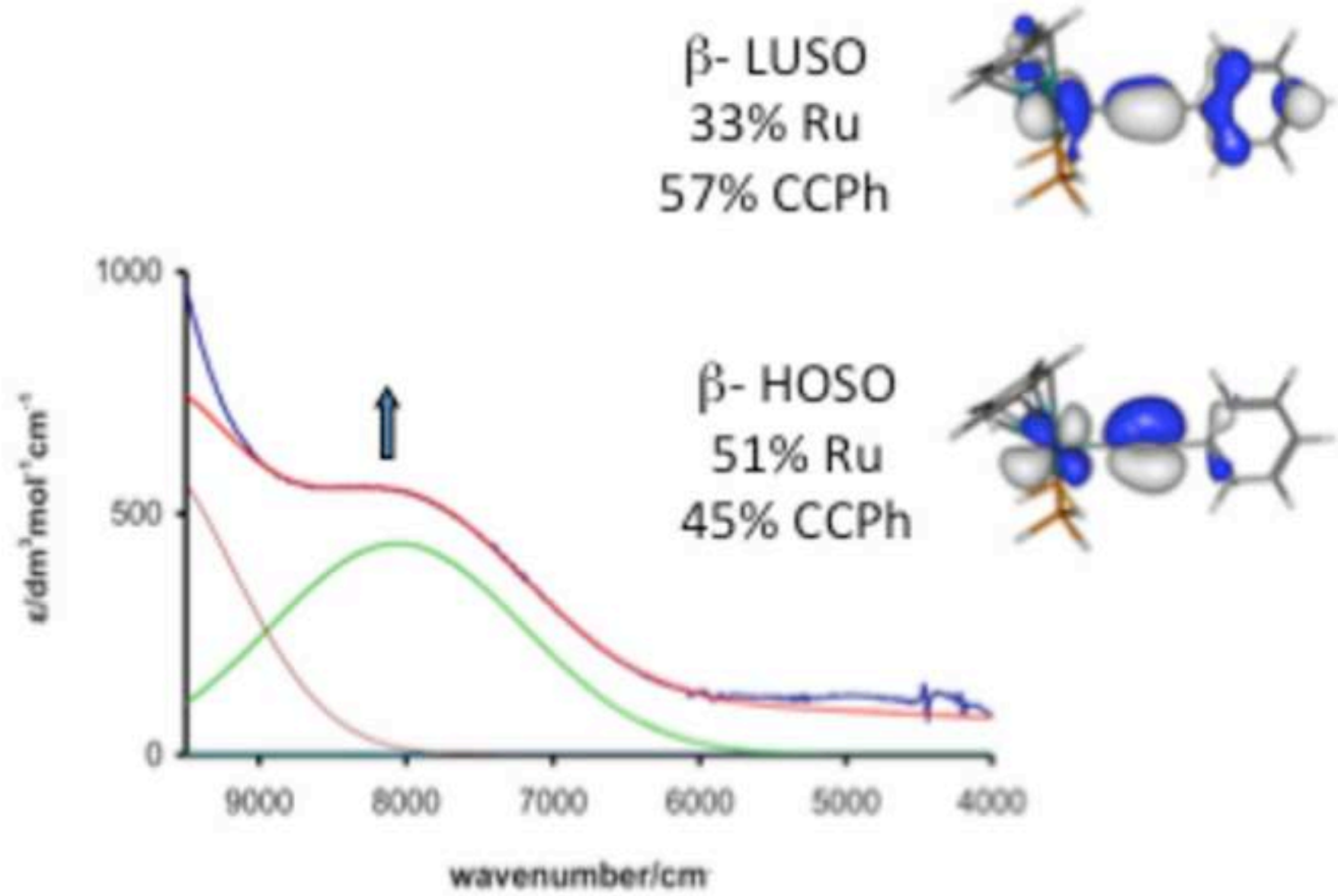

Figure 9

Click here to download high resolution image

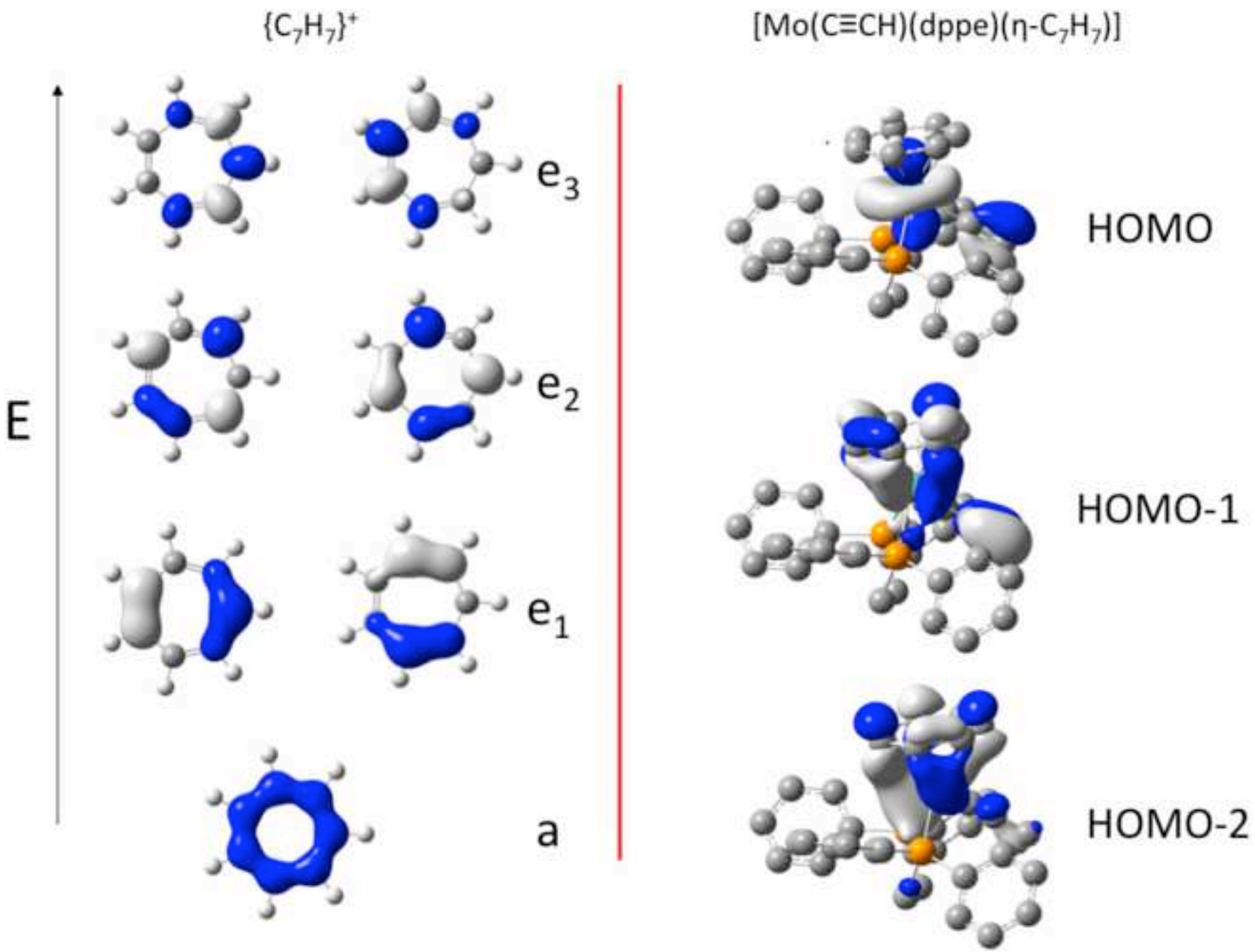

Figure 10

Click here to download high resolution image

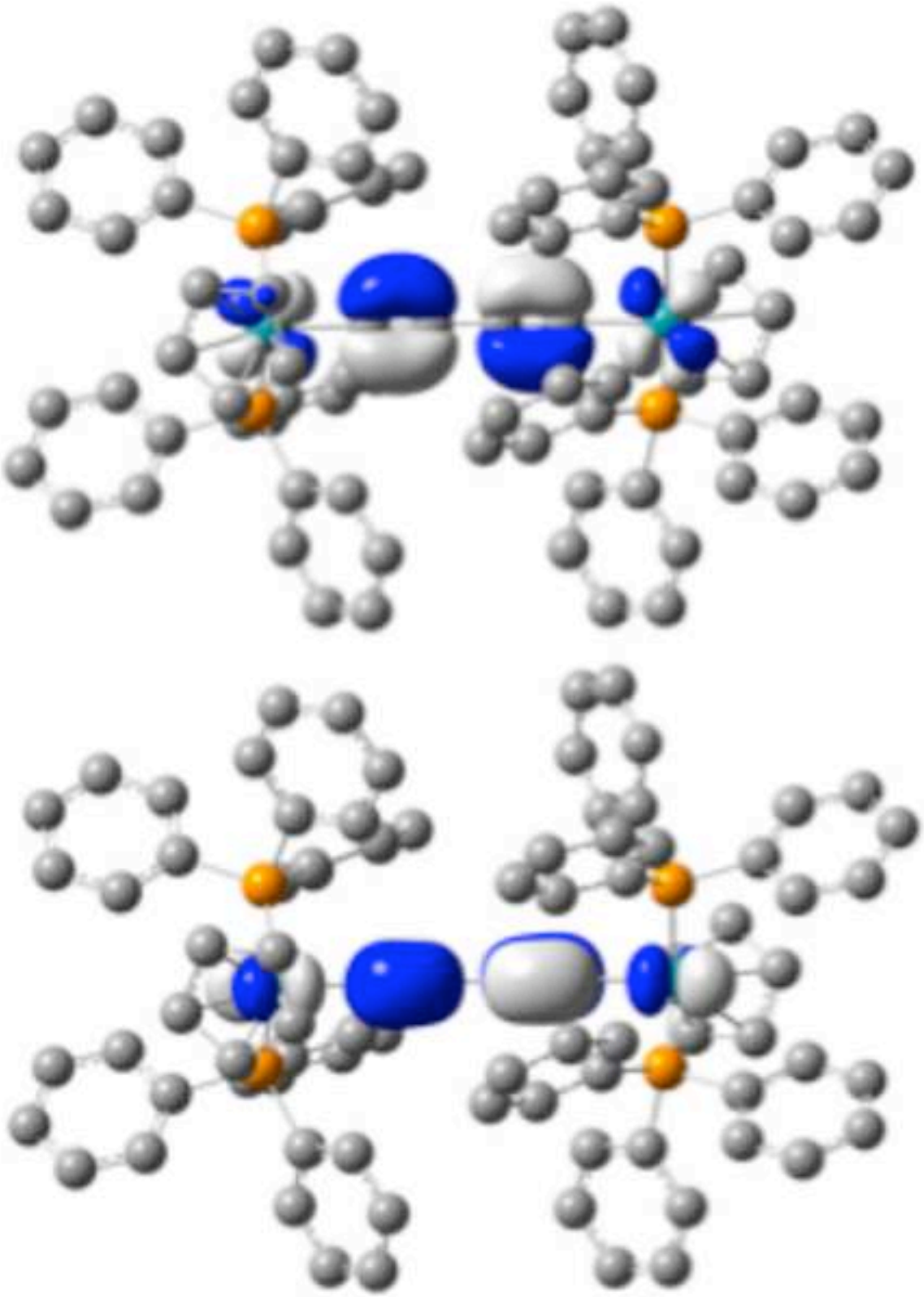

Figure 11

Click here to download high resolution image

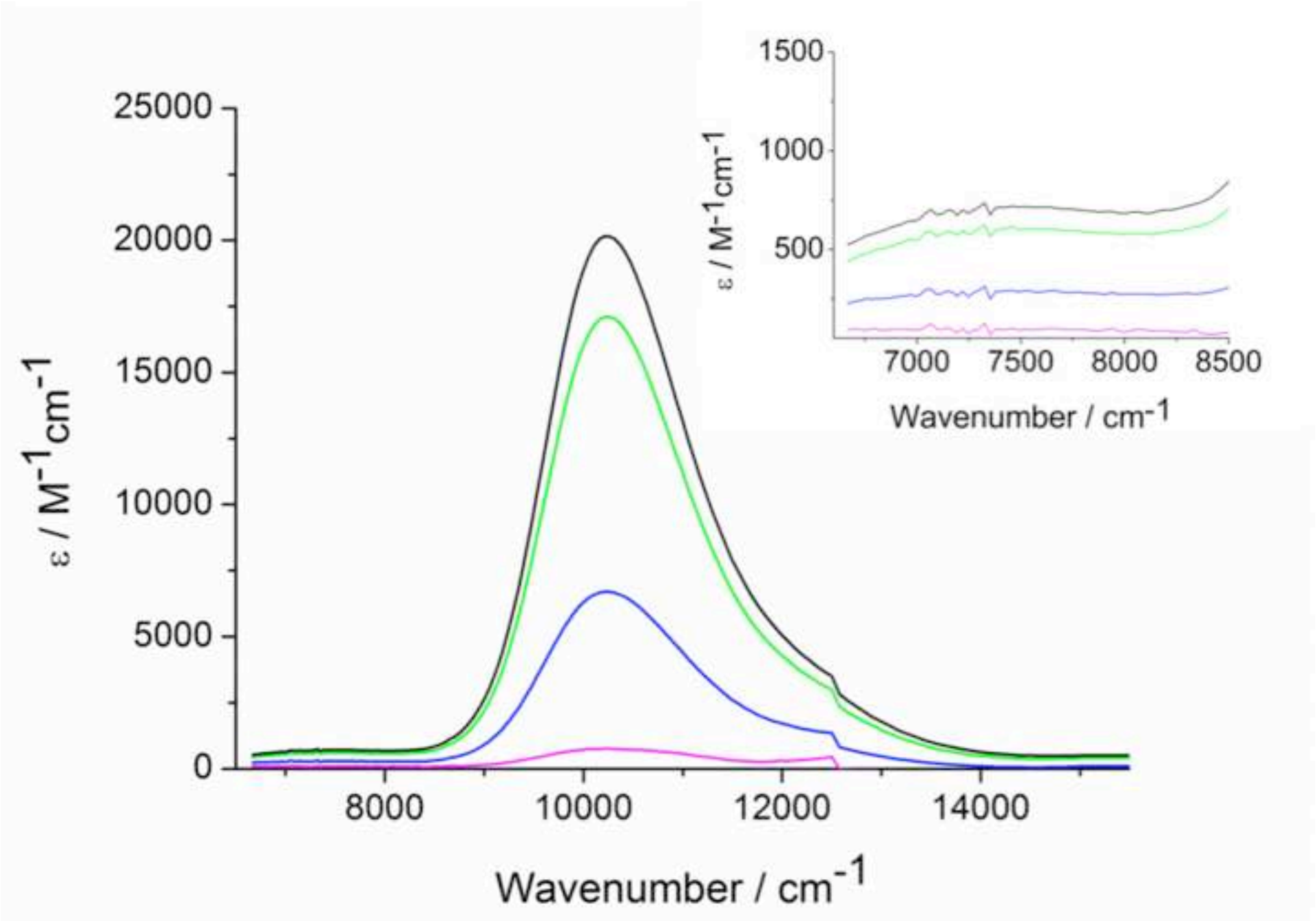

Figure 12

Click here to download high resolution image

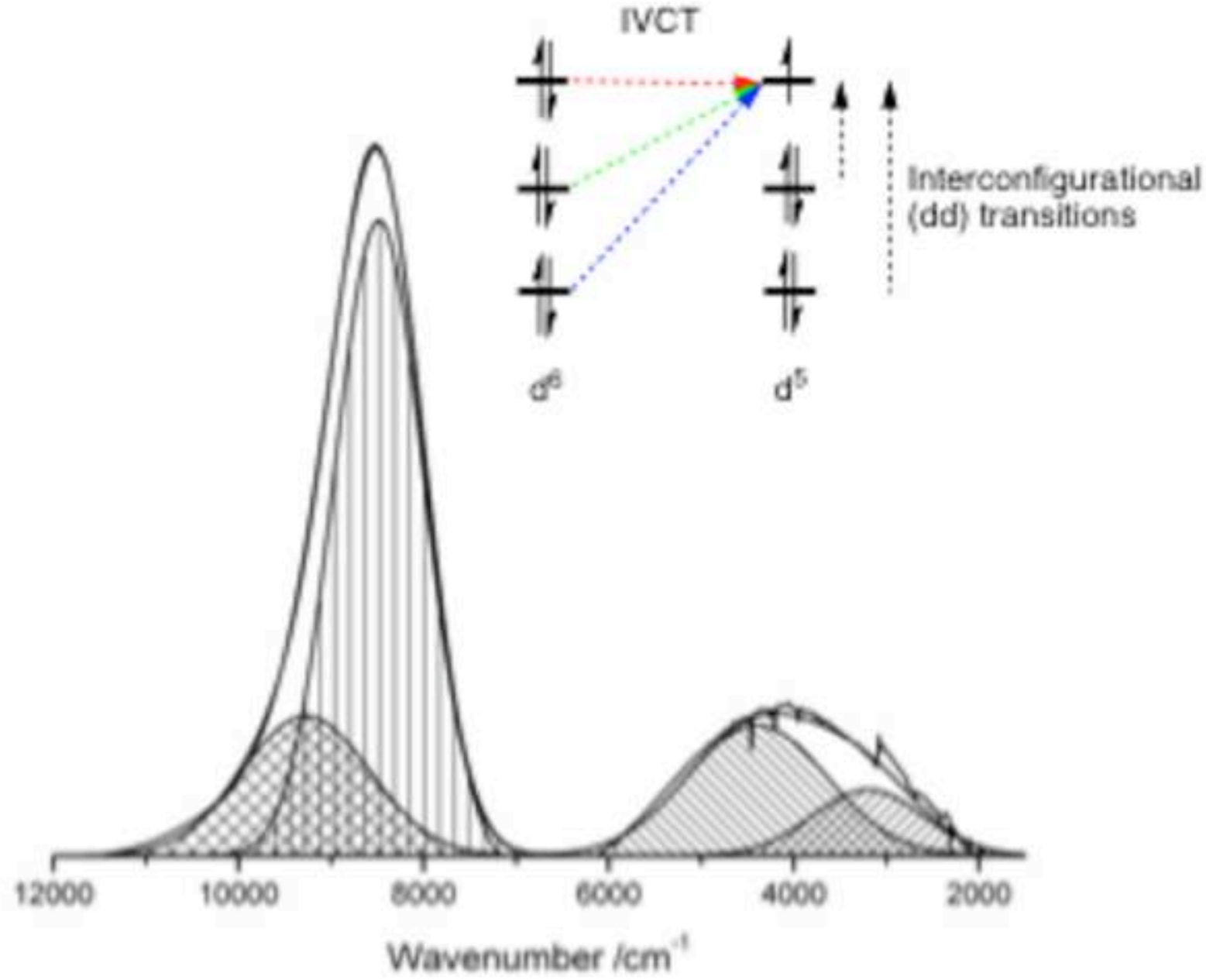

Figure 13

Click here to download high resolution image

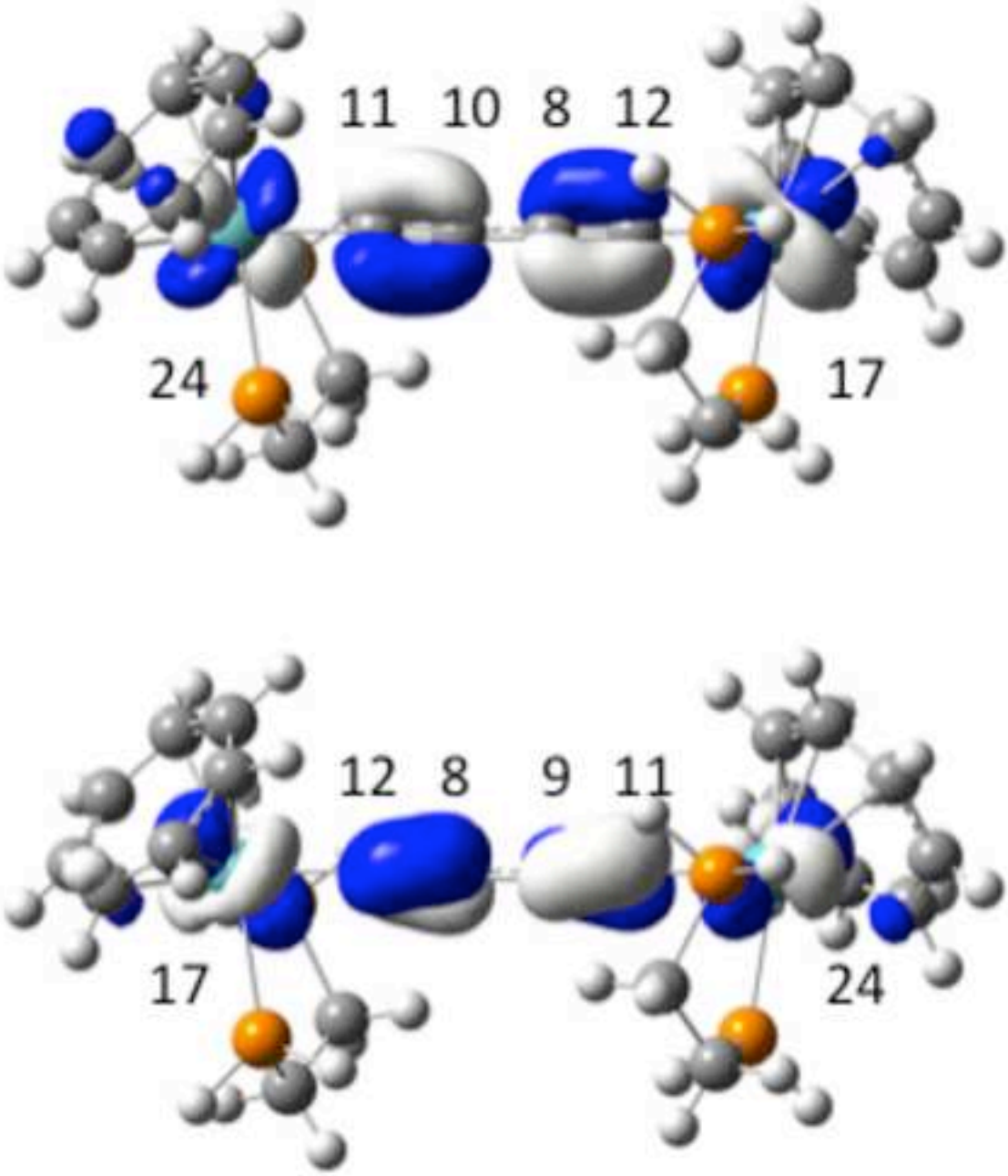

Figure 14
Click here to download high resolution image

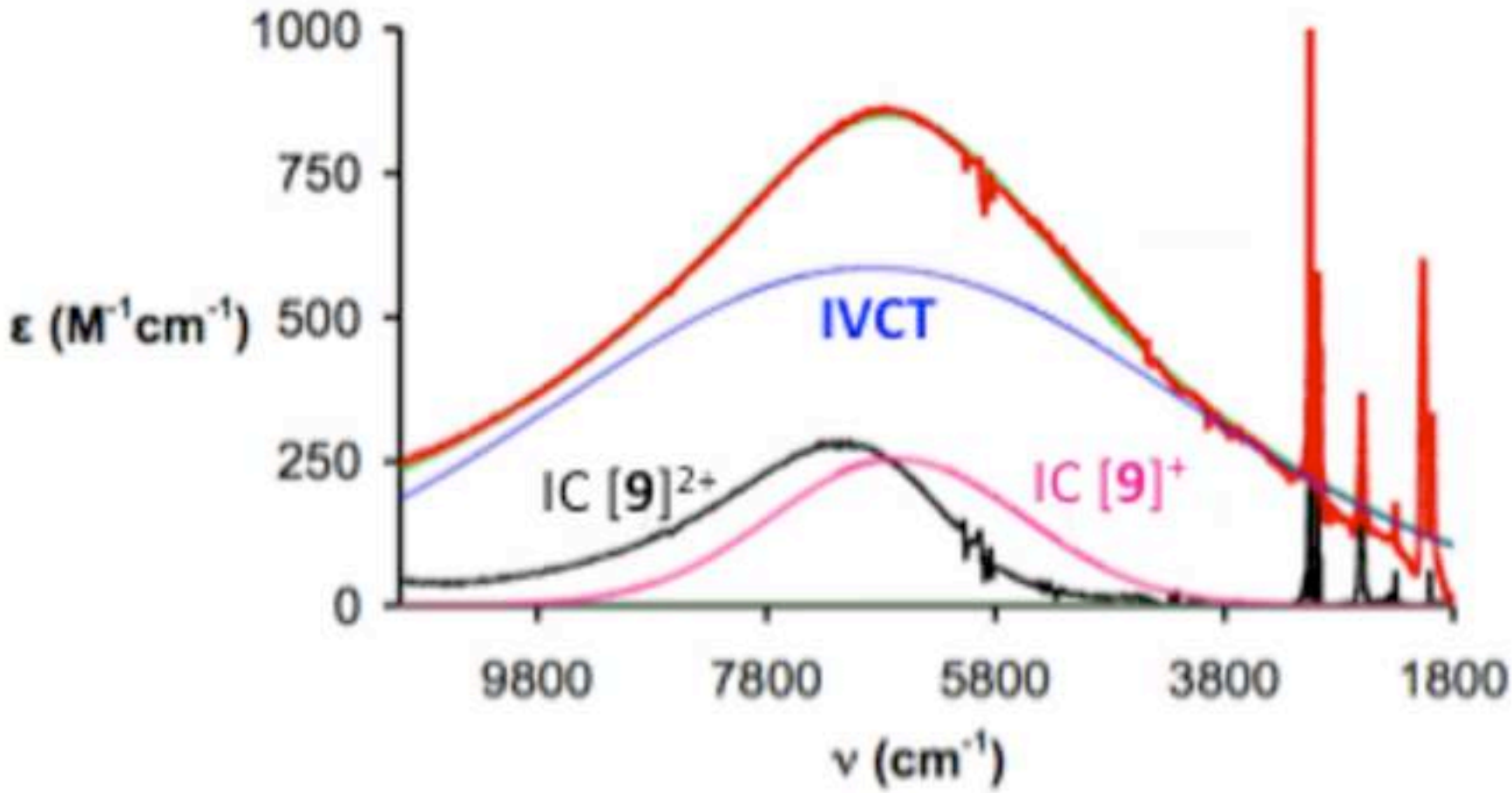

Figure 15

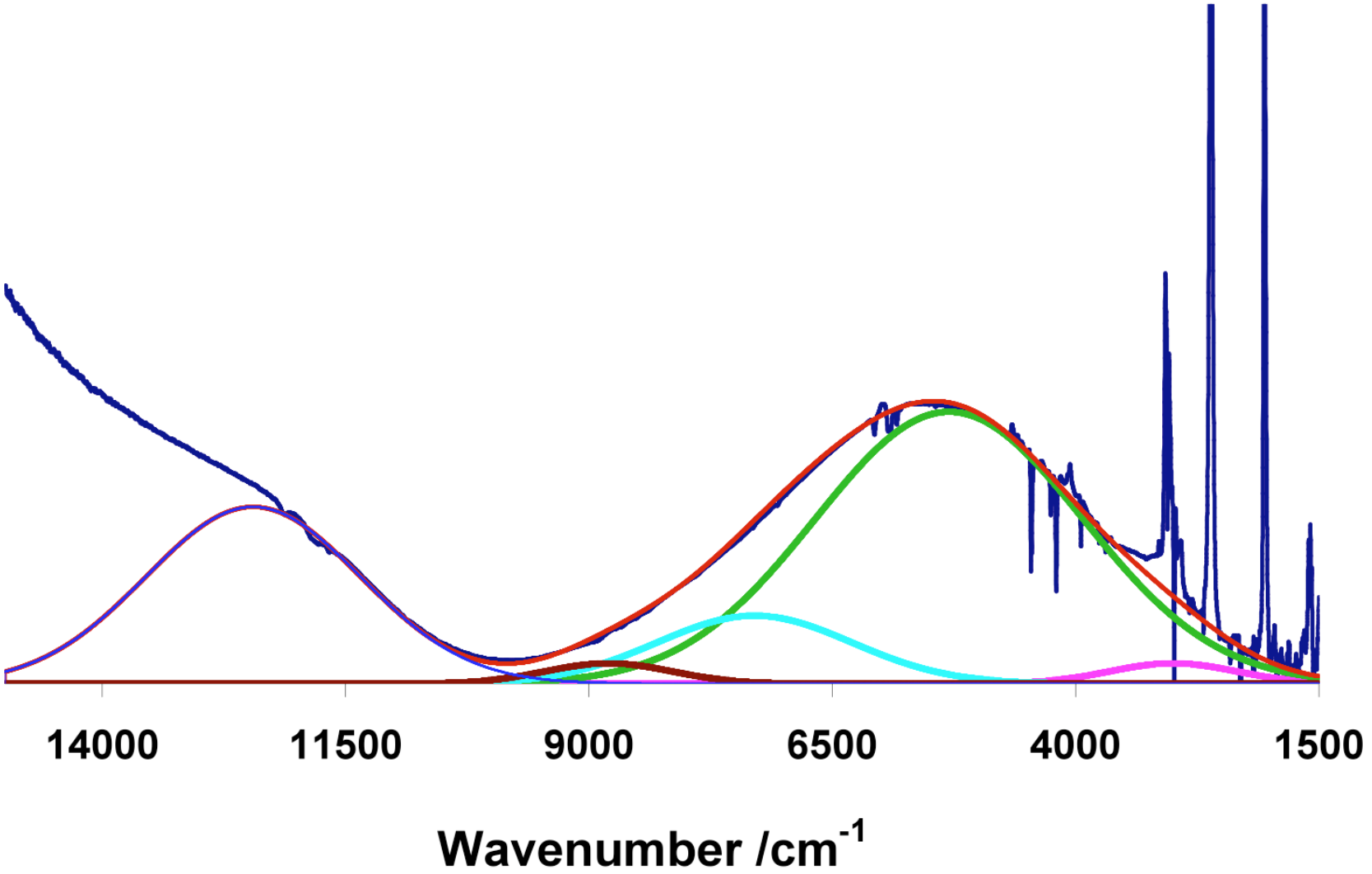

Figure 16

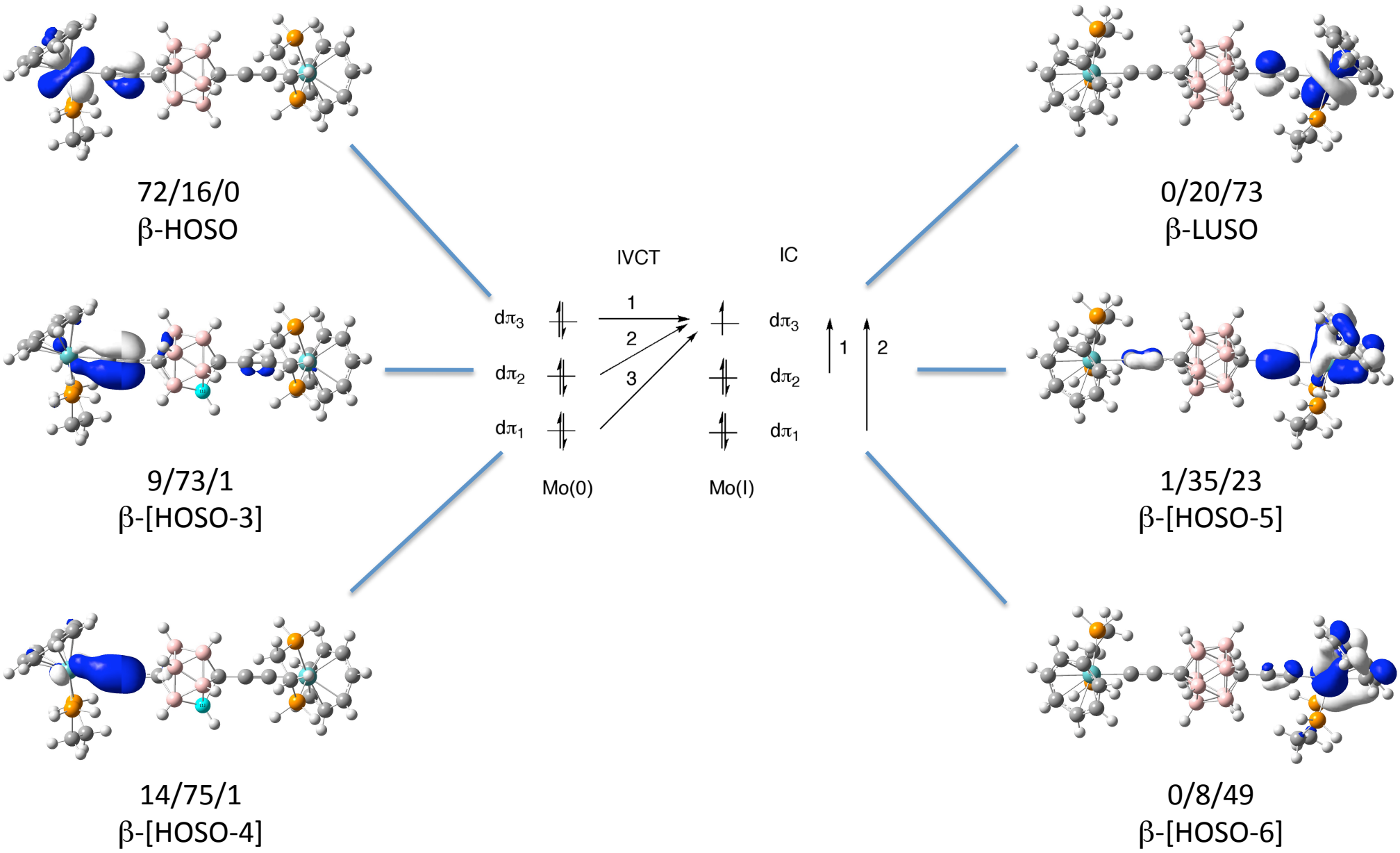
72/16/0
β-HOSO
9/73/1
β-[HOSO-3]
14/75/1
β-[HOSO-4]
0/20/73
β-LUSO
1/35/23
β-[HOSO-5]
0/8/49
β-[HOSO-6]
IVCT
IC
dπ3
dπ2
dπ1
1
2
3
Mo(0)
Mo(I)

Figure 17
Click here to download high resolution image

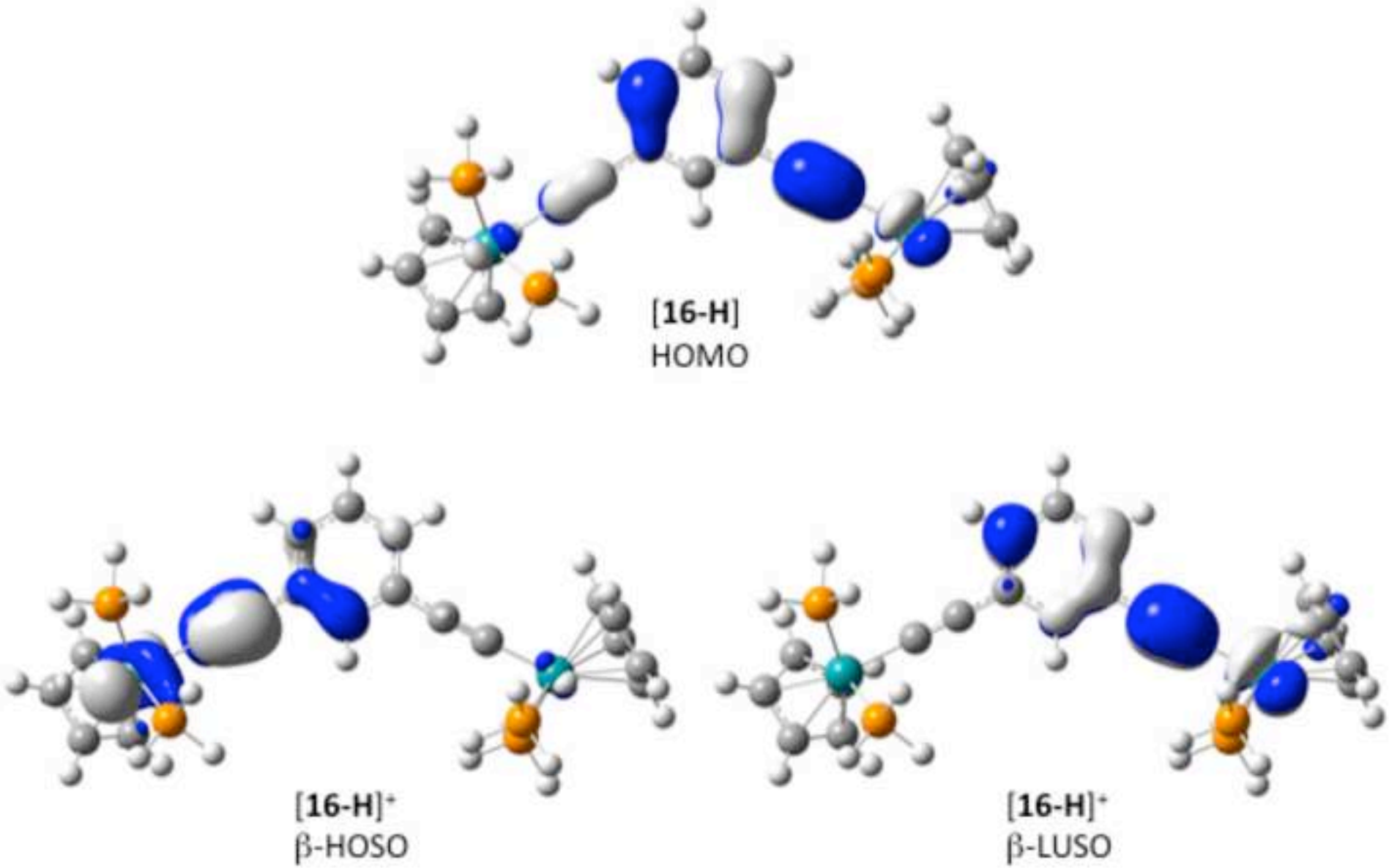

Figure 18

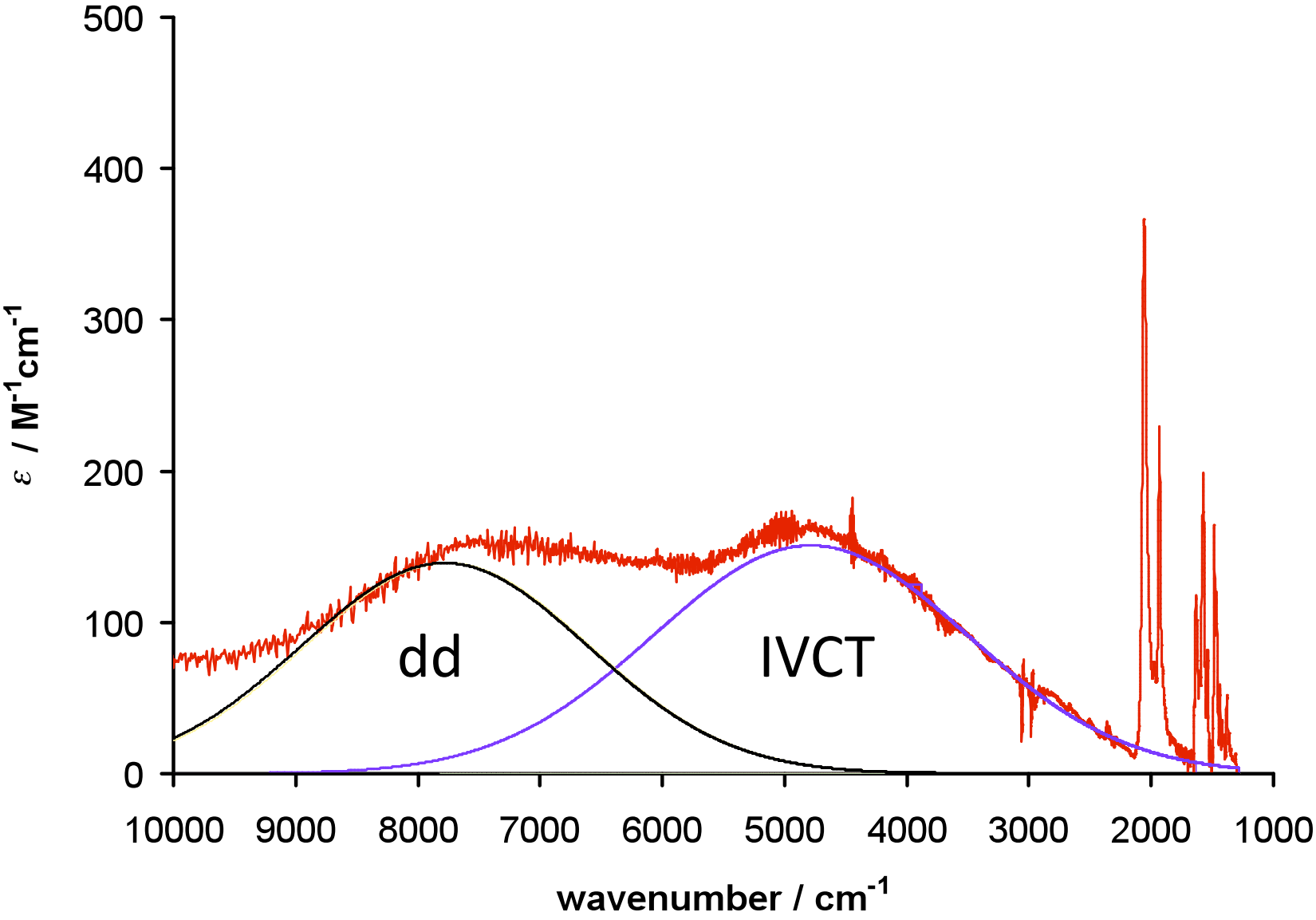
500
400
300
200
100
0
ε / M-1cm-1
dd
IVCT
10000
9000
8000
7000
6000
5000
4000
3000
2000
1000
wavenumber / cm-1

Figure 19
Click here to download high resolution image

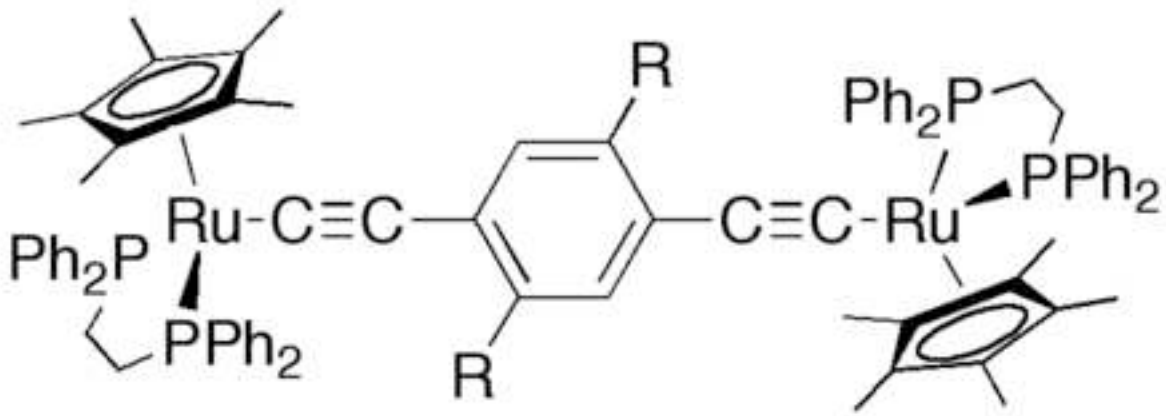

R = H (**17**), OMe (**18**)

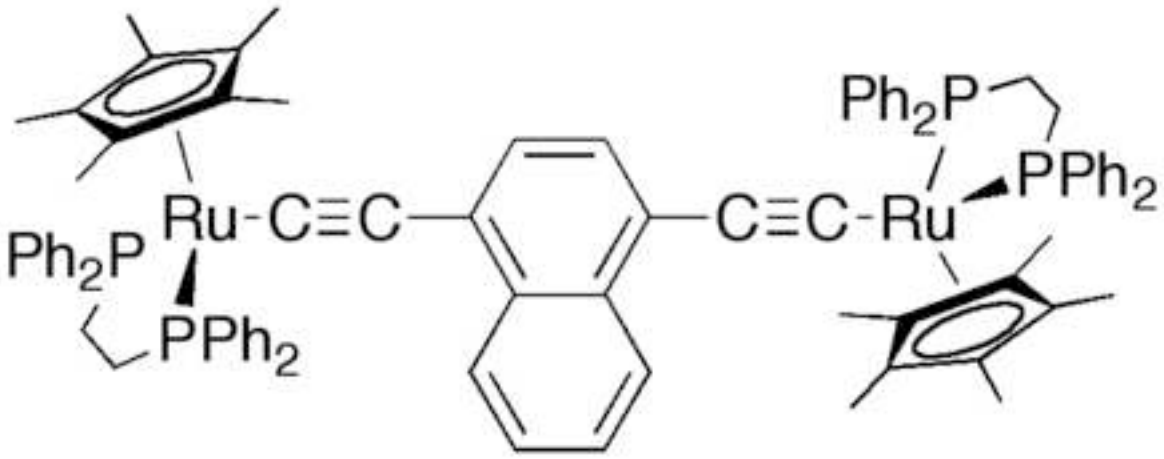

19

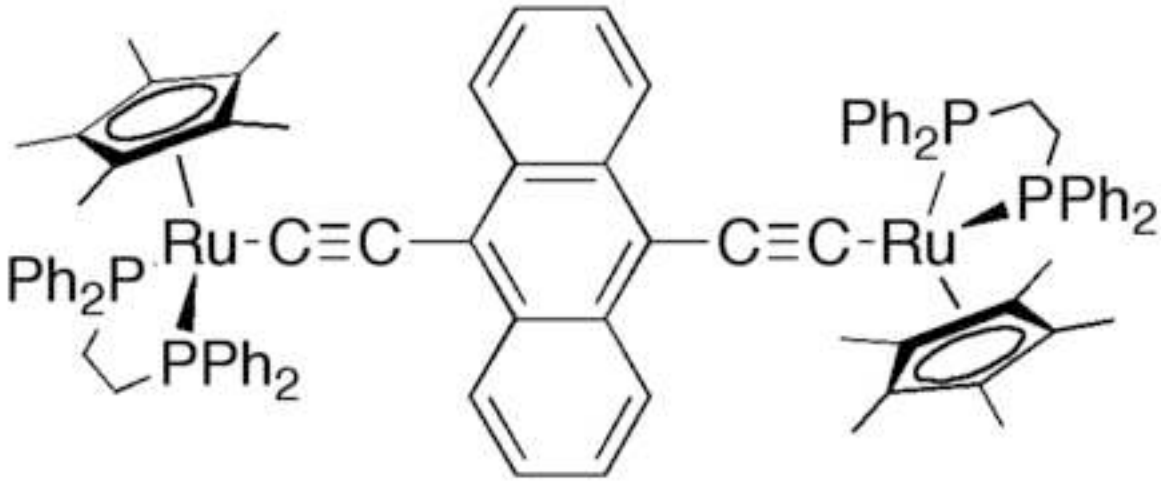

20

Figure 20

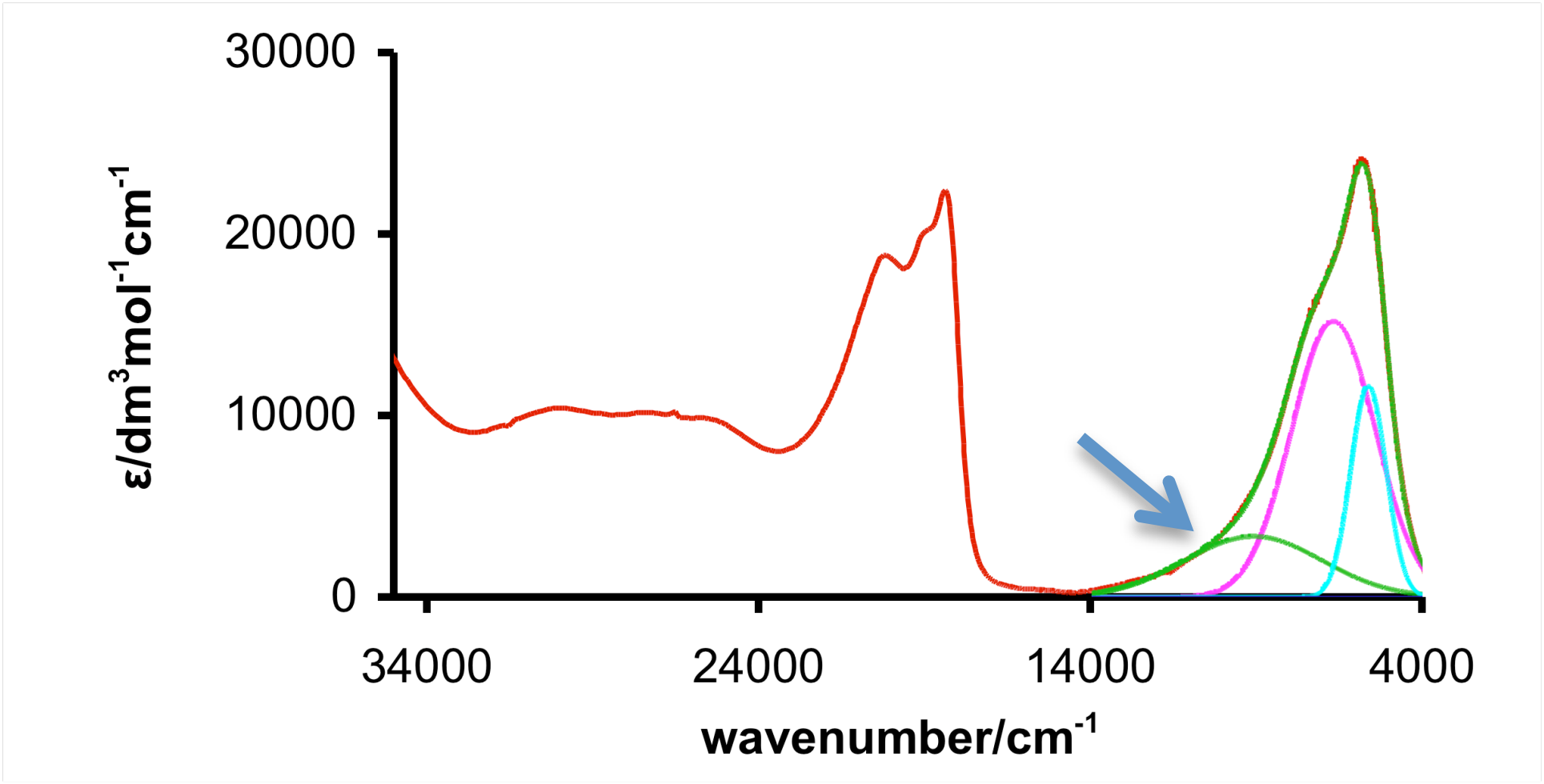
30000
20000
10000
0
ε/dm3mol-1cm-1
34000
24000
14000
4000
wavenumber/cm-1

Figure 21

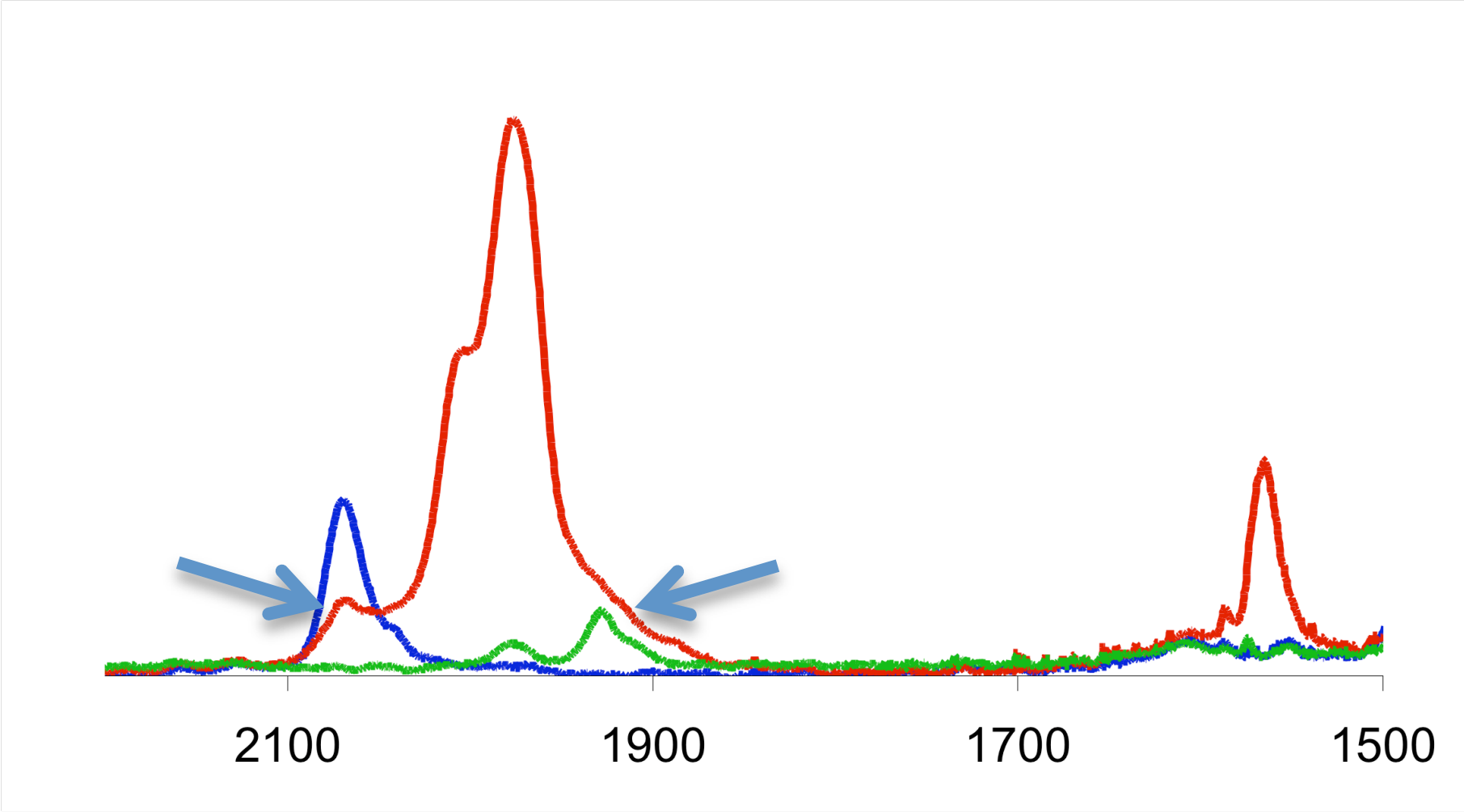

Figure 22

[21]

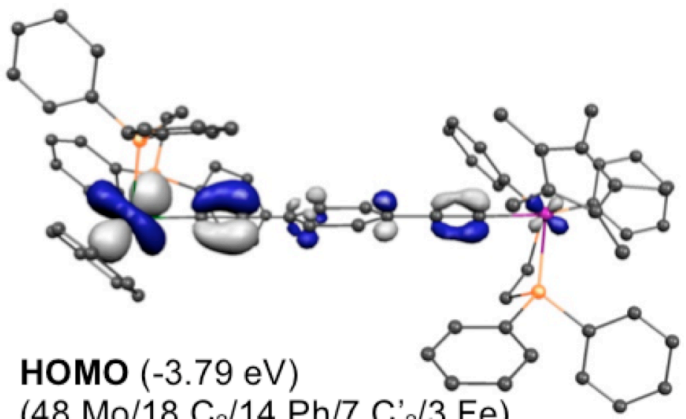

HOMO (-3.79 eV)
(48 Mo/18 C_2/14 Ph/7 C'_2/3 Fe)

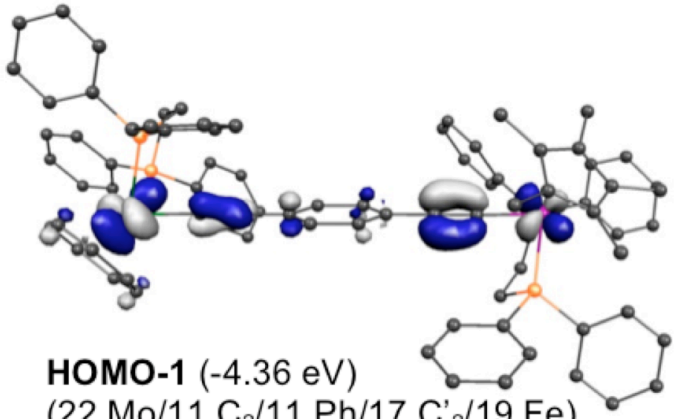

HOMO-1 (-4.36 eV)
(22 Mo/11 C_2/11 Ph/17 C'_2/19 Fe)

[22]

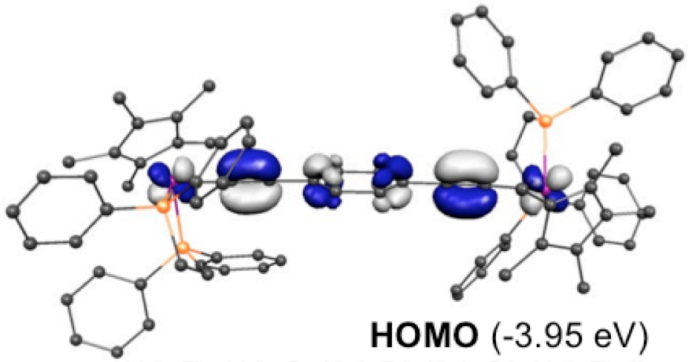

HOMO (-3.95 eV)
(13 Fe/18 C_2/24 Ph/21 C'_2/15 Fe')

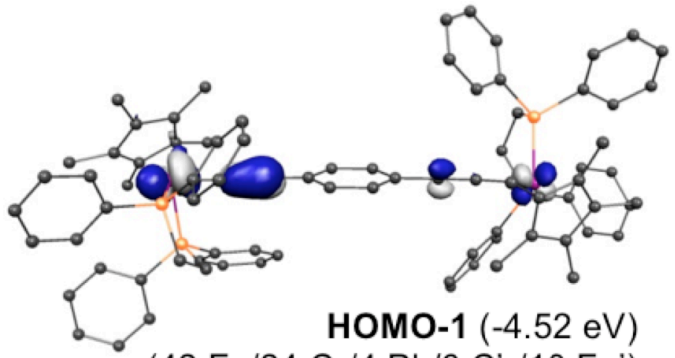

HOMO-1 (-4.52 eV)
(42 Fe/24 C_2/4 Ph/6 C'_2/10 Fe')

[23]

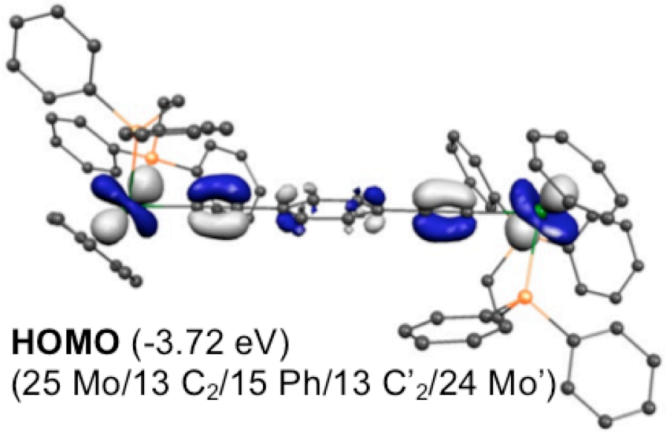

HOMO (-3.72 eV)
(25 Mo/13 C_2/15 Ph/13 C'_2/24 Mo')

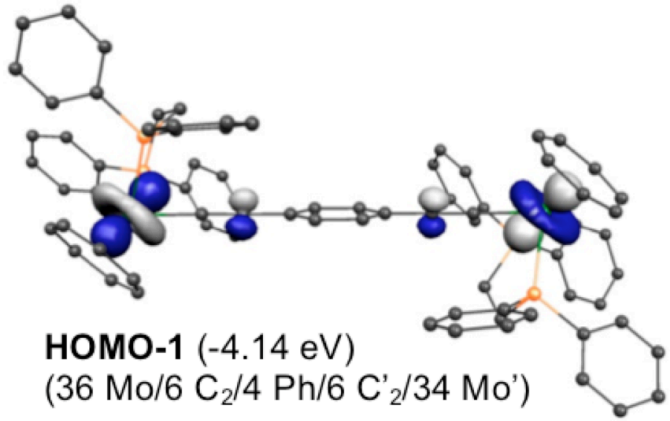

HOMO-1 (-4.14 eV)
(36 Mo/6 C_2/4 Ph/6 C'_2/34 Mo')

Figure 23

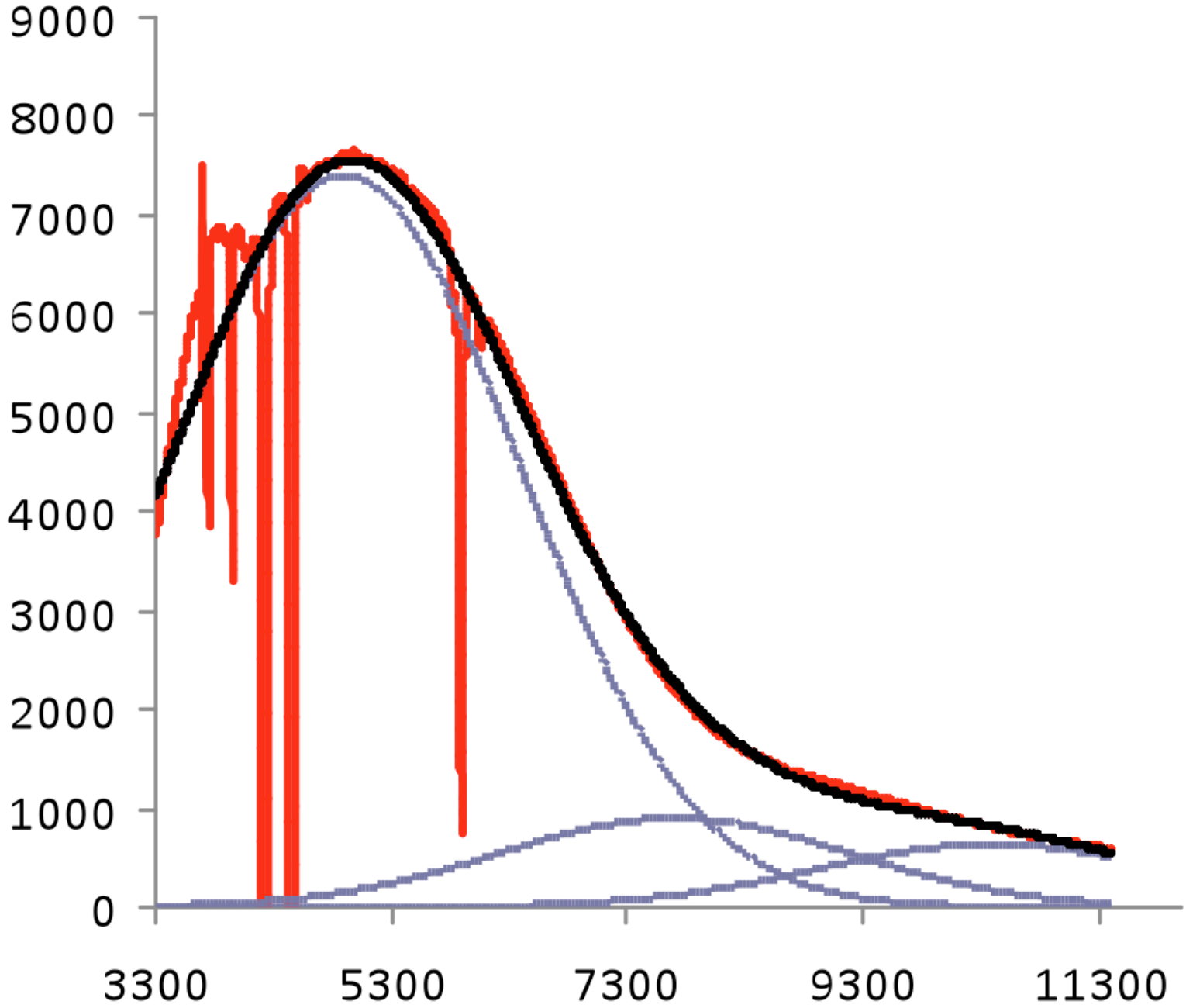
9000
8000
7000
6000
5000
4000
3000
2000
1000
0
3300
5300
7300
9300
11300

Figure 24

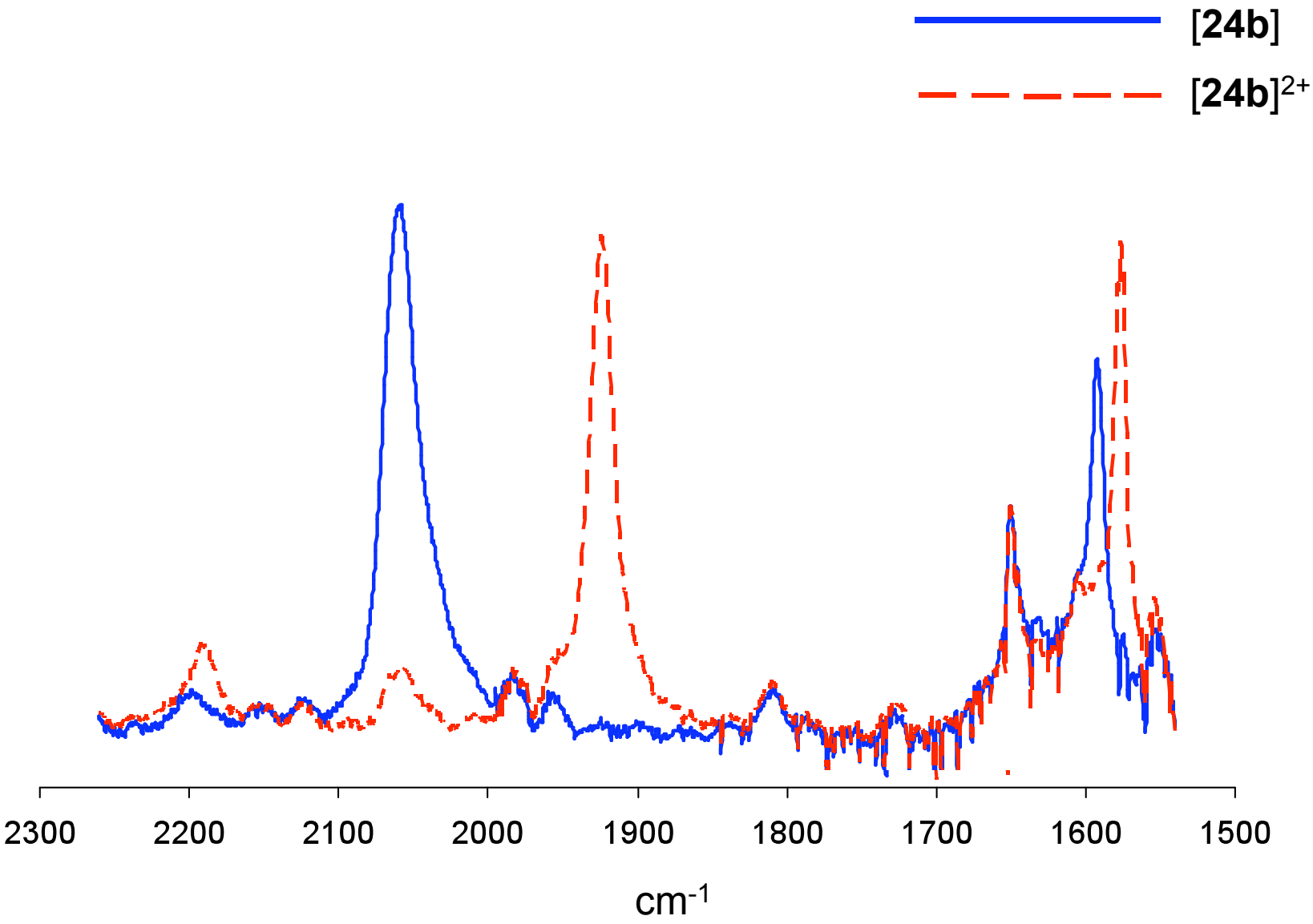

Figure 25

Click here to download high resolution image

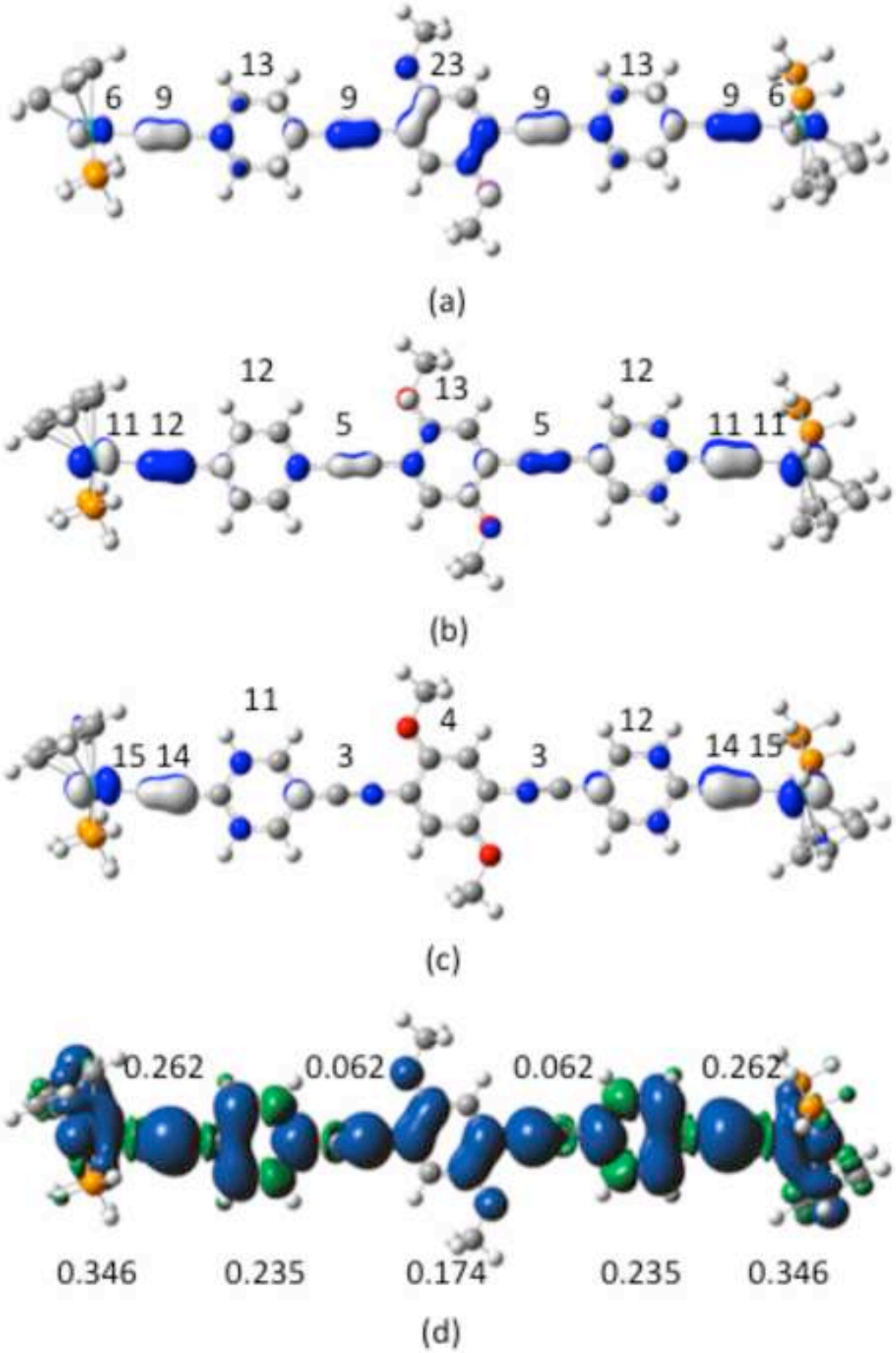

Scheme 1

Click here to download high resolution image

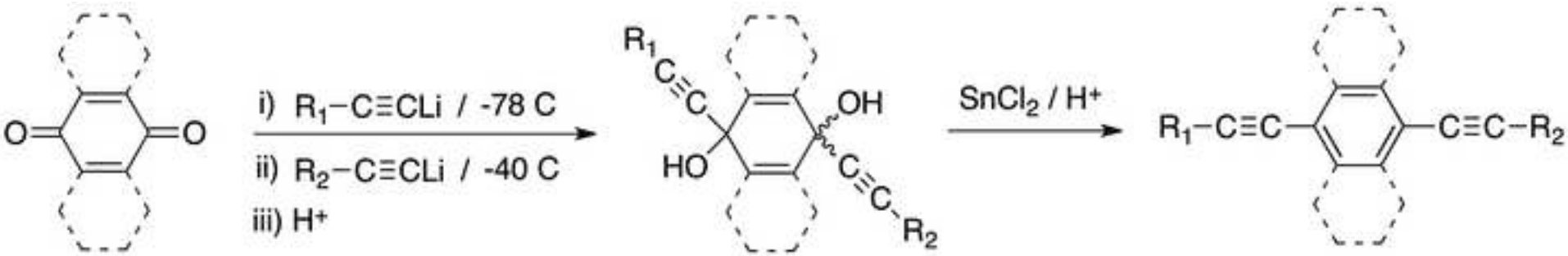

Scheme 2

Click here to download high resolution image

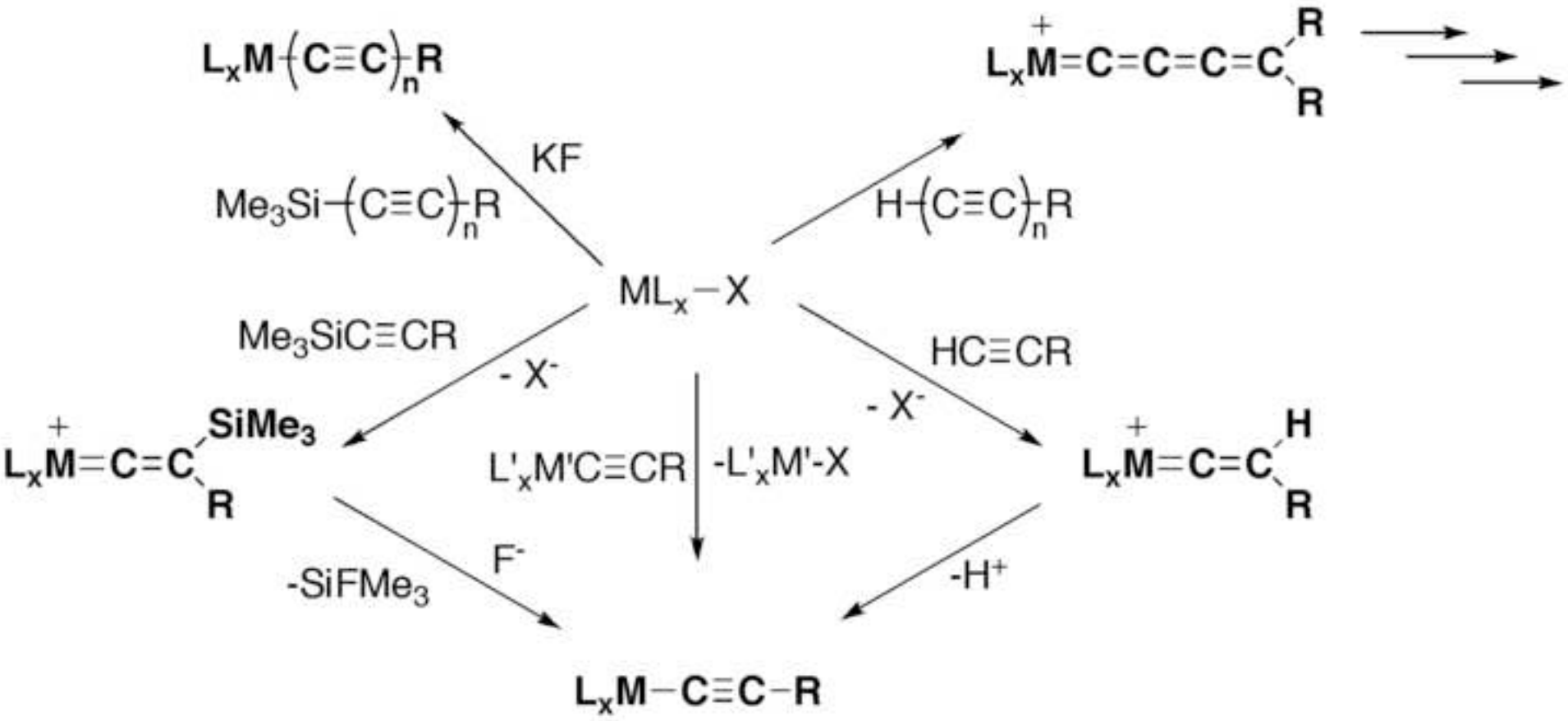

Scheme 3

Click here to download high resolution image

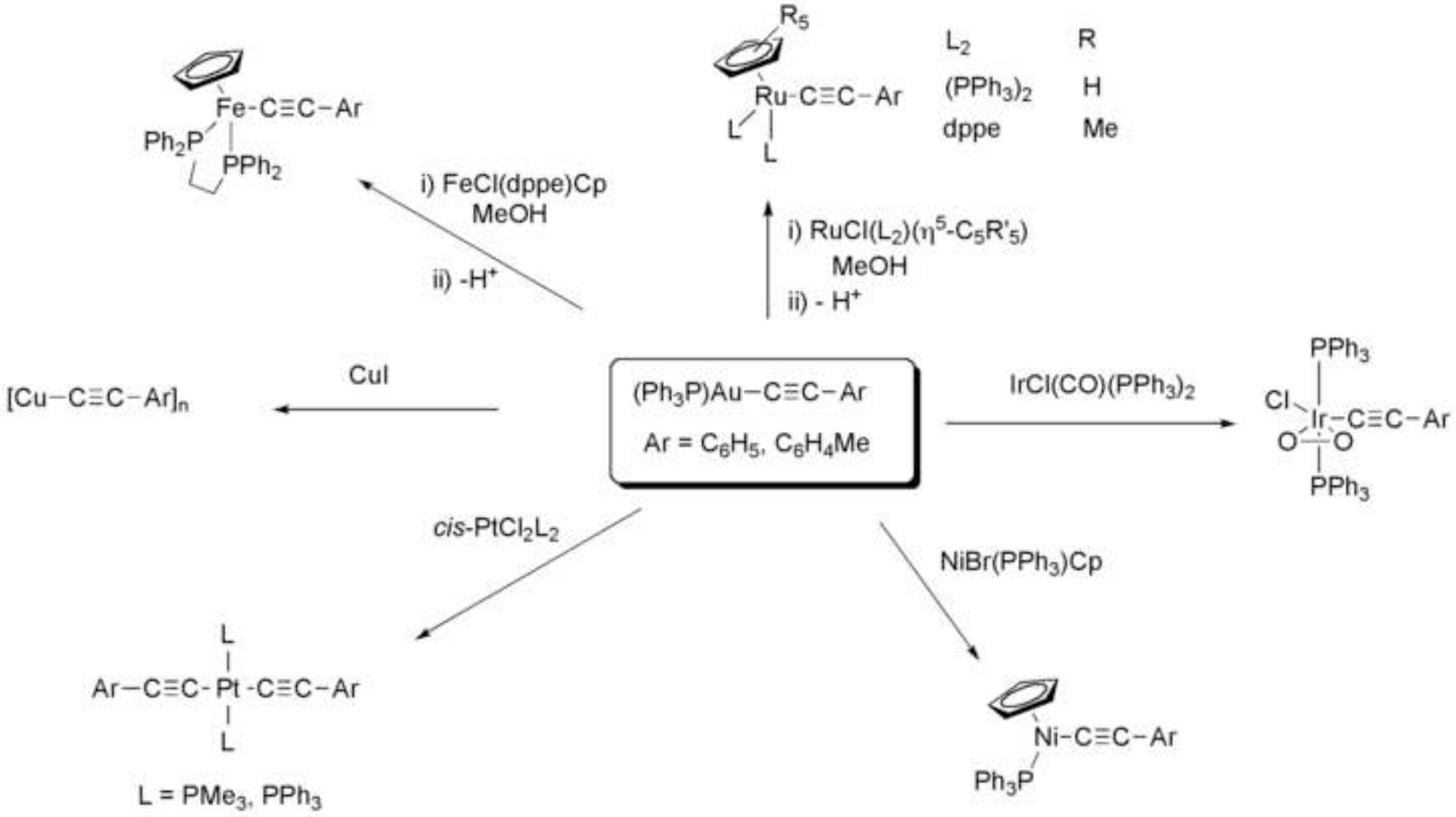

Scheme 4

Click here to download high resolution image

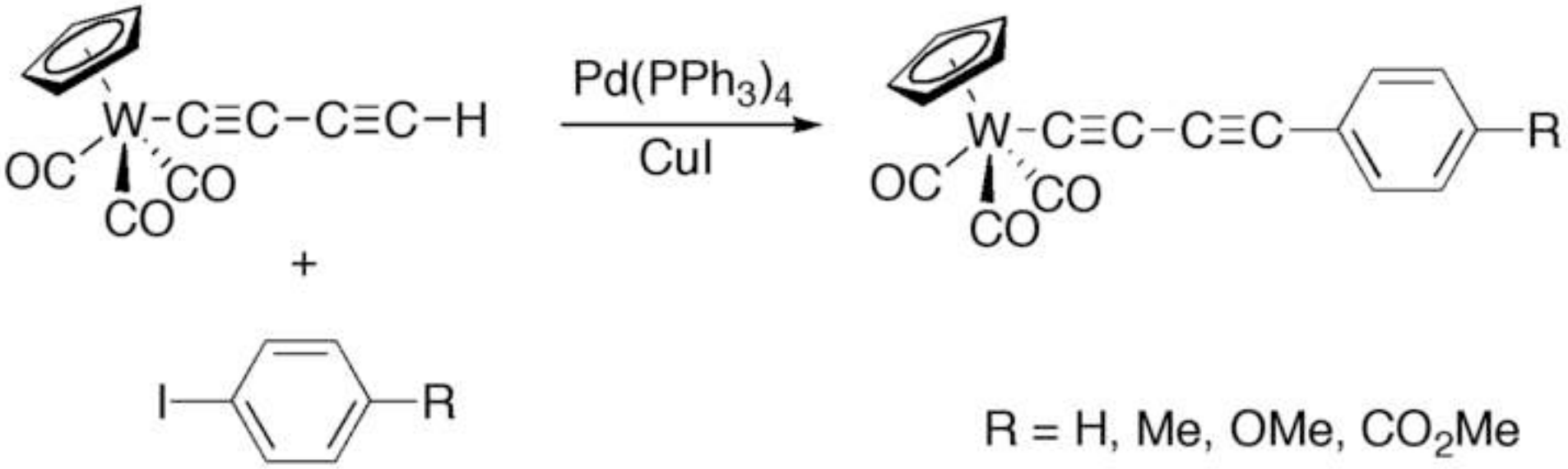

Scheme 5

Click here to download high resolution image

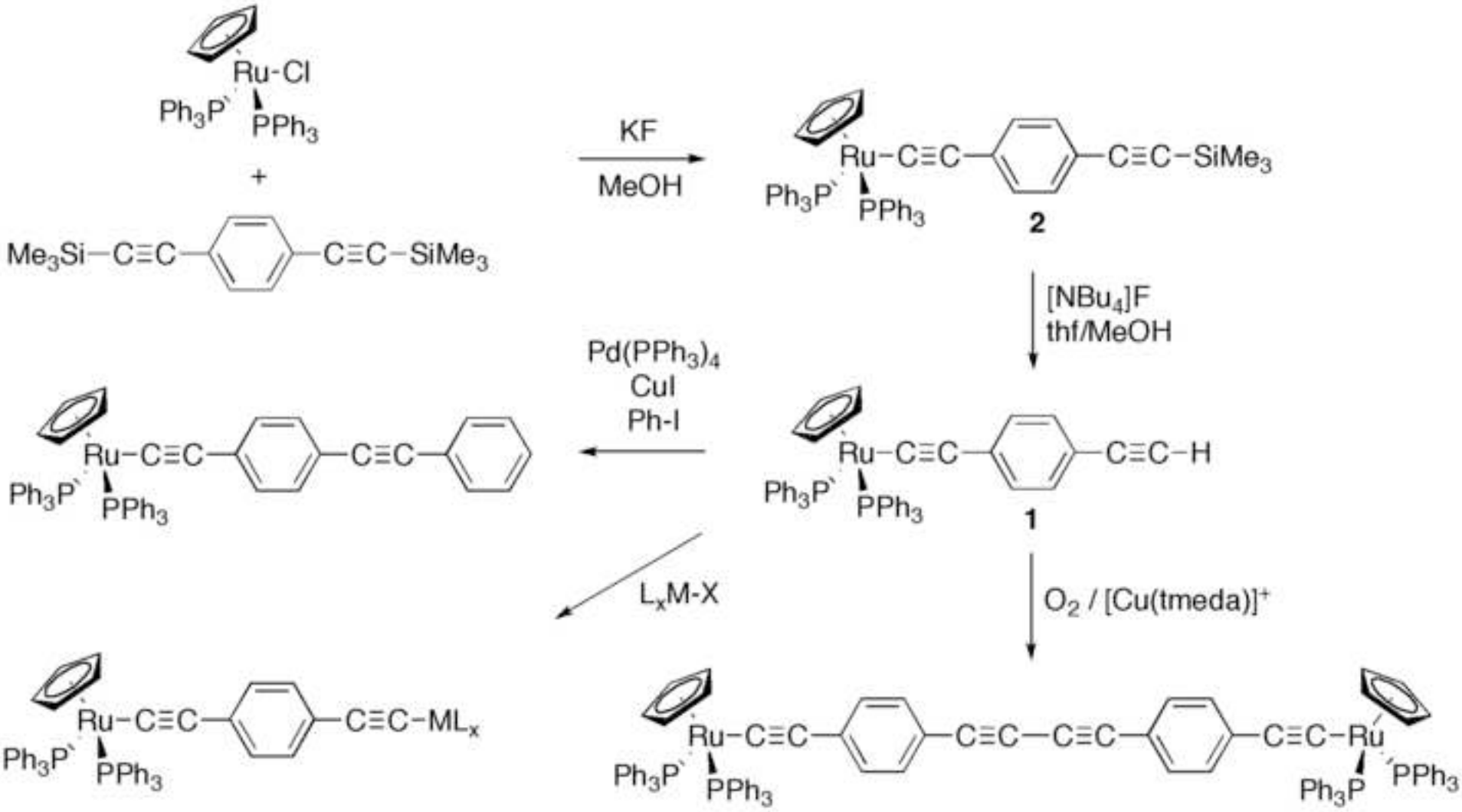

Scheme 6

Click here to download high resolution image

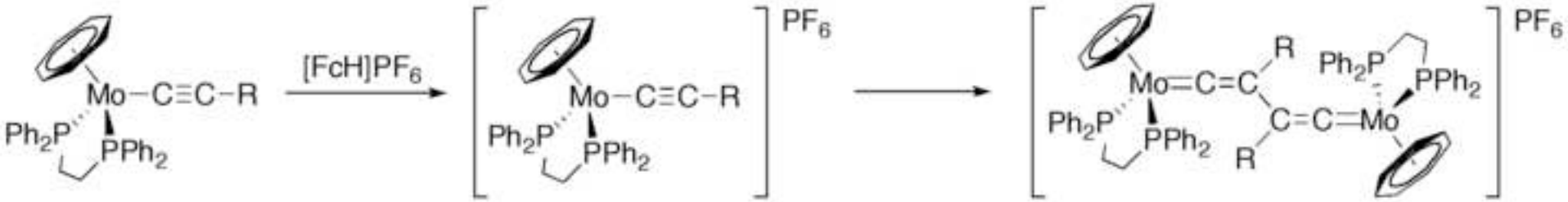

R = Ph, ^{n}Bu, C≡CSiMe$_3$

Scheme 7

Click here to download high resolution image

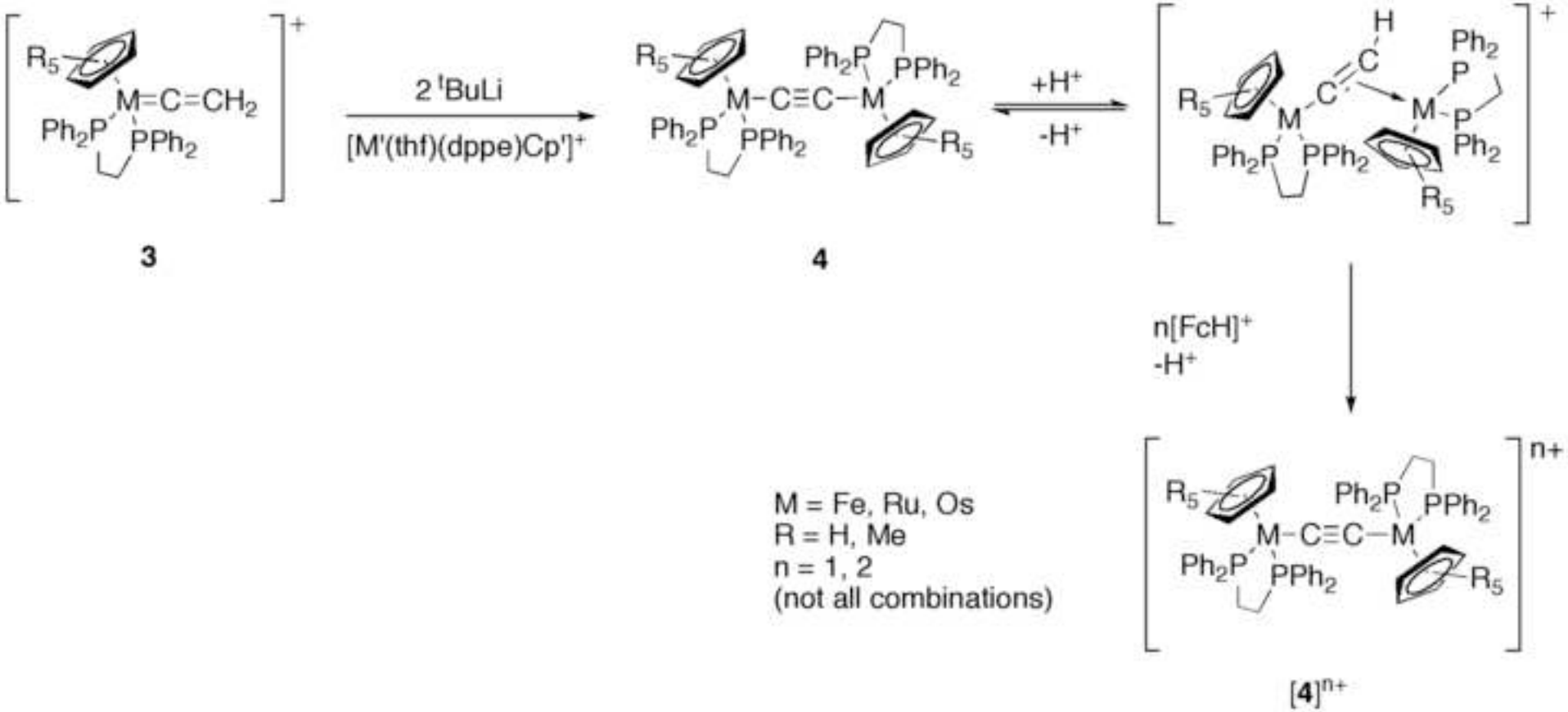

Scheme 8

Click here to download high resolution image

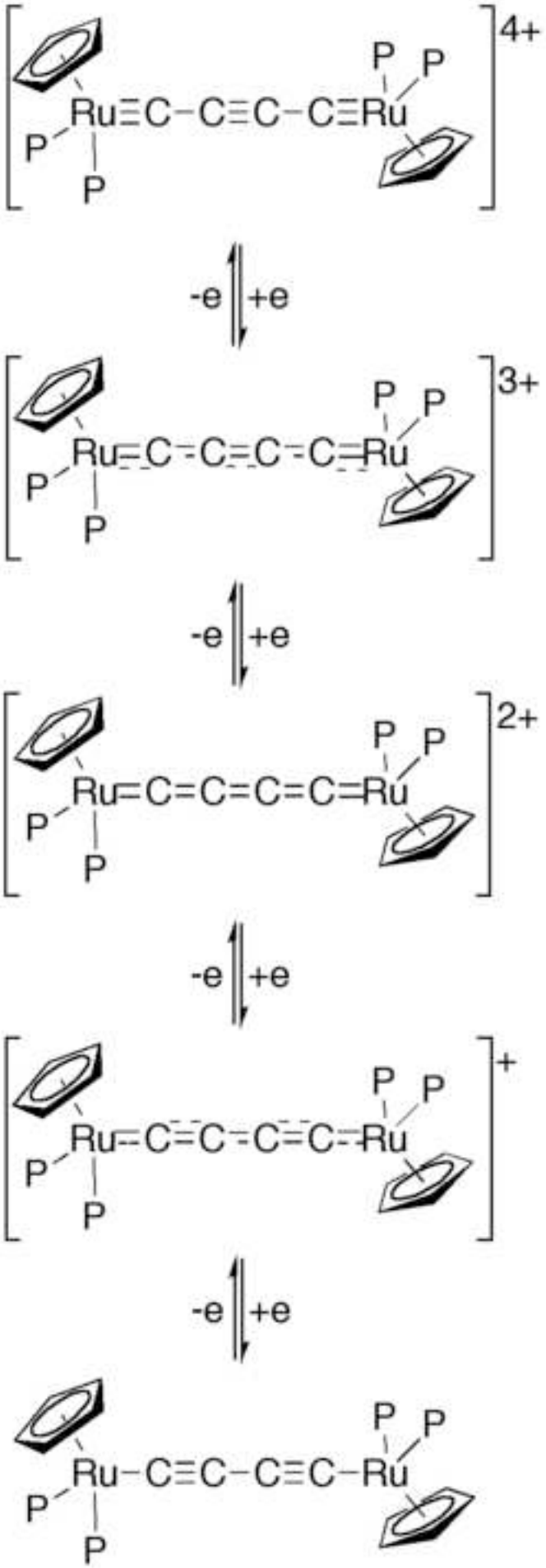

Scheme 9

Click here to download high resolution image

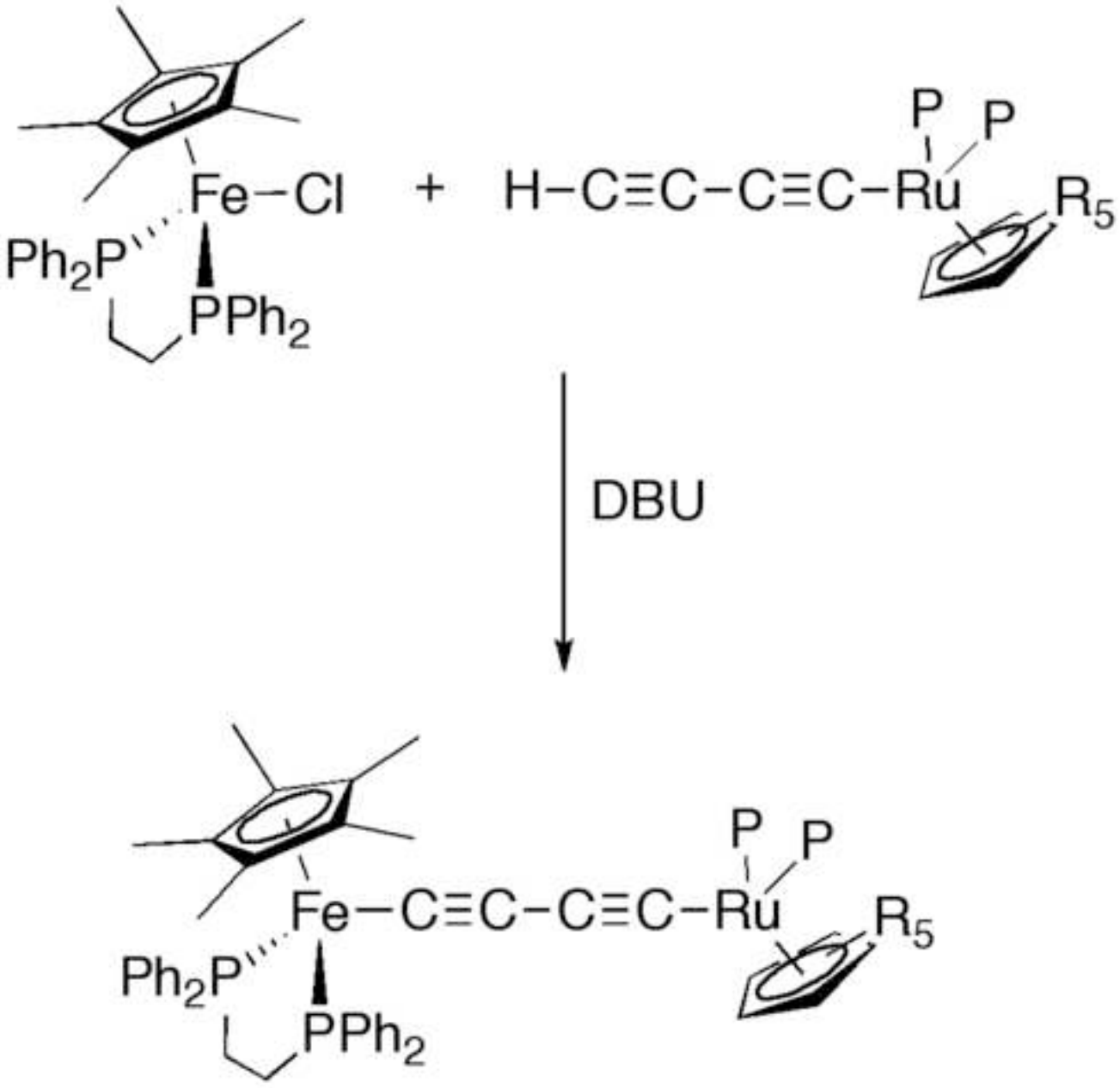

Ru(PP)Cp' = $Ru(PPh_3)_2Cp$ (**6**); Ru(dppe)Cp* (**7**)

Scheme 10

Click here to download high resolution image

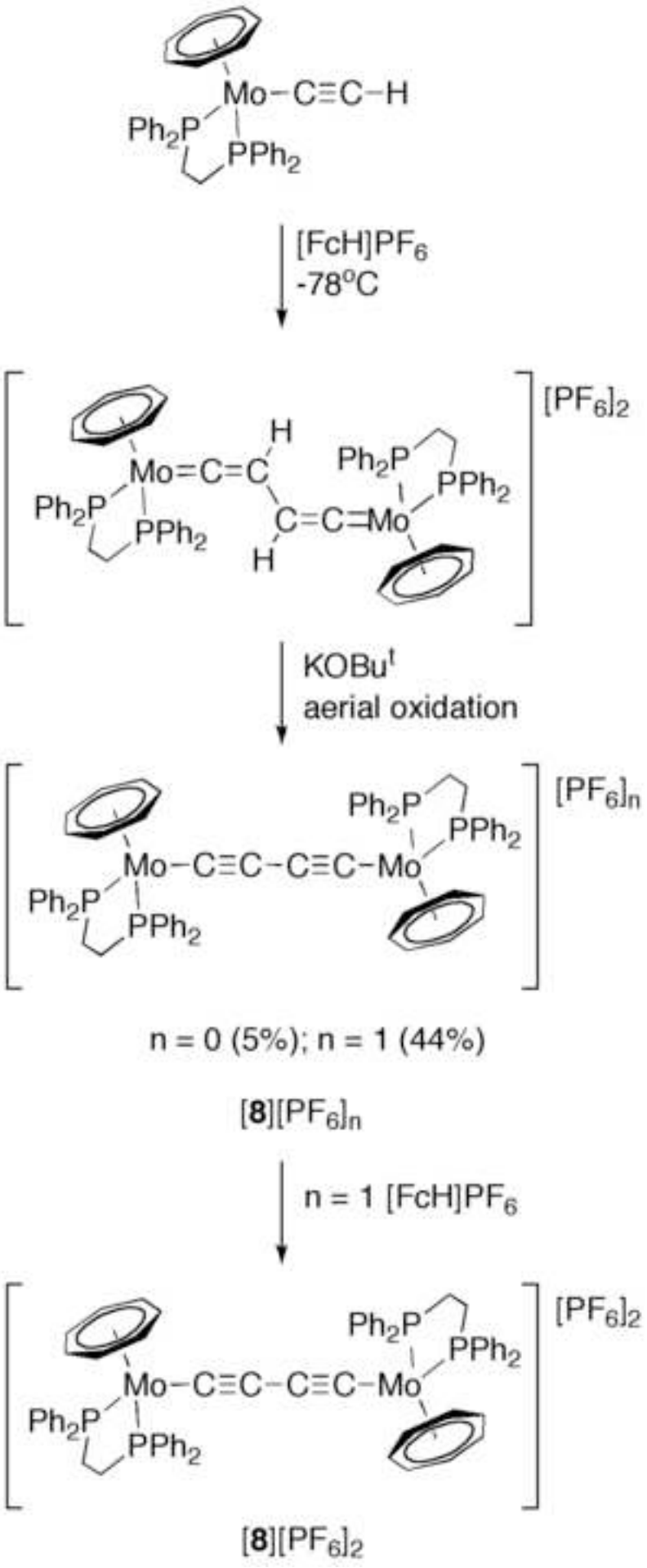

Scheme 11

Click here to download high resolution image

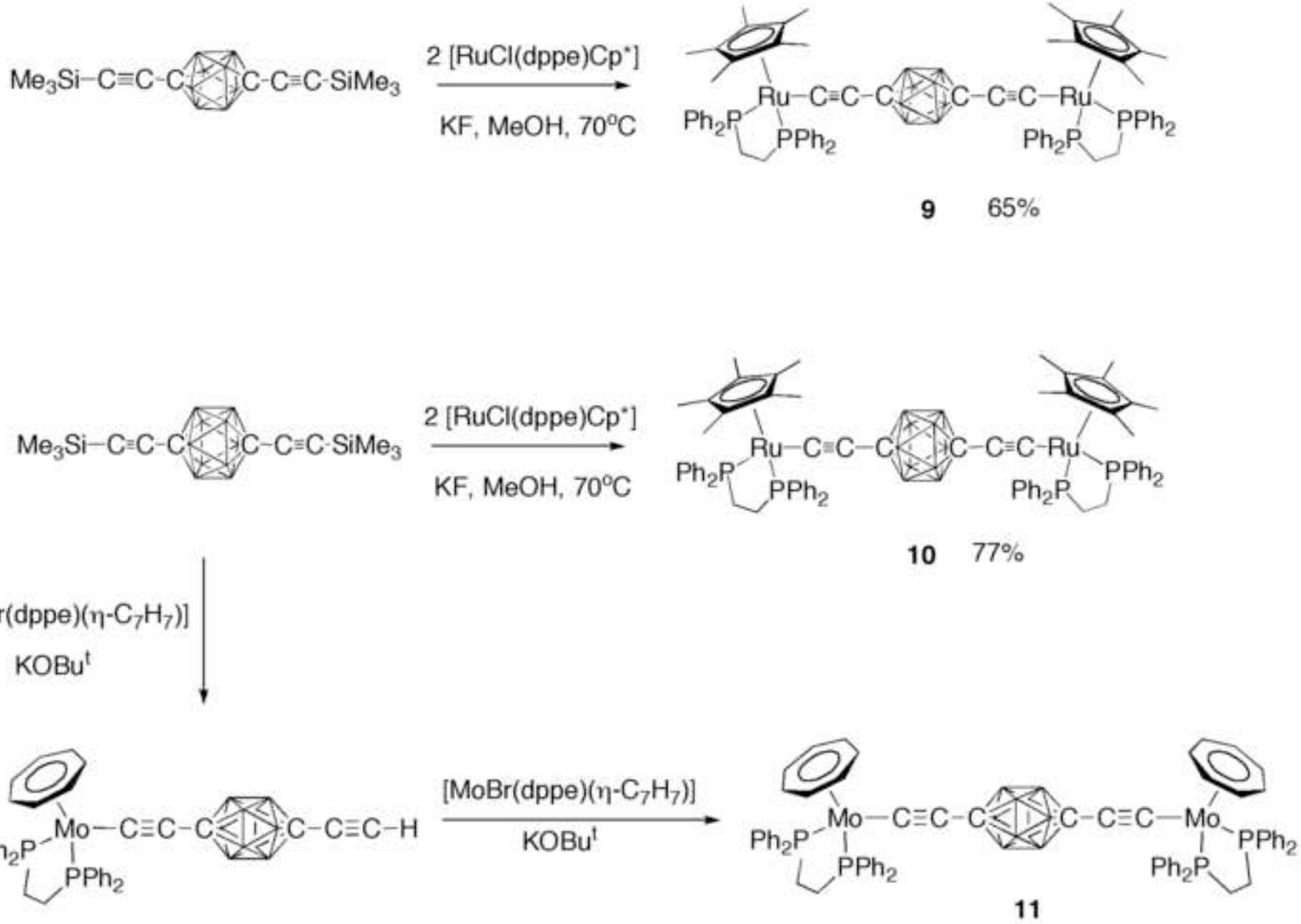

Scheme 12

Click here to download high resolution image

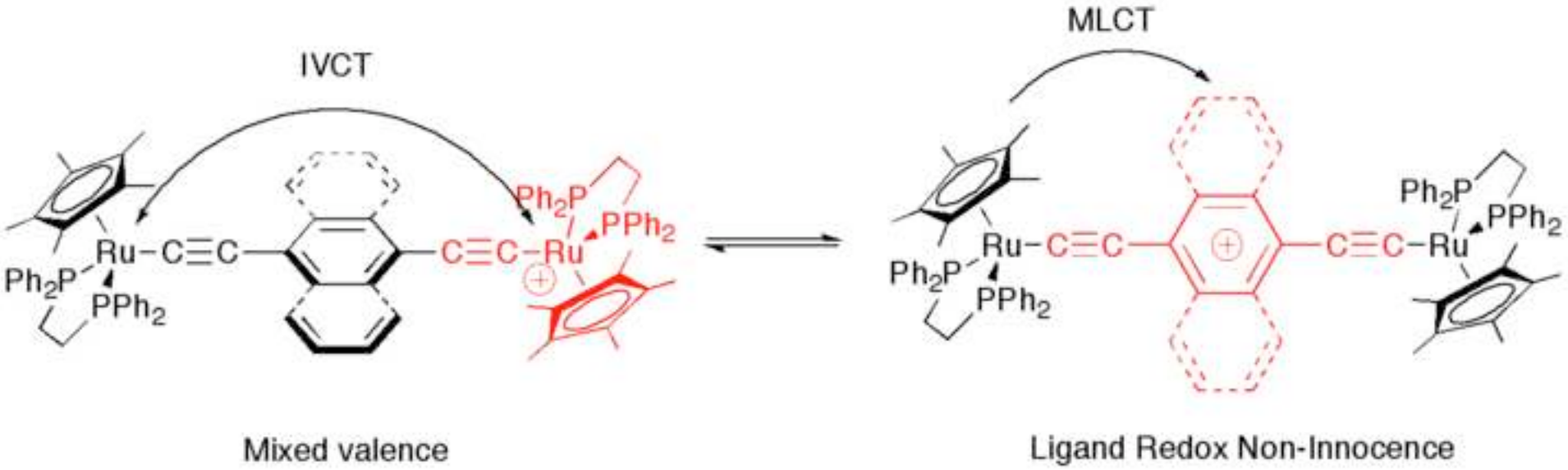

Scheme 13

Click here to download high resolution image

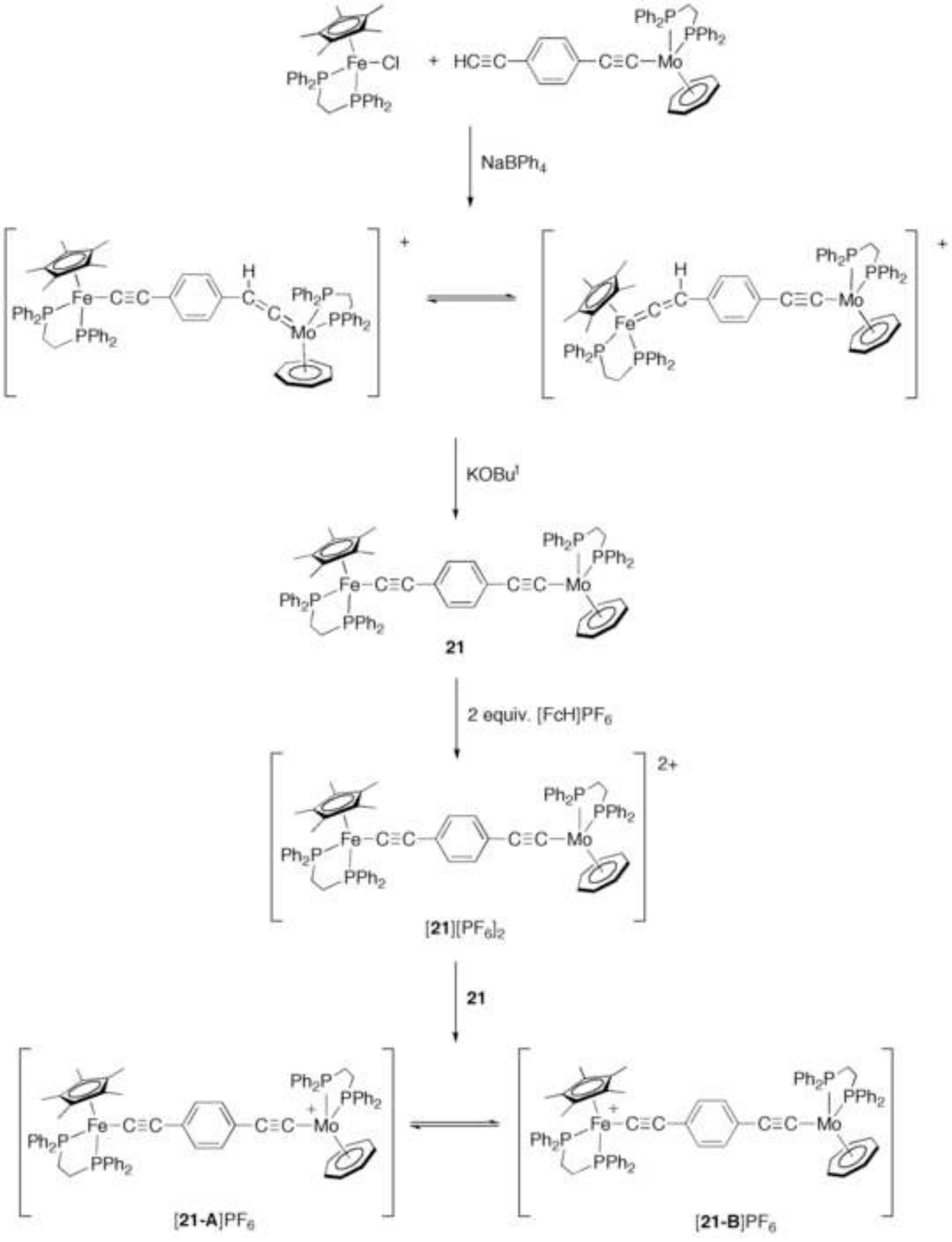

Table 1

Table 1. Summary of ν(C≡C) frequencies for selected complexes.

compound	n = 0	n = 1	n = 2
[*trans*-RuCl(C≡CPh)$(dppe)_2$]$^{n+}$	2075	1910	
[Ru(C≡CPh)(dppe)Cp*]$^{n+}$	2072	1929	
[{*trans*-RuCl$(dppe)_2$}(μ-1,3-C≡CC_6H_4C≡C)]$^{n+}$	2063	2049, 1905	1909
[{Ru(dppe)Cp*}(μ-1,3-C≡CC_6H_4C≡C)]$^{n+}$	2063	2060, 1934	1938

Table 2

Table 2. Summary of electrochemical data from selected alkynyl complexes, in CH_2Cl_2 / 0.1 M NBu_4BF_4, reported against SCE (FcH / FcH^+ = 0.46 V, Fc*H / Fc^*H^+ = –0.07 V).

compound	E_1 / V	E_2 / V	DE / mV	K_C	reference
[Ru(C≡CPh)(dppe)Cp*]	0.25				183
[Ru(C≡C$C_6H_4NH_2$-4)(dppe)Cp*][a]	0.05				183
[Ru(C≡C$C_6H_4NO_2$-4)(dppe)Cp*][a]	0.40				183
[{Ru(dppe)Cp*}$_2$(μ-1,10-C≡C-1,10-$C_2B_8H_8$)]	0.27	0.39	0.12	116	247
[{Ru(dppe)Cp*}$_2$(μ-1,12-C≡C-1,12-$C_2B_{10}H_{10}$)]	0.32	0.41	0.09	35	247
[{Ru(dppe)Cp*}(μ-1,3-C≡CC_6H_4C≡C)]	0.18	0.34	0.16	500	282
[{Ru(dppe)Cp*}(μ-1,4-C≡CC_6H_4C≡C)]	0.01	0.30	290	0.8×10^5	299
[{Ru(dppe)Cp*}(μ-1,4-C≡C$C_6H_2(OMe)_2$C≡C)]	–0.14	0.17	310	1.7×10^5	299
[{Ru(dppe)Cp*}(μ-1,4-C≡C$C_{10}H_6$C≡C)]	–0.06	0.24	290	0.8×10^5	299
[{Ru(dppe)Cp*}(μ-9,10-C≡C$C_{14}H_8$C≡C)]	–0.17	0.13	300	1.2×10^5	299

[a] in 0.1 M NBu_4PF_6 / CH_2Cl_2 [183].

Response to Reviewers

Reviewer 1:

- The Salomon et al review is now cited (ref 23b)
- the typographical corrections have been made as indicated
- A minor edit to Figure 1 and the associated caption has been made to address comments 14 and 15

Reviewer 2:

- The directive for the manuscript was to maintain a tight focus on one's own work. I have included the additional references suggested by the reviewer, but have NOT substantially extended the scope of the text of the review.
- All typographical corrections have been made as suggested with the exception of the inclusion of the dithiocarbamate work; again, more for reasons of space and desire to restrict the possible overlap with other authors than any other.
- A revised Figure 12 with inset showing the low energy transition is included.